Faculty of Medicine
at the
University Duisburg-Essen

Institute of Pathology and Neuropathology

Pulmonary Neuroendocrine Tumours – Different Biological Entities?

Inaugural – Dissertation
in order to achieve the academic degree of
Doctor rerum medicinarum (Dr. rer. medic.)
at the University Duisburg-Essen
Faculty of Medicine

submitted by
Fabian Dominik Mairinger
in Innsbruck (Austria)
2014

Dekan	Herr Univ.-Prof. Dr. med. J. Buer
1. Gutachter:	Herr Priv.-Doz. Dr. med. J. Wohlschläger
2. Gutachter:	Frau Univ.-Prof. Dr. Dr. med. D. Führer-Sakel
3. Gutachter:	Herr Priv.-Doz. Dr. med. J. Verheyen

Tag der mündlichen Prüfung: 12. November 2015

First authorships concerning this dissertation:

- Mairinger FD, Walter RFH, Werner R, et al.: **Activation of angiogenesis differs strongly between pulmonary carcinoids and neuroendocrine carcinomas and is crucial for carcinoid tumourgenesis.** *J Cancer*. 2014; 5(6):465-71.

- Mairinger FD, Ting S, Werner R, et al.: **Different micro-RNA expression profiles distinguish subtypes of neuroendocrine tumors of the lung: results of a profiling study.** *Mod Pathol*. 2014 May 30. doi: 10.1038/modpathol.2014.74.

- Mairinger FD, Walter RFH, Theegarten D, et al.: **Gene Expression Analysis of the 26S Proteasome Subunit PSMB4 Reveals Significant Upregulation, Different Expression and Association with Proliferation in Human Pulmonary Neuroendocrine Tumours.** *J Cancer* 2014; 5(8):646-654.

Table of Contents

1. Introduction

1.1 Epidemiology

Lung cancer is the leading cause of cancer-related deaths worldwide, with a poor five-year survival rate of approximately 15%. It accounts for more deaths than the next four most lethal cancer types combined (Jett and Midthun 2004; Eramo et al. 2008; Mallick et al. 2010) (Figure 1). Lung cancer is usually detected as an accidental finding at an advanced stage or when symptoms are clinically present (Brambilla et al. 2003). In order to decrease these high mortality rates, screening techniques and reliable biomarkers are needed.

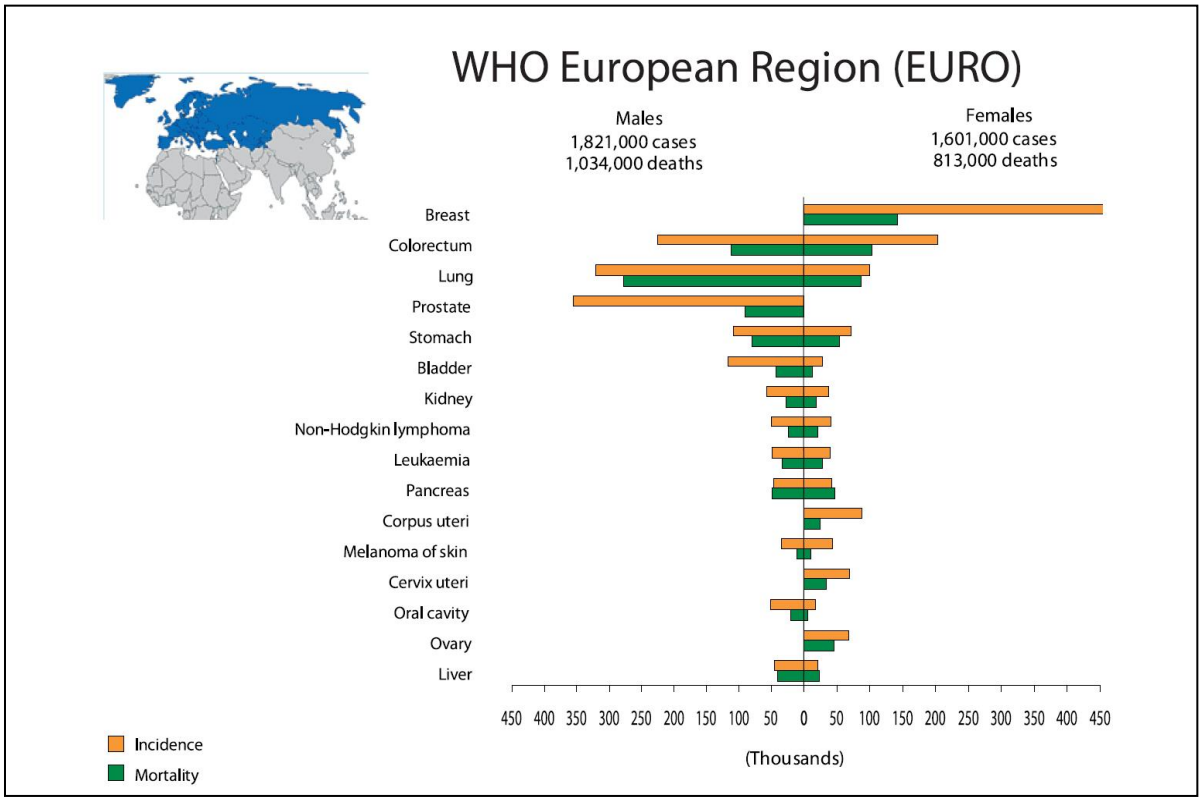

Figure 1: Incidence and mortality rates of different cancers, evaluated by the WHO World Cancer Report 2008 for the European region (Boyle 2008). Lung cancer accounts for more deaths than the next four most lethal cancer types combined.

Twenty-five percent of all lung tumours are neuroendocrine tumours (NETs) (Rekhtman 2010). This subset of tumours encompasses small-cell lung carcinoma (SCLC), large-cell neuroendocrine carcinoma (LCNEC) and both typical (TC) and atypical carcinoid (AC) (Takei et al. 2002). Although the incidence of pulmonary carcinoids has increased during the past 30 years, their combined incidence (both TCs and ACs) in 2003 was just 1.57 per 100,000 inhabitants in the USA (Swarts et al. 2012). Patients suffering from TC have excellent survival rates of 87-100%, but some present lymph node metastasis (4-15%) (Travis et al. 1998; Beasley et al. 2000; Fink et al. 2001; Thomas et al. 2001; Cardillo et al. 2004; Pelosi et al. 2005; Asamura et al. 2006; Garcia-Yuste et al. 2007; Rea et al. 2007; Travis 2009). ACs are more aggressive and show higher frequency of nodal metastasis (35-64%). The survival rate is 61-88% (Beasley et al. 2000; Fink et al. 2001; Scott 2003; Cardillo et al. 2004; Pelosi et al. 2005; Asamura et al. 2006; Garcia-Yuste et al. 2007; Rea et al. 2007). Patients suffering from TC and AC have a mean age at diagnosis of 45-55 years (Travis 2009).

LCNEC was only recognized for the first time about a decade ago. LCNEC belongs to the non-SCLC tumours according to the 1999 WHO classification, but it shows a similar clinical progression to SCLC, with a five-year survival between 15% and 57%, depending on the reporting source (Asamura et al. 2006; Rekhtman 2010). Approximately 15% of all lung cancers are SCLCs, showing definite neuroendocrine differentiation (Rekhtman 2010), and metastasize early (Takei et al. 2002; Asamura et al. 2006; Travis 2009). Ninety-five percent of all small-cell carcinomas (SCCs) are found in the lung, whereas non-pulmonary SCCs are very rare (Rekhtman 2010). The five-year survival for SCLC is <5% (Rekhtman 2010). Even when diagnosed at an early stage, SCLCs and LCNECs show the poorest clinical outcome compared to

other lung tumours due to their aggressive biological behaviour. However, the molecular characteristics of these tumours remain incompletely understood (Takei et al. 2002). They grow rapidly and occur almost exclusively in patients with a history of heavy smoking, whereas lung carcinoids occur frequently in never smokers and younger patients (Travis et al. 1998; Travis et al. 2004; Travis 2009; Swarts et al. 2012). Although both LCNEC and SCLC are still more common in males, the proportion of women suffering from these has significantly increased due to the altered smoking habits of women (Govindan et al. 2006; Swarts et al. 2012).

Table 1 summarizes the outcomes for patients suffering from pulmonary tumours with neuroendocrine features from a recent study.

Table 1. Comparison of clinical parameters from patients suffering from NET (Asamura et al. 2006).

	Histologic Type									
	TC (n=55)		AC (n=9)		LCNEC (n=141)		SCLC (n=113)		Total (N=318)	
Outcome	No. of Patients	%	No. of Patients	%	No. of Patients	%	No. of Patients	%	No. of Patients	%
Tumour recurrence	2	3.6	3	33.3	68	48.2	54	47.8	124	39
Locoregional	1		1		17		10		30	
Distant	1		2		34		18		55	
Both	0		0		16		16		36	
Unknown	0		0		1		1		4	
All deaths	3	5.5	2	22.2	84	59.6	69	61.1	158	49.7
Cancer death	0	0.0	0	0.0	62	73.8	43	63.2	106	67.5

Abbreviations: TC, typical carcinoid; AC, atypical carcinoid; LCNEC, large-cell neuroendocrine carcinoma; SCLC, small-cell lung carcinoma; NE, neuroendocrine

1.2 Tumorigenesis

Tumorigenesis is a complex event on the cellular level comprising the following six deregulation criteria: (I) autonomous growth, (II) insensitivity to external growth-regulating signals and (III) resistance to apoptotic signals, (IV) increased proliferation,

(V) as well as permanent angiogenesis and (VI) metastatic behaviour (Zhu et al. 2006).

During carcinogenesis, cells accumulate multiple molecular-genetic and epigenetic abnormalities that lead to immortalisation, uncontrolled proliferation and spread of these cells (Brambilla et al. 2003).

Cell of Origin

Both pulmonary carcinoids and SCLCs were previously reported to arise from serotonin producing Kulchitsky-type cells, currently known as pulmonary neuroendocrine cells (PNECs), which are the first cells to differentiate in the epithelium during lung development (Bensch et al. 1968; Warburton et al. 2000; Swarts et al. 2012). Sometimes they aggregate to form small nodules named neuroepithelial bodies (NEBs). PNECs only comprise about 0.4% of bronchial epithelial cells, playing an important role as local modulators of lung growth and pulmonary differentiation during prenatal development and as airway chemoreceptors during adult life (Boers et al. 1996; Linnoila 2006; Swarts et al. 2012). In the prenatal phase, PNECs express serotonin, neuron-specific enolase (NSE) and gastrin-releasing peptide, whereas in adults, NEBs have been described as being involved in hypoxia response by secretion of serotonin and thereby regulating local vasoconstriction (Cutz and Jackson 1999; Linnoila 2006; Swarts et al. 2012).

Because gene expression profiling has shown that SCLCs cluster together with LCNECs, and combined SCLC-LCNEC tumours are not uncommon, it is suggested that LCNEC and SCLC originate from the same or similar precursor cells (Jones et al. 2004; Swarts et al. 2012). However, it remains unclear how carcinoids can be integrated into this scheme (Figure 2).

Precursor Lesions

Precursor lesions of pulmonary carcinoid tumours comprise diffuse idiopathic pulmonary neuroendocrine cell hyperplasia (DIPNECH), a linear proliferation of PNECs or NEBs, as well as tumourlets (Swarts et al. 2012). Tumourlets are 2-5mm extraluminal lesions which share histopathological features with carcinoids and originate when proliferating PNECs penetrate through the basal membrane and form small aggregates; by definition, a tumourlet >5mm in size is termed a “carcinoid tumour” (Finkelstein et al. 1999). Although tumourlets are thought of as benign tumours, some have been reported to behave like carcinoids, cause Cushing’s syndrome and to metastasize to lymph nodes or even distant organs (D'Agati and Perzin 1985; Arioglu et al. 1998; Liu et al. 2003; Swarts et al. 2012). In contrast to tumourlets related to DIPNECH, tumourlets resulting from reactive PNEC hyperplasia do not progress to carcinoid tumours (Swarts et al. 2012).

In contrast, no precursor lesions for high-grade lung NETs have been identified thus far, although genomic changes typical of these tumours have been observed in phenotypically normal cells (Lantuejoul et al. 2009).

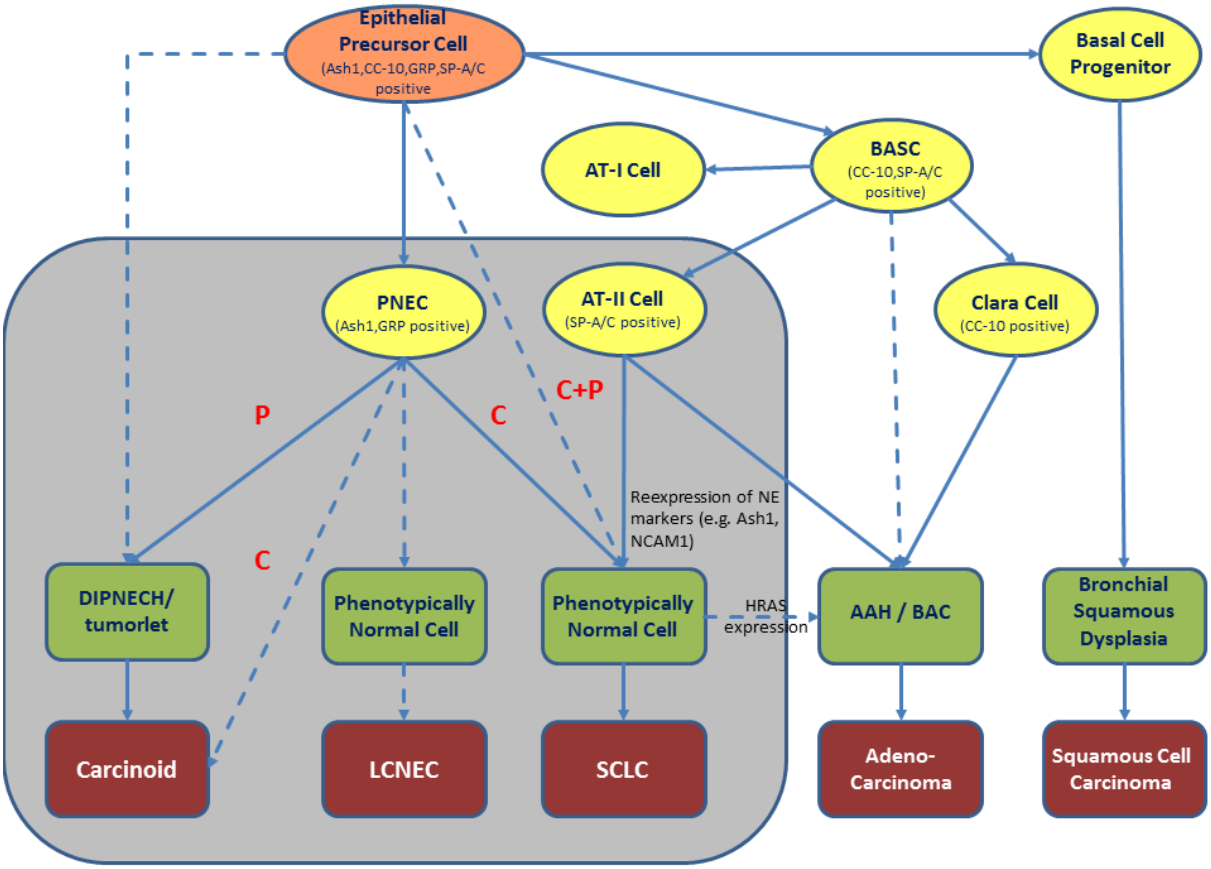

Figure 2 Current model for the cells of origin of the main types of lung cancer. An Ash1 expressing precursor cell is considered a stem cell giving rise to pulmonary neuroendocrine cells (PNECs), but also bronchoalveolar stem cells (BASC) and basal cell progenitors. Diffuse idiopathic pulmonary neuroendocrine cell hyperplasia (DIPNECH) and tumourlets comprise precursor lesions for pulmonary carcinoids, while for LCNEC and SCLC no precursor lesions have been identified. For adenocarcinoma, the precursor lesions seem to be atypical adenomatous hyperplasia (AAH) and bronchoalveolar carcinoma in situ (BAC). for squamous cell carcinoma, the bronchial squamous dysplasia is a suspected precursor lesion. (Swarts et al. 2012) C: central; P: lung periphery

Models of Tumorigenesis

A hypothetical model for carcinogenesis of pulmonary neuroendocrine tumours suggests an Ash1-positive pulmonary precursor cell capable of differentiation into PNECs, BASCs and basal cell progenitors (Swarts et al. 2012).

In carcinoids, the transition towards tumourlets is initiated via a linear expansion of PNECs or NEBs into DIPNECH and a subsequent resistance to apoptotic mechanisms due to increased Bcl-2 expression (Gosney et al. 2011). Evasion of cell

cycle control must also be amongst the earliest stages (Swarts et al. 2012). Epigenetic silencing of tumour suppressor genes is also likely to occur in early tumorigenesis, e.g., involving *RASSF1A* methylation (Toyooka et al. 2001; Swarts et al. 2012). Subsequent steps in carcinoid progression may include abrogation of the Menin pathway, deletions of the telomeric part of chromosome 11q and CD44 downregulation (Granberg et al. 1999; Swarts et al. 2012). Progression to a metastatic stage may result from epithelial-mesenchymal transition (EMT), probably induced by abolition of *CDH1* (E-cadherin) or *CTNNB1* (β-catenin) function along with an increase of the PSA variant of neural cell adhesion molecule 1 (*NCAM*; CD56) (Figure 3).

The majority of steps in SCLC carcinogenesis can be related to direct exposure to tobacco carcinogens. Early events in carcinogenesis of this tumour include epigenetic changes and allelic imbalances such as 3p regions, comprising *FHIT* and *RASSF1A,* which can both be inactivated by promoter hypermethylation (Gorgoulis et al. 2005). Furthermore, aberrations of the intrinsic apoptosis pathway by inversion of the Bcl-2/Bax ratio are an early event, possibly preceding p53 alterations (Brambilla et al. 1998; Swarts et al. 2012). It is still unclear whether 3p deletions precede or follow 17p losses and associated p53 mutations (Swarts et al. 2012). A strict sequence of events in SCLC and LCNEC tumorigenesis like those reported for other human malignancies is therefore unlikely (Swarts et al. 2012). It is possible that p53 mutations pave the way for subsequent chromosomal instability and further chromosomal losses like 9p, 17p and/or 5q, and might cause an inactivation of pRb and an increase in the PSA variant of *NCAM* downstream of this process, the next important events in tumorigenesis of high-grade pulmonary NET (Swarts et al. 2012).

Continued cigarette smoking may induce EMT, crucial for metastatic SCLC in association with MYC overexpression (Wong et al. 1986; Takahashi et al. 1989). Because there is a major lack of information regarding LCNEC, this tumour entity could not be included in this model (Swarts et al. 2012) (Figure 3).

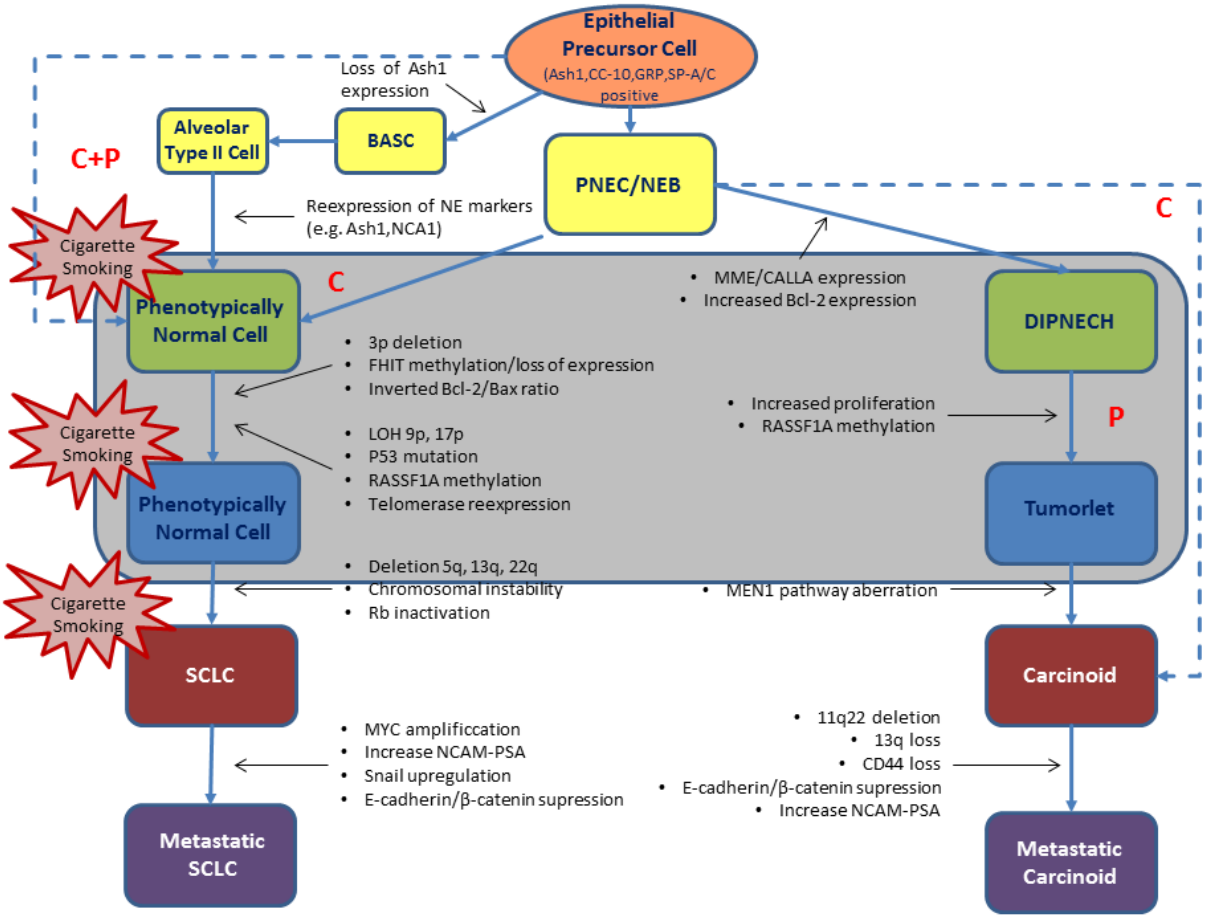

Figure 3 Tumorigenesis model for pulmonary neuroendocrine tumours excluding LCNEC. Precursor lesions are indicated in the grey area. The occurrences of specific aberrations in the primary tumour are shown. The dotted lines indicate hypothetical relationships (Swarts et al. 2012). C: central; P: lung periphery

1.3 Diagnosis

The morphologic features of carcinoid tumours have been accurately described: neuroendocrine cytology including coarsely granular “salt and pepper” chromatin, lack of prominent nucleoli and overall uniformity (Figure 4) (Travis et al. 2004; Rekhtman 2010). In addition, architectural patterns, like organoid nests, trabeculae or

rosettes, are morphological features of carcinoids (Figure 4 to Figure 5) (Travis et al. 2004; Rekhtman 2010). Further diagnostic criteria for typical carcinoids include a mitosis rate of not more than 1 per 10 high power fields (HPF, approx. 2mm^2) and an absence of necrotic areas. Atypical carcinoids are defined as showing a mitosis rate of 2-10 per 10 HPF and may exhibit areas of comedo-like necrosis (Travis et al. 2004; Rekhtman 2010).

Travis *et al.* (Travis et al. 1991) introduced LCNECs in the 2004 WHO classification and described their components. The high mitotic rate (>10 per 10 HPFs) and necrotic areas are criteria for these high grade carcinomas. The morphology is characterised by neuroendocrine architecture like organoid nesting, trabecular growth and palisade or rosette patterns (Figure 6). Cytology demonstrates prominent nucleoli, vesicular clumpy chromatin and large cell size (Travis et al. 2004; Rekhtman 2010).

Morphologically, SCLC are characterized by finely granular nuclear chromatin, nuclear moulding, lack of prominent nucleoli and crush artefacts with nuclear streaming and incrustation of vessels (Figure 7) (Travis et al. 2004; Rekhtman 2010). The size of the cells is normally less than three resting lymphocytes in extension (Travis et al. 2004; Rekhtman 2010). Other diagnostic features of SCLC include the high mitosis rate (>10 per 10 HPF) and undefined cell borders with apoptotic or necrotic areas (Hirsch et al. 1982; Travis et al. 2004).

Diagnostic discrimination of LCNEC versus atypical carcinoids and SCLCs on solely morphological grounds is difficult due to overlapping morphological features.

Therefore, diagnosis by immunohistochemical (IHC) staining is a routine tool for differential diagnosis of neuroendocrine tumours.

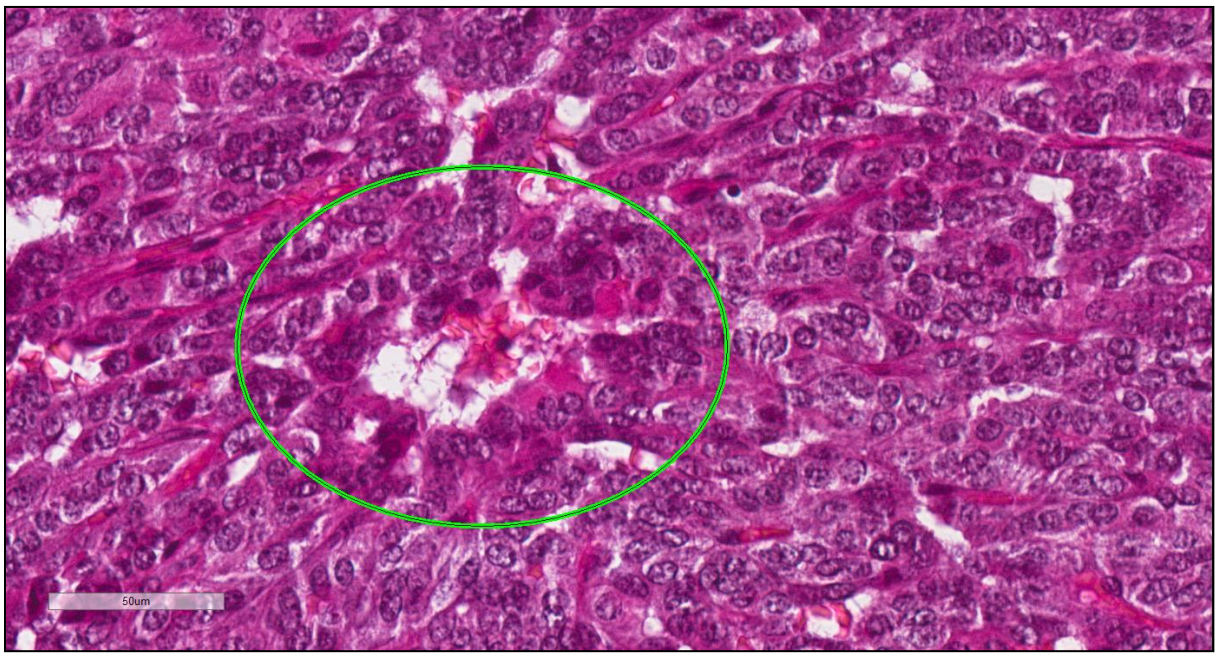

Figure 4 Typical carcinoid stained with haematoxylin and eosin (HE) showing neuroendocrine features such as rosettes (marked) and granular chromatin (400x magnification). Note the dense vascularisation of the tumour tissue.

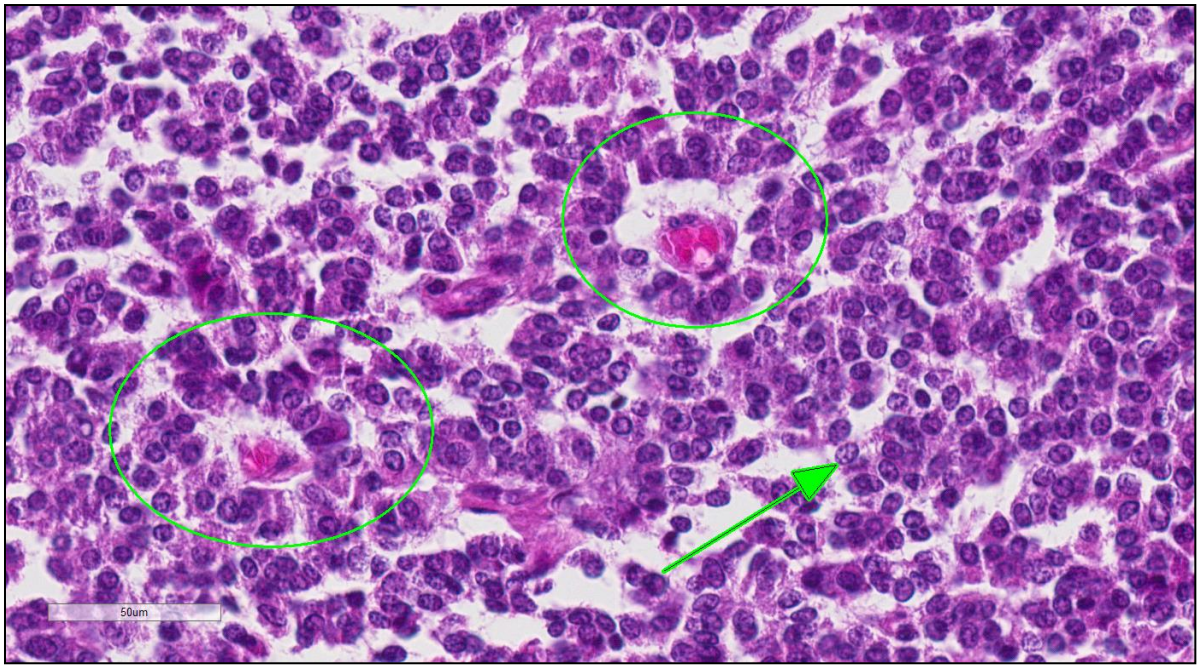

Figure 5 Atypical carcinoid with two rosette structures (circles) and "salt and pepper chromatin" (arrow) stained with HE (400x magnification).

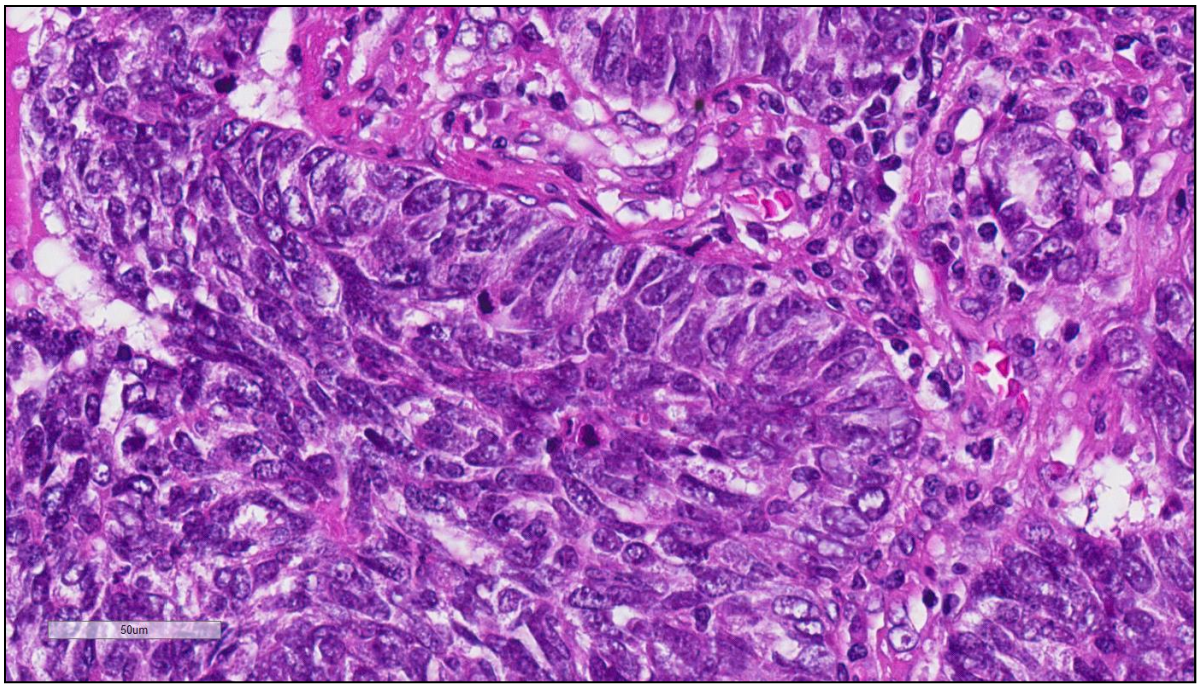

Figure 6 Large-cell lung cancer forming a so-called palisade structure (400x magnification).

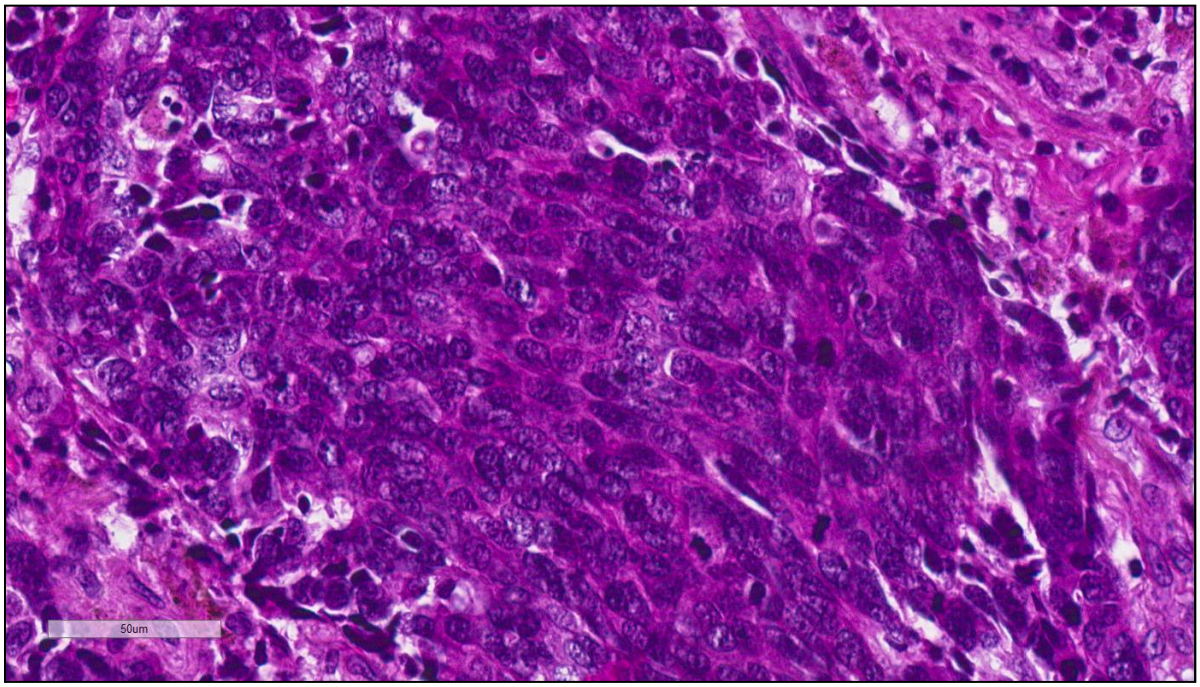

Figure 7 Small-cell lung cancer with HE staining (400x magnification). The neuroendocrine properties like granular chromatin and lack of prominent nucleoli serve as diagnostic criteria for diagnosis of SCLC.

The most important markers for the diagnosis of pulmonary neuroendocrine tumours by IHC are neural cell adhesion molecule 1 (also known as CD56 or *NCAM1*), chromogranin A (*CHGA*), synaptophysin (*SYP*), thyroid transcription factor 1 (also known as TTF-1 or *NKX21*) and *MKI67* (marker of proliferation Ki-67, also known as MIB1) (Takei et al. 2002; Asamura et al. 2006; Rekhtman 2010). As with all subjective imaging methods, these techniques are prone to significant intra- and interobserver variability, reducing the reproducibility and reliability of this methodology (Jagoe et al. 1991; Jarlov 2000; Asamura et al. 2006; Rekhtman 2010). Furthermore, differentiating LCNECs and SCLCs via IHC is hindered by their related biological characteristics, leading to false identification (Takei et al. 2002; Asamura et al. 2006; Rekhtman 2010). A reproducibility study by Travis *et al.* achieved unanimous agreement among five pathologists diagnosing LCNEC only 40% of the time (Travis et al. 1998). Furthermore, in an intraobserver variability study, only 12% of diagnoses were unanimous for a group of nine pathologists (den Bakker et al. 2010).

Zhu *et al*. (Zhu et al. 2006) performed a meta-analysis of literature focusing on tumour markers and their prognostic values based on IHC analysis. Table 2 shows the results of their broad investigation, revealing that a large number of potential markers exist, but that results obtained can differ significantly (Zhu et al. 2006).

Table 2 Summary of meta-analyses of the results of studies on candidate immunohistochemistry markers for survival of patients with non-small cell lung cancer (Zhu et al. 2006).

Marker	First author	Published studies	Number of eligible studies	Number of patients	Overall HR*	95% CI	Significance/ comment
EGFR	Meert(Meert et al. 2002)	Until July 2001	8	1987	1.13	1.00 to 1.28	Weak significance
P21RAS	Mascaux(Mascaux et al. 2005)	Until July 2003	7	989	1.08	0.86 to 1.34	Not significant
HER-2	Nakamura (Nakamura et al. 2005)	Until August 2004	18	2579	1.32	1.14 to 1.65	17/25 negative studies excluded for lack of detailed survival data
P53	Steels (Steels et al. 2001)	Until July 1999	8 (Pab 1801) 16 (DO-7)	1035	1.57	1.28 to 1.91	True significance requires prospective and multivariante confirmation by a standardised technique, scoring criteria and cut-offs
Ki-67	Martin (Martin et al. 2004)	Until December 2002	16	1863	1.55	1.34 to 1.78	
Bcl-2	Martin (Martin et al. 2003)	1993 to December 1999	18	2909	0.72	0.64 to 0.82	

CI, confidence interval; EGFR, epidermal growth factor receptor; HER; human epidermal growth factor receptor; HR, hazard ratio of death for high expression of the marker.

*HR> 1 implies worse survival for the group with increased expression of the marker, whereas HR< 1 (Bcl-2) indicates better survival for the group with high expression. For p53, the prognostic significance of studies that used Pab1801 and DO7 antibodies were separately analysed.

Tumour staging is performed based on several factors, trying to link them to the patients' clinics and outcome. Tumour size, lymph node metastasis and distant metastasis as a part of TNM-staging cannot be taken as *ultima ratio* for prognosis. In general, late detection of a tumour with widespread metastases is associated with significantly decreased patient survival. As noted above, morphologic differentiation between LCNEC and SCLC can fail because of related histology, making molecular markers a favourable tool for more accurate tumour assessment (Asamura et al. 2006).

1.4 Treatment of Pulmonary Neuroendocrine Tumours

Due to the different treatment options for each malignant neuroendocrine lung tumour, accurate pathohistological diagnosis is crucial. Carcinoid tumours are predominantly surgically treated, based on the general principle of complete resection when locally limited. Metastatic tumours are commonly not sensitive to chemotherapeutic regimes or radiation therapy (Rekhtman 2010; Gridelli et al. 2012). Recurrence after surgical resection occurs in 3-5% of all TC (Gridelli et al. 2013). In AC, 25% of deaths are due to recurrences (Ducrocq et al. 1998; Gridelli et al. 2013). A mediastinal lymph node dissection is recommended for AC without the detection of lymph node invasion (Gridelli et al. 2013). TCs are polyp-like endobronchial structures without extension through the cartilaginous wall in 5-10% of patients; however, endobronchial removal should be reserved for very specific patients (Luckraz et al. 2006; Brokx et al. 2007). In the presence of central carcinoids with clinical invasion of lymph nodes, surgical resection and mediastinal lymph node dissection is recommended (Gridelli et al. 2013). Adjuvant treatment, chemotherapy or radiotherapy should be considered in completely resected ACs with mediastinal lymph node involvement (Thomas et al. 2001; Mackley and Videtic 2006; Gridelli et al. 2013). Combined chemotherapies are usually platinum- or streptozoticin-based approaches (Gridelli et al. 2013).

For SCLCs, chemotherapy with cisplatin plus etoposide is an established treatment since the tumours are notably sensitive to chemotherapeutical and radiation therapy (Rekhtman 2010). A prophylactic cranial irradiation should be performed in SCLCs with a chemosensitive shape. Since 50-80% of patients develop brain metastases, a proper pathological diagnosis is vital (Rekhtman 2010). Considering the relative rarity of LCNEC (~3% of neuroendocrine lung tumours), an optimal treatment for this entity

is still under investigation (Rekhtman 2010). Under the WHO classification guidelines, LCNEC belongs to non-SCLCs, and based on this classification therapeutic strategies for LCNEC leave it up to clinicians whether to treat it similarly to SCLCs or non-SCLCs (Asamura et al. 2006). In fact, patients in stage IV receiving SCLC-based regimens had a significantly better overall survival rate compared with those receiving standard regimes for NSCLC (Rossi et al. 2005; Gridelli et al. 2013). The chemotherapy regimens usually administered in SCLC therapy, including platinum plus etoposide, should be the preferred option (Gridelli et al. 2013). Unfortunately, there is even less information available concerning the treatment of unresectable and advanced LCNEC (Gridelli et al. 2013).

Most LCNECs are poor candidates for surgical resection due to local or systemic spread (Gridelli et al. 2013). In early stages, lobectomy or pneumonectomy are preferred (Zacharias et al. 2003; Gridelli et al. 2013).

The American Society for Clinical Oncology (ASCO) and the European Society for Medical Oncology (ESMO) summarize these recommendations in their clinical practice guidelines (Rinaldi et al. 2006; Gridelli et al. 2013; Vansteenkiste et al. 2013).

Figure 8 provides a suggested algorithm for treatment decisions in non-small cell neuroendocrine lung tumours.

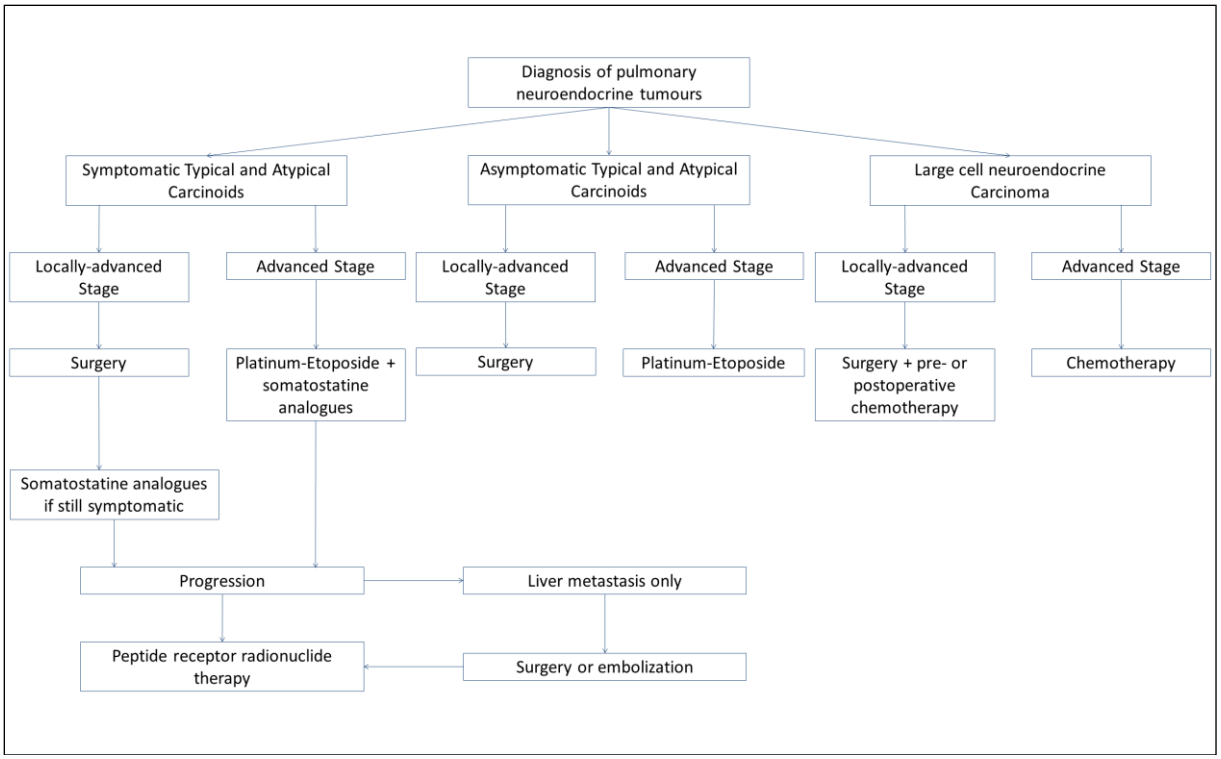

Figure 8 Suggested algorithm for the treatment of non-small cell pulmonary neuroendocrine tumours (Gridelli et al. 2013).

Targeted Therapies

Octreotide was developed as a pharmacologically stable, long-acting repeatable (LAR) analogue of the hormone somatostatin and has proven to be an effective agent for symptoms of carcinoid syndrome (Gridelli et al. 2013). Several results supported the recommendation of somatostatin analogues such as octreotide and lanreotide in treating the carcinoid syndrome, but their use for any other purpose, including the management of asymptomatic metastatic carcinoids, is still subject to fierce debate (Filosso et al. 2002; Waldherr et al. 2002; Srirajaskanthan et al. 2009; Bushnell et al. 2010; Oberg et al. 2010; Gridelli et al. 2013).

The mammalian target of rapamycin (*mTOR*) pathway may be involved in the pathogenesis of neuroendocrine tumours and can be inhibited by everolimus (Gridelli et al. 2013). The upregulation of upstream insulin-like growth factor-1 (*IGF1*) pathway should be a potential resistance mechanism for everolimus (O'Reilly et al. 2006). In

contrast, octreotide has been shown to reduce serum *IGF-1* levels in patients with solid tumours (Pollak et al. 1989).

Overexpression of vascular endothelial growth factor (*VEGF*) and VEGF receptor (*VEGFR*) subtypes has been observed in carcinoid tumours, suggesting that autocrine activation of the *VEGF* pathway may promote tumour growth (La Rosa et al. 2003; Gridelli et al. 2013). In addition, neuroendocrine tumours also express platelet derived growth factor (*PDGF*) and PDGF receptor (*PDGFR*) (Chaudhry et al. 1992), targets drugable with sunitinib, an orally administered small molecule with activity against *VEGFR-1, -2, -3*, *PDGFR-α* and *–β* (Mendel et al. 2003; Gridelli et al. 2013). Results from the use of bevacizumab are also promising, but need to be confirmed in larger studies (Gridelli et al. 2013). Additionally, interferon-α (*IFNA1*) has been described as having antiangiogenic properties and has also been studied in carcinoids. In fact, it was approved by the European Medicines Agency (EMA) for the treatment of metastatic carcinoid tumours with syndrome (Gridelli et al. 2013).

The role of the ErbB family signalling was investigated for this class of tumours (Rickman et al. 2009). The analysis showed that 45.8% of TCs and 28.6% of ACs expressed epidermal growth factor receptor (*EGFR*), all tumours lacked expression of ErbB2 and all had moderate or intense staining for ErbB3 and ErbB4. No *EGFR* mutations were found in a recent study and all investigated tumours were *KRAS* wildtype (Rickman et al. 2009). Moreover, in a lung carcinoid cell line expressing *EGFR*, erlotinib reduced proliferation. These findings suggest a potential clinical use of *EGFR* inhibitors in the treatment of patients with pulmonary carcinoids (Rickman et al. 2009; Gridelli et al. 2013).

Targeted therapy of tyrosine kinase receptors also seems promising in SCLC. In particular, expression c-Kit receptor (*KIT*) has been widely studied within SCLC, showing that 56-70% of these tumours are positive for c-Kit expression (Swarts et al.

2012). *PDGFR-β* is also frequently expressed in SCLC (Shinohara et al. 2007; Swarts et al. 2012). As a result, an inhibitory effect of mesylate, a small molecule inhibitor which targets *KIT* as well as *PDGFR* and Bcr-Abl, could be shown in SCLC cell lines (Krystal et al. 2000). Hedgehog signalling reveals potential targets for therapy, because this pathway is implicated in the development and maintenance of SCLC. In particular, sonic hedgehog is expressed in a subset of SCLC (Watkins et al. 2003; Park et al. 2011; Swarts et al. 2012).

1.5 Molecular Differences and Similarities

Genomic DNA Alterations

Several genome-wide (array) comparative genomic hybridization (CGH) studies as well as other technical approaches were performed to identify chromosomal alterations in pulmonary carcinoids (Walch et al. 1998; Zhao et al. 2000; Leotlela et al. 2003; Petzmann et al. 2004), high grade lung NETs (Petersen et al. 1997; Michelland et al. 1999; Ullmann et al. 2001; Peng et al. 2005) or both (Peng et al. 2005; Swarts et al. 2012) (Table 3). In general, chromosomal alterations of more than 10 Mb in size are much more frequent in SCLCs and LCNECs than ACs and TCs (SCLC: 18.8/tumour, LCNEC: 13.7/tumour, AC: 6.1/tumour, TC: 2.8/tumour) (Swarts et al. 2012). Although most alterations occur frequently in both high-grade tumour types, it must be noted that loss of chromosome 17p (harbouring the *TP53* gene locus) and gain of 3q occur twice as frequently in SCLCs compared to LCNECs (Swarts et al. 2012).

The most important chromosomal alteration in neuroendocrine lung carcinomas, which is infrequently present in lung carcinoids, is deletion of chromosome 3p (Swarts et al. 2012). This deletion is often followed by overrepresentation of 3q and

precedes other chromosomal alterations such as deletions of 5q, 9p and 17p (Wistuba et al. 1999; Swarts et al. 2012). Putative tumour suppressors located at chromosome 3p are identified in four separated areas, including 3p12-13 (*DUTT1, ROBO1*), 3p14.2 (*FHIT*), 3p21.3 (*BAP1, CTNNB1, FUS1, HYAL2, MLH1, RASSF1A, SEMA3B, SEMA3F*) and 3p24.6 (*VLH, RARB*) (Zienolddiny et al. 2001; Wistuba and Gazdar 2006; Swarts et al. 2012). Additionally, *RARB* (in approximately 50%) and *RASSF1A* (in approximately 85%) are frequently methylated in SCLCs but less often in carcinoids (Toyooka et al. 2001).

Deletion of 11q is the most frequently observed alteration in pulmonary carcinoids; its telomeric portion is associated with AC and is an important prognostic factor for these tumours, representing a marker of tumour progression rather than initiation of tumorigenesis (Swarts et al. 2011; Swarts et al. 2012). Deletion of 11q is the only chromosomal aberration with comparable frequency in carcinoids (28%) and neuroendocrine carcinomas (32%) (Swarts et al. 2012). These deletions are mostly centred around regions with a high density of genes (11p13, 11p22, 11p23, 11p24), and only in few cases could a deletion of the whole chromosome arm be observed (Koreth et al. 1999). Tumour suppressor genes identified in these regions include *ADAMTS8* (11q24.3), *ATM* and *TSLC1* (11q22.3), *SDHD* (11q23.1) and particularly the *MEN1* gene encoding menin (11q13).

Menin, a complex tumour suppressor protein with many different functions in multiple pathways, is responsible for the familial hereditary syndrome multiple endocrine neoplasia type 1 (*MEN1*-syndrome). Patients with *MEN1*-syndrome have inherited mutations of the *MEN1* gene, predisposing them to the formation of multiple NETs, including bronchial carcinoids (Swarts et al. 2012). In contrast, neither SCLCs nor LCNECs have been reported to develop in association with *MEN1*-syndrome (Sachithanandan et al. 2005). The frequency of sporadic lung carcinoids that actually

display *MEN1* gene mutations is approximately 18%, but the percentage of loss-of-heterozygosity LOH of the *MEN1* region at chromosome 11q13 is nearly 36% (Swarts et al. 2012). Importantly, *MEN1* mutations are largely absent from sporadic neuroendocrine lung carcinomas (Debelenko et al. 2000; Swarts et al. 2012).

The other important shared genomic alteration between pulmonary carcinoids and high-grade tumours are deletions on chromosome 13q, although they appear in much higher frequencies in the high-grade group (Swarts et al. 2012). The most important tumour suppressor genes located at this region are *RB1* (13q14), *BRCA2* (13q12.3) and *ING1* (13q34).

Table 3 Molecular characteristics that distinguish lung carcinoids from SCLC (Swarts et al. 2012).

Molecular Characteristic	Carcinoids	SCLC	Relation to Smoking
Number of chromosomal alterations	3.8	14.4	Yes
Chromosomal instability	Rare	Frequent	Yes
Telomerase activity	7% (TCs)	93%	Unknown
3p loss	10%	92%	Yes
FHIT protein expression	100%	0%	Yes
4q loss	5%	79%	Unknown
5q loss	4%	79%	Yes
13q loss	14%	83%	Yes
pRb downregulation	9-21% (TC-AC)	90%	Unknown
17p loss	7%	73%	Yes
p53 mutation	6%	90%	Yes
p53 upregulation	< 10%	> 50%	Yes
Bcl-2:Bax ratio> 1	5%	90%	Unknown
CASP8 methylation	18%	41%	Unknown
B-Catenin dislocation	11-41%	90-93%	Unknown
E-Cadherin dislocation	17-46%	67-90%	Yes
CDH1 methylation	~ 25%	~ 60%	Unknown
Fascin protein expression	< 35%	100%	Unknown
Snail protein expression	Weak	Strong	Probably
Ki67 proliferative index	< 5%	> 25%	Unknown
Cyclin B1 protein overexpression	4%	84%	Unknown
c-Kit protein expression	11%	56%	Unknown
MEN1 mutation	18-36%	0%	Unknown
NCAM1-PSA protein expression	53%	95%	Unknown

Gene Expression Profiles

Only a limited number of studies describe genome-wide expression profiling of pulmonary neuroendocrine tumours including carcinoids (Anbazhagan et al. 1999; Bhattacharjee et al. 2001; Virtanen et al. 2002; He et al. 2004; Jones et al. 2004; Swarts et al. 2012). There are only a few genes that have been consistently reported to show a differential expression between carcinoids, LCNECs and/or SCLCs, respectively. The findings in these studies show that carcinoid tumours and high-grade NETs share only a few overlapping genetic alterations, while a distinct group of genes are specifically associated with these two groups. Moreover, SCLCs and LCNECs cluster separately, but more closely to each other than to carcinoid tumours. Bhattacharjee et al. showed that SCLCs and carcinoids shared high-level expression of neuroendocrine genes such as *INSM1*, *ASCL1* and *CHGA* (Bhattacharjee et al. 2001; Swarts et al. 2012). In contrast, another study observed low frequencies of *ASCL1* expression in TCs compared to high-grade NETs of the lung (Jiang et al. 2004). Immunohistochemistry for *CHGA* has been reported as being positive in a higher frequency in carcinoids than in poorly differentiated neuroendocrine lung tumours (Lantuejoul et al. 1998). While *NCAM1* has been reported as being overexpressed in both SCLC and carcinoids (Jones et al. 2004; Swarts et al. 2012), several immunohistochemical studies showed that the *NCAM*-PSA variant was more often present in SCLCs (95.2%) than in pulmonary carcinoids (52.8%) (Kibbelaar et al. 1989; Komminoth et al. 1991; Michalides et al. 1994; Patriarca et al. 1997; Lantuejoul et al. 1998). While the majority of LCNECs have been reported as being positive for this variant, ACs show variable frequencies of positivity (Michalides et al. 1994; Patriarca et al. 1997; Swarts et al. 2012).

Tumour Suppressors and Oncogenes

Several tumour suppressor genes and oncogenes have been related to pulmonary tumorigenesis, including Bcl-2 family members, *CDH1*, *FHIT* and *TP53* (Swarts et al. 2012).

The protein expression levels of p53, the mutation frequencies of the *TP53* gene and the percentage of LOH at the *TP53* locus differ greatly between lung carcinoids and high-grade neuroendocrine lung tumours (Swarts et al. 2012). Mutations of *TP*53 are reported to be rare or absent in lung carcinoids (Lohmann et al. 1993; Przygodzki et al. 1996; Couce et al. 1999), but are present in up to 90% of high-grade NETs (Leotlela et al. 2003; Swarts et al. 2012). Also the frequency of LOH rises considerably from carcinoids towards neuroendocrine carcinomas (Onuki et al. 1999). Similarly, there is a significant increase in p53 expression, indicating a TP53 mutation, when comparing carcinoids to lung carcinomas (Brambilla et al. 1996; Swarts et al. 2012). In addition, alterations of the p53 main regulator Mdm2 may be involved; 30% of neuroendocrine lung tumours show overexpression of this gene (Eymin et al. 2002).

Epithelial to mesenchymal transition is characterized by decreased *CDH1* expression and increased expression of tyrosine kinase receptors, including *EGFR*, *FGFR* and *IGFR* (Swarts et al. 2012). *CDH1* interacts with *CTNNB1*, a main transducer of Wnt-signalling to the nucleus. *CDH1* is expressed in most NETs and *CTNNB1* in all lung NETs, although a disruption of normal membrane associated expression of these proteins has been observed (Salon et al. 2004; Pelosi et al. 2005; Swarts et al. 2012). This dislocation to the cytoplasm gradually increases in both frequency and severity from low-grade TCs to high-grade SCLCs.

The pRb pathway is altered significantly more often in high-grade NETs than in carcinoids. In general, pRb protein expression is gradually lost when comparing

tumours with a higher differentiation with poorly differentiated NETs (Swarts et al. 2011; Swarts et al. 2012). Also LOH at 13q14.2 appears approximately three times more frequently in high-grade neuroendocrine lung tumours than in pulmonary carcinoids (Onuki et al. 1999).

Pulmonary carcinoids need to expand, although these tumours show a very low proliferation rate. However, the intrinsic apoptosis pathway, including *BCL2*, *BCL2L1* (Bcl-X) and *BAX* family genes, is more often inhibited in high-grade pulmonary NETs in comparison to carcinoids, and SCLCs in particular display very low apoptotic indices (Brambilla et al. 1996; Swarts et al. 2012). LCNECs show high (1-7%) apoptotic indices compared to SCLCs (<0.1%) (Brambilla et al. 1996; Swarts et al. 2012). Furthermore, an inversion in the Bax/Bcl-2 ratio towards cell survival (Bcl-2) in high-grade lung NETs has been reported, e.g., 90% in SCLCs compared to 5% in carcinoids (Brambilla et al. 1996; Swarts et al. 2012). Other studies showed comparable results, with an almost intact intrinsic apoptotic pathway in TCs, a moderately affected pathway in ACs and a largely disordered pathway in the high-grade NELCs (Swarts et al. 2012). Similar to expression of mutant p53, upregulation of Bcl-2 and downregulation of Bax, resulting in an inverted Bax/Bcl-2 ratio was observed in preneoplastic lesions adjacent to lung cancers (Brambilla et al. 1998; Gosney et al. 2011; Swarts et al. 2012).

1.6 Applied Detection Methods

A common and cost-effective method for long-term storage of tissues in the pathological routine diagnostic is formalin-fixation followed by paraffin embedding (FFPE). These FFPE tissues are the most prominent source of nucleic acids in pathological laboratories. This procedure makes it possible to connect the genetic

information of the samples with their clinical follow-up data and therefore provide the requirements for large-scale retrospective studies with extensive patient collectives.

During the fixation process, chemical modifications such as crosslinking and oxidative deamination of the nucleic acids occur, decreasing the reliability of the material for molecular biological analysis (Ibusuki et al. 2011). In addition, storage conditions like temperature, exposition to ultraviolet light and oxygen exposure affect the integrity of the nucleic acids (von Ahlfen et al. 2007; Ludyga et al. 2012). This led to intense discussions about FFPE material as a source for DNA and RNA, but recent studies have shown that FFPE can be used for reliable DNA and RNA investigations (von Ahlfen et al. 2007; Walter et al. 2013).

miRNA expression profiles can be screened in a broad manner through different methodical approaches, such as next generation sequencing (NGS), microarray hybridizations or quantitative polymerase chain reaction (qPCR) based screening methods.

Quantitative real-time PCR correlates exonuclease digestion-induced increase of fluorescence, triggered by the Förster resonance energy transfer (FRET) effect, with the initial quantity of nucleic acids of a specific target in the measured sample. Therefore, specific systems using probes (e.g., TaqMan® probes) complementary to the region of interest (ROI) are used. These probes are labelled with both a fluorophore (reporter) for detection and its counterpart fluorophore (quencher) proximate to each other to induce FRET. Digestion via the 5’ – 3’ exonuclease activity of the DNA-polymerase used leads to separation of the two fluorophores and therefore to the loss of FRET, resulting in measurable laser-induced fluorescence of the reporter fluorophore.

An additional problem caused by the small size of miRNA-molecules is the synthesis of the cDNA necessary for subsequent amplification. These cDNA-molecules have to be long enough to provide the space for hybridization of at least one primer and the real-time probe. Due to the short length of miRNA nucleotide sequences, normal cDNA-synthesis is not feasible for this application; a special, looped reverse transcriptase primer is needed. The additional loop structure elongates the miRNA-cDNA amplicon to a sufficient length during this process.

The NanoString nCounter technology is a robust, fast and reproducible technique with low costs enabling the detection of multiple molecular markers simultaneously (Geiss et al. 2008). A non-enzymatic, multiple sequence-specific probe assay is used to assess the number of targeted molecules. A capture probe tagged with biotin and a reporter probe with specific fluorescent dyes hybridise specifically to the target molecule. Each reporter probe contains a sequence-specific barcode labelled with six different fluorescent dyes. Excess probes are removed and the biotin of the capture probe is linked to streptavidin on a surface. All molecules are arranged in one direction to prevent false assignment. The fluorescent dyes are excited by a laser and photographic images are taken. The quantity of the detected barcodes is equal to the amount of molecules. Since there are many sequence-specific barcodes available, the method could be used for an 800-plex application. Measuring reference genes allows a relative quantification to determine gene expression. Personalized or standard probe sets are available, allowing customized application of the method. The beneficial feature of this colour-coded barcode technology is its repeatable measurement ability. Even though the fluorescent signal fades after each laser induction, the barcode sequence is still the same. This technology allows gene expression analysis, miRNA assessment and copy number variation (CNV) analysis

in a highly professional way, making it a superior method for validating results or even as a principal research method (Northcott et al. 2012).

Due to the increasing number of genetic variations relevant for prediction of therapeutic success of modern anti-cancer therapies, new sequencing methods are necessary to analyse multiple targets and/or samples simultaneously in a time- and cost-effective manner, thus resulting in the development of different NGS-platforms. Despite all the differences between these platforms, they all share the properties of analysing clonally amplified molecules. This results in an additional quantitative assessment of mutated alleles, even within an extensive wildtype background (Vollbrecht et al. 2013). To reach such sensitivity with conventional sequencing methods like Sanger, special preparation protocols like the COLD-PCR would be necessary (Mairinger et al. 2014).

During conventional Sanger or pyrosequencing, the ROI contained within the entire sample gets amplified. The measured signal represents the whole population. For NGS, individual nucleic acid molecules are immobilised and separated on a surface. Afterwards, these single spots, also called ‘clusters’, are clonally amplified directly at this spot and then sequenced in parallel. Therefore, the measured signal for each cluster represents a single allele; the sum of all clusters originating from one ROI represents the whole population of alleles in the proper stochastic proportion. The sequencing methods differ from platform to platform and range from sequencing by synthesis using removable terminators (MiSeq, Illumina, San Diego, CA, USA) and pyrosequencing (454, Roche Applied Sciences, Penzberg, Germany) to sequencing by ligases (SOLiD, Thermo Fisher Scientific, Waltham, Massachusetts, USA) and physical sequencing using semiconductors (Ion Torrent, Thermo Fisher Scientific).

Some of these high-throughput sequencing methods need masses of input material (e.g. 250ng gDNA for MiSeq TruSeq library preparation); however, preamplification methods like isothermal multiple displacement amplification (IMDA) can solve such problems for daily routine applications (Mairinger FD 2014).

Table 4 gives a technical summary of the detection methods used.

Table 4 Comparison of the different high-throughput methods used

Method	NanoString nCounter	TaqMan Array Human MicroRNA Cards	Illumina MiSeq
Input Material	DNA; RNA	RNA	DNA; RNA
Capacity	800-plex	759-plex	2-8 Gigabases
Sample preparation	none	cDNA synthesis	Bridge-PCR
Preparation duration	15 minutes-2 hours	≥ 2 hours	2 days - 1 week
Process duration	2 days	1.5 hours	1 day

1.7 Aims

Both pulmonary carcinoids and SCLCs have been previously reported to arise from serotonin producing Kulchitsky-type cells, currently known as pulmonary neuroendocrine cells (PNECs), which are the first cells to differentiate in the epithelium during lung development (Bensch et al. 1968; Warburton et al. 2000; Swarts et al. 2012). Nevertheless, lung carcinoids and high-grade neuroendocrine lung carcinomas show a very different clinical outcome, with a five-year overall survival of 92-100% for TCs and 61-88% for ACs, compared to 13-57% for LCNECs and 5% for SCLCs (Rossi et al. 2005; Travis 2010). Morphological differences

classify them as at least three different entities, termed carcinoids, LCNECs and SCLCs.

The studies summarized in this dissertation were conducted to examine whether neuroendocrine tumours of the lung are a distinct entity with different forms of differentiation or are different independent tumour entities. These tumours were also screened for possible biomarkers useful for diagnostic purposes, improving the current diagnostic tools and prognostic factors in this subset of tumours and potentially predicting the response to different chemotherapeutic regimes and small-molecule inhibitors for targeted tumour therapy.

2. Material and Methods

2.1 Patient Collective

Two hundred-one patient samples of primary pulmonary neuroendocrine tumours were collected including atypical and typical carcinoids as well as LCNEC and SCLC. All samples were resected between 2005 and 2012 at the Ruhrlandklinik, West German Lung Centre of the University Hospital Essen, Essen (NRW, Germany). Patient samples were recruited from the biobank-database of the Institute of Pathology of the University Hospital Essen (NRW, Germany). All samples were formalin-fixed and paraffin embedded (FFPE). A reevaluation of all samples was done by two experienced pathologists. Out of this collective, the 80 most representative specimens were used for all further analysis. Inclusion criteria were sufficient tumour material and a minimum of contamination by non-tumorous lymphocytic and stromal cells. The complete clinical data set and all IHC and qPCR-based parameters determined for diagnostic purposes were collected.

The collective encompassed 107 male and 94 female patients. The patients' age at time of diagnosis ranged from 19 to 85 years (median: 61; mean: 60). Forty-six patients were suffering from TC, 26 from AC, 57 from LCNEC and 72 from SCLC. TNM staging was performed according to the WHO classification guidelines (Travis et al. 2004). Forty-two tumours were classified as pT1, eleven as pT1a, three as pT1b, 38 as pT2, five as pT3, five as pT4 and two as pTX with no conclusive classification of the pathological stage. The evaluation of tumour grade showed 52 G1, 17 G2, 61 G3 and 47 G4 tumours. Lymph node status (N) was finally determined in 130 cases (87 pN0, 23 pN1, 17 pN2, 3 pN3) as well as the distant-metastasis

status (M) in all cases (191 M0 and 10 M1). Blood vessel (V) and lymph node status (L) could be conclusively clarified in 109 cases, 11 V1 and 16 L1 infiltrations could be found.

Follow up was collected in 75 cases. 36 were already deceased at the time of data collection. Clinical follow-up data concerning disease progression could be collected from 47 patients. Seventy-three of them showed progressive disease (PD), six stable disease (SD) and four partial remission (PR).

Additionally, 20 non-tumorous lung tissues obtained from resections in patients with pneumothorax were used as benign tissue controls. These 20 samples were recruited from the Department of Pathology, Helios Klinikum Emil von Behring, Berlin (Berlin, Germany), and were evaluated by an experienced pathologist (PD. Dr. T. Mairinger). Only samples without an inflammatory reaction served as normal controls.

.

2.2 Study Design

The studies included in this doctoral thesis were designed to clarify, whether pulmonary neuroendocrine tumours form one distinct group of tumours or have to be considered as different independent entities.

In order to address this question, 74 representative tumour specimens were used for sequencing analysis including TC, AC, LCNEC and SCLC. Sequencing was performed on a MiSeq instrument (Illumina, San Diego, CA, USA) using the TruSeq sequencing-chemistry (Illumina). A commercially available primer-pool covering the 221 most important mutation hotspots related to human malignant neoplasias was used (TruSeq Amplicon Cancer Panel, Illumina).

Additionally, mRNA-expression profiles of 80 tumour samples were determined. Measurement of mRNA profiles of 91 selected genes was performed by the

NanoString nCounter technology (NanoString Inc., Seattle, US). The majority of these patient samples is in concordance with the specimens used for SNP genotyping. These 91 genes include the most important regulators of angiogenesis, apoptosis, cell cycle regulation, DNA-repair mechanisms, folic acid metabolism, growth factor signalling, MET downstream signalling, MTOR pathway regulation, neuroendocrine differentiation, SOX signalling and tumour environment.

Three unequivocal samples of each tumour entity were chosen to be tested for their miRNA signature by 384 well TaqMan low-density array real-time qPCR. Special inclusion criteria for this analysis were well differentiated cells, high content of tumour tissue and a for each entity representative clinical course. Analysis were performed using the TaqMan Array Human MicroRNA Card A and TaqMan Array Human MicroRNA Card B v3.0 (both Applied Biosystems), respectively. These cards contain primer sets for 759 of the believed most important and most investigated miRNA species.

Finally, the same pulmonary neuroendocrine tumour samples were analysed via TaqMan qPCR (Applied Biosystems) for expression of the five most important subunits of the 26S proteasome.

The investigations conform to the principles outlined in the declaration of Helsinki and were approved by the ethical committee of the University Hospital of Essen (ID: 13-5382-BO) and for the patients from Berlin, used for control-purposes, informed consent was obtained.

2.3 Parallel Sequencing by Synthesis

Procedure and Panel Design

Sample preparation was done using the TruSeq Amplicon - Cancer Panel (Illumina Inc., San Diego, CA, USA) followed by sequencing on the MiSeq Personal Sequencer (Illumina) according the protocols provided by the manufacturer. The Cancer Panel covers 48 tumour-relevant genes including 221 mutation hotspots. The list of these genes is summarised in table 5.

Table 5 Summary of investigated genes provided by the TruSeq Amplicon-Cancer Panel.

ABL1	*AKT1*	*ALK*	*APC*	*ATM*	*BRAF*	*CDH1*	*CDKN2A*
CSF1R	*CTNNB1*	*EGFR*	*ERBB2*	*ERBB4*	*FBXW7*	*FGFR1*	*FGFR2*
FGFR3	*FLT3*	*GNA11*	*GNAQ*	*GNAS*	*HNF1A*	*HRAS*	*IDH1*
JAK2	*JAK3*	*KDR*	*KIT*	*KRAS*	*MET*	*MLH1*	*MPL*
NOTCH1	*NPM1*	*NRAS*	*PDGFRA*	*PIK3CA*	*PTEN*	*PTPN11*	*RB1*
RET	*SMAD4*	*SMARCB1*	*SMO*	*SRC*	*STK11*	*TP53*	*VHL*

DNA Extraction and Library Preparation

For DNA-isolation FFPE tissue was used. Tumour tissue blocks were cut by a microtome Cool Cut HM 355S (MICROM International, Walldorf, Germany) to generate 4 µm thick slides. Three to five paraffin tissue slides per sample were deparaffinised with xylene prior to DNA extraction. Genomic DNA was isolated via Maxwell® 16 Research (Promega Corporation, Madison, USA) as recommended by the manufacturer. Subsequently, DNA quantification was performed by using the Nanodrop ND-1000 (PEQLAB Biotechnologie GmbH, Erlangen, Germany) and Qubit 2.0 (Life Technologies, Carlsbad, USA). Samples of isolated gDNA were prepared according to the TrueSeq Custom Amplicon – Library Preparation guide. Prior

sequencing, constructed library pools were denaturised with NaOH leading to a final concentration of 8 mM NaOH. Additionally, a TruSeq Cancer Amplicon (TSCA)-control was spiked into each library pool. A Sample Sheet was created with the Illumina Experiment Manager software (Illumina).

Library Construction and Sequencing

Paired-end sequencing (2x 150 base-pairs, 302 cycles in total) was performed with eight index reads and MiSeq v2 chemistry. Each cartridge (300 cycles, Illumina) was loaded with a library pools containing 23 or 24 samples and control DNA (TrueSeq Control Amplicon (TSCA), Illumina) to achieve a calculative mean coverage of 800-1000x.

Alignment of Raw Reads and Preliminary Analysis

FastQ-files were generated by the MiSeq reporter software and data sets were aligned against the human genome (Hg19). For analysis of the aligned reads including variant calling, the software Avadis NGS (Strand Scientific Intelligence, California, USA) was used. Reads with a quality score < 30 were discarded by the used algorithm. Detected nucleotide changes were checked for known variants using the db135SNP database. Additionally data filtering was done by excluding variants with less than 25 effective reads (total reads*(percent variant reads/100)) or below 10% variant reads. Afterwards, synonymous variants were removed. The samples were subdivided into tumour types and for every investigated gene a basic statistical analysis was done (sum and mean value of mutations and sum, mean value and frequency of variants for every tumour entity, respectively).

2.4 Gene Expression Profiling by NanoString Technology

RNA Extraction and RNA Integrity Assessment

Three to five paraffin sections per sample were deparaffinised with xylene prior to RNA extraction using the miRNeasy FFPE kit (Qiagen, Hilden Germany) as recommended by the manufacturer, using adapted times and volumes (e.g. overnight digestion). RNA concentration was measured using a Nanodrop 1000 instrument (Nanodrop, PEQLab Biotechnologie GmbH, Erlangen, Germany). RNA integrity was assessed via RIN-values using an Agilent 2100 Bioanalyzer (Agilent, Santa Clara, CA, US) at the NanoString nCounter Core Facility at the University of Heidelberg, Germany. Smear analysis was performed using the Agilent 2100 expert software to determine the proportion of RNA ≥300 nucleotides within a given sample.

RNA not immediately used was stored at –20°C until use.

NanoString CodeSet Design and Expression Quantification

Important genes of different tumour pathways and genes involved in neuroendocrine differentiation were included in the custom CodeSet. The CodeSet was designed to consist of a total of 91 genes with different signature genes for each subgroup. Investigated genes and corresponding pathways are summarised as follows: SOX signalling *(MYB, MYBBP1A, OCT-4, PAX6, PCDHB, RBP1, SDCBP, SOX2, SOX4, SOX11, TEAD2*); MET pathway (*GAB1, GRB2, MET, MST1R, PAX5*); MTOR signalling (*MTOR, RHOA, RICTOR, RPTOR*); angiogenesis (*CRHR2, FIGF, FLT4, HIF1A, KDR, MMP3*); apoptosis (*ASCL1, BAX, BCL2, CASP-8, CASP-10, FAS, MDM2, TP53, PNN*); neuroendocrine differentiation (*CHGA, GABBR2, NCAM1, NTS, RTN1, SEMA3B, SYP*); folate metabolism (*ATIC, DHFR, FOLR1, FPGS, GART, GGT1, SLC19A1, TYMS*); DNA-repair (*ERCC1, MLH1, MSH2, MSH6, XRCC1*); cell cycle regulation (*CCND1, CCNE1, CDK1, CDK2, CDK4, CDK6, CDKN1A, CDKN1B,*

CDKN2A, MIB-1); tumour environment (*LDHA, LDHB, LDHC, MAN2A1, MAN2B1, MAN2C1, TKTL1*); growth factors (GF), GF-receptors and downstream signalling (*IGF-1, IGF-2, MET, EGFR, FGFR1, AKT1, ALK, PTEN*) and miscellaneous (*CAT, CYP1A1, FN1, MDM2, NES, NKX21, TP53; SOD1, STK11, TWSG1, UCHL1*). Three reference genes (*ACTB, GAPDH*, and *HPRT1*) were also included in the CodeSet for biological normalisation purposes. Probe sets for each gene in the CodeSet were designed and synthesised by NanoString Technologies. All designed Probe Sets were re-evaluated using the BLAST-Algorithm (Basic Local Alignment Search Tool). An overview of all targets is given in table 6.

Table 6 Summary of investigated genes involved in different pathways or cellular mechanisms.

Cellular mechanism	Gene
Angiogenesis	*CRHR2, FIGF, FLT4, HIF1A, KDR, MMP3*
Apoptosis	*ASCL1, BAX, BCL2, CASP-8, CASP-10, FAS, MDM2, TP53, PNN*
Cell cycle regulation	*CCND1, CCNE1, CDK1, CDK2, CDK4, CDK6, CDKN1A, CDKN1B, CDKN2A, MIB-1*
DNA-repair	*ERCC1, MLH1, MSH2, MSH6, XRCC1*
Folate metabolism	*ATIC, DHFR, FOLR1, FPGS, GART, GGT1, SLC19A1, TYMS*
Growth factors (GF), GF-receptors and downstream signalling	*IGF-1, IGF-2, MET, EGFR, FGFR1, AKT1, ALK, PTEN*
Reference genes	*ACTB, GAPDH, HPRT1*
MET pathway	*GAB1, GRB2, MET, MST1R, PAX5*
Miscellaneous	*CAT, CYP1A1, FN1, NES, NKX21, SOD1, STK11, TWSG1, UCHL1*
MTOR signalling	*MTOR, RHOA, RICTOR, RPTOR*
Neuroendocrine differentiation	*CHGA, GABBR2, NCAM1, NTS, RTN1, SEMA3B, SYP*
SOX signalling	*MYB, MYBBP1A, OCT-4, PAX6, PCDHB, RBP1, SDCBP, SOX2, SOX4, SOX11, TEAD2*
Tumour environment	*LDHA, LDHB, LDHC, MAN2A1, MAN2B1, MAN2C1, TKTL1*

Total RNA (100 ng) including miRNAs originating from FFPE material was hybridised overnight and afterwards analysed on the DigitalAnalyzer (NanoString).

NanoString Data Processing

Raw NanoString counts for each gene were subjected to a technical normalisation using the counts obtained for positive control probe sets prior to a biological normalisation using the three reference genes included in the CodeSet.

2.5 TaqMan® Array Human MicroRNA Cards

RNA Extraction and RNA Integrity Assessment

For details according to the RNA extraction and RNA integrity assessment please refer to 2.4.

cDNA Synthesis and Preamplification

For cDNA synthesis the Megaplex RT Human Primer Pools A and B (Applied Biosystems, Foster City, CA, USA) in combination with the TaqMan miRNA Reverse Transcription Kit (Applied Biosystems) were used. cDNA not immediately used was stored at -20°C. Preamplification was also conducted with Megaplex Preamplification Primer Pools A and B (Applied Biosystems) in combination with the TaqMan miRNA Preamplification Kit (Applied Biosystems). Preamplified samples were stored at -20°C until usage.

TaqMan real-time qPCR for miRNA Expression Determination

For 384 well TaqMan low-density array real-time qPCR, preamplification products were pressed through microchannels into wells fixed in the card, preloaded with immobilised, dehydrated target-specific primer-probe pairs. PCR analysis was run on the ABI PRISM 7900 System. Analysis was done with TaqMan Array Human MicroRNA Card A and TaqMan Array Human MicroRNA Card B v3.0 (both Applied Biosystems), respectively. Quantitative PCR was performed using the ready-to-use TaqMan Universal PCR Master Mix (Applied Biosystems). Of note, qPCR analysis was performed in concordance to the MIQE-guidelines (Bustin et al. 2009).

Bioinformatical Data Analysis

miRNA target-sites were descriptively determined using the miRanda-database (miRanda), inhibition scores were calculated by the mirSVR algorithm. The ten most differentially regulated miRNA-targets in the various neuroendocrine tumours were selected for further analysis. In addition, all targets with a score higher than 2.00 were selected for the identification of possibly deregulated pathways. Associated pathways, which were affected by differences in the miRNA expression levels, were discovered and, if possible, correlated to gene- and protein expression levels available. Additionally, a gene ontology (GO)-term analysis to classify differentially regulated biological processes was performed.

Databases used for pathway identification were uniprot.org and the NCBI website gene-search and BioSystems-search, respectively.

2.6 Determination of 26S-Proteasome Genexpression via qPCR

The subunits α1 and α5, β4 and β5 (*PSMA1, PSMA5, PSMB4, PSMB5*) as well as δ1, also known as *RPN2*, which is part of the proteasome capping structure, of the 26S-Proteasome were investigated. To evaluate the expression levels of the subunits of the 26S proteasome in the pulmonary neuroendocrine tumours, TaqMan real-time qPCR was applied. Twenty samples of each entity as well as 20 benign samples represented by spontaneous pneumothorax tissue of otherwise healthy patients were analysed.

RNA Extraction and RNA Integrity Assessment

For details according to the RNA extraction and RNA integrity assessment please refer to 2.4.

cDNA Synthesis

For cDNA synthesis the "iScript® Select cDNA Synthesis Kit" (BioRad, Hercules, CA, USA) was used. cDNA synthesis was done with the total RNA-samples. cDNA not immediately used was stored at –20°C. Ct-values were normalised to the mean of two different endogenous reference genes, namely β-actin (*ACTB*) and glyceraldehyde-3-phosphate dehydrogenase (*GAPDH*).

TaqMan real-time qPCR Analysis

Relative cDNA quantification of *PSMA1, PSMA5, PSMB4, PSMB5* and *PSMD1* and two reference genes (*GAPDH* and *ACTB*) as internal reference for biological normalisation were measured. For qPCR, commercial TaqMan® Gene Expression-assays (Applied Biosystems®, AoD, Assay-ID: Hs03023943-g1, Hs01027362-g1, Hs00932059-m1, Hs01123843-g1, Hs01002826-g1, Hs00160631-m1) with optimised primer and probe concentrations were used. 10µl was sufficient as total reaction volume. The AoD were chosen because of their short amplicon size (90 to 110bp) to overcome FFPE-specific problems and additionally, they spanned exon-exon boundaries. Each target was measured in triplicate.

For assay validation, standard curves were calculated using six different concentrations of a pool out of all isolated RNAs. Calculation was performed automatically with the Roche® LightCycler® 480 II data analysis program.

qPCR analysis was performed in concordance to the MIQE-guidelines (Bustin et al. 2009).

Preliminary Data Analysis

qPCR and determination of Ct-values was performed on a Roche® LightCycler® 480 II. Ct-values were calculated by the fit-points method. For consecutive statistical analysis, $2^{-\Delta\Delta Ct}$ values were calculated in relation to the benign control samples.

2.7 Immunohistochemistry

For immunohistochemical characterisation staining of whole tissue slides with antibodies directed against Pan-Cytokeratin (DAKO, Clone MNF116, Hamburg, Germany), CD56 (Zytomed, clone RCD56, Berlin, Germany), ChromA (Novocastra, clone 5H7, Wetzlar, Germany) and TTF-1 (DAKO, Clone 8G7G3/1, Hamburg, Germany) was performed. The proliferation index was determined by staining with antibodies directed against the proliferation associated marker Ki67 (Zytomed, clone K-2, Berlin, Germany) using a fully automated stainer (Dako AutostainerPlus, Copenhagen, Denmark). Apoptosis was determined by IHC against cleaved caspase 3 (Cell Signalling, Beverly, MA, USA). 26S-Proteasome expression was determined by IHC directed against *PSMB4* (Sigma Aldrich, polyclonal antibody, Taufkirchen, Germany).

An overview of the different pretreatment protocols and the dilution factors is given in Table 7.

Table 7 Pretreatment protocols and dilutions of the different used antibodies

Company	Target	Clone	Temperature	pH	Pretreatment	Incubation	Dilution
DAKO	Pan-Cytokeratin	MNF116	37°C	-	4’ Pronase	30’	1:1000
Zytomed	NCAM	RCD56	98°C	6.0	30’ Citrate	30’	1:1000
Novocastra	CHGA	5H7	98°C	6.0	20’ Citrate	30’	1:100
DAKO	TTF1	8G7G3/1	30°C	9.0	20’ EDTA	30’	1:1000
Zytomed	TKI67	K-2	98°C	6.0	30’ Citrate	30’	1:2000
Cell Signalling	CASP3	polyclonal	98°C	6.0	20’ Citrate	60’	1:100
Sigma Aldrich	PSMB4	polyclonal	30°C	9.0	20’EDTA	60’	1:20

Preliminary Data Analysis

The immunoexpression of Ki67 was quantified by applying an internally evaluated four stage score (0= 0%, 1 ≤10%, 2 = 11 - 50%, 3 ≥ 50% stained cells), whereas cleaved caspase was scored by a different system (0 = 0%, 1 ≤ 5%, 2 = 5-10%, 3 ≥ 10%).

Pan-Cytokeratin, CD56 (*NCAM1*), *CHGA* and *TTF1* immunohistochemistry was determined just by presence (positive) or absence (negative). For *PSMB4* immunohistochemical expression, the H-Score was first preferred. Due to the universal and strong staining of all tumours against *PSMB4*, also its expression was determined in a dichotomous way.

2.8 Statistical Analysis

To determine a correlation between affected genes and clinical parameters, the R statistical software environment (The R Foundation for Statistical Computing, Institute for Statistics and Mathematics, Vienna, Austria; v2.15.2) was used. Correlation analysis was performed with a customized algorithm for the R software.

The exact Wilcoxon Mann-Whitney Rank Sum test was used to test associations between miRNA expression and dichotomous variables (e.g., gender). For the analysis of possible associations between miRNA and clinical variables (age, age of blocks, etc.), a Spearman's rank correlation test was performed. Additionally, Spearman's rank correlation test was done to test associations between tumour type and expression levels of different miRNAs.

Similar to the analysis of miRNA-expression, association between mRNA-counts and $2^{-\Delta\Delta Ct}$-values, respectively, and linear vectors (clinical variables) were calculated using the Spearman's rank correlation rho test.

For dichotomous features regarding gender and gene expression level, the Wilcoxon Mann-Whitney rank sum test was applied.

For variables with more than two categories the Kruskal-Wallis test was performed.

Overall survival (OS) and progression free survival (PFS) were calculated using the Wald-test, likelihood-ratio test and Score (logrank) test.

To check correlations between protein expression levels and variables represented by linear vectors, the Spearman's rank correlation rho test was chosen again. The Spearman's rank correlation test was done to test associations between gene expression and IHC staining scores.

The exact Wilcoxon Mann-Witney Rank Sum test was used to test associations between protein expression and dichotomous variables (gender).

Survival analysis for overall and progression-free survival was done by Cox-regression (COXPH-model), statistical significance was determined using Likelihood ratio test, Wald test and Score (logrank) test.

For illustration of the overall survival (OS) and progression-free survival (PFS), Kaplan-Meier curves were generated.

For association analysis of the number of variants occurring in each gene and the tumour entity, the Kruskal-Wallis Rank Sum Test was used. The Kruskal-Wallis test was also used to analyse the association of mutations occurring in a gene and tumour type.

Because the mutation-status of each gene leads to dichotomous factors (yes/no), association between genetic variants and clinical variables were calculated using the exact Wilcoxon Mann-Witney Rank Sum test.

For additional dichotomous variables like patient's gender and number of mutations occurring, the exact Wilcoxon Mann-Witney Rank Sum test was used.

Correlations between linear vectors (e.g. clinical variables) and count of mutations were assessed by Spearman's rank correlation rho test.

Survival analysis for mutation-dependent overall and progression-free survival was done by Cox-regression (COXPH-model), statistical significance was determined using Likelihood ratio test, Wald test and Score (logrank) test.

The results concerning survival were graphically illustrated by Kaplan-Meier curves.

All calculated p-values were corrected by a Bonferroni-Correction for multiple testing. Statistical significance was assigned as $p \leq 0.05$.

3. Results

miRNA Expression Profiling

qPCR analysis was accomplished successfully in all cases. The endogenous control was detected between Ct 12.5 and 13.9 on both plates. All further analysis was performed using log(miR)-values.

In the complete collective including the four entities (AC, TC, SCLC, LCNEC), 44 miRNAs with significantly different expression were identified, eleven of them showing highly significant correlation with a p-value <0.01. Seven showed an inverse correlation to aggressiveness of the tumour (miR-22, miR-29a, miR29b, miR-29c, miR-367*; miR-504, miR-513C, miR-1200), the remaining a direct correlation (miR-18a; miR-15b*, miR-335*, miR-1201). Data are summarised in Table 8.

Table 8 Detected significant association of miRNA expression with tumour type. Highly significant miRNAs are bolded. Data are presented in Figure 9 and 18.

miRNA	Tumour Type	
	p-value	rho
hsa-miR-15b	0.047	0.5830
hsa-miR-18a	**0.007**	**0.7341**
hsa-miR-22	**0.004**	**-0.7557**
hsa-miR-27b	0.037	-0.6046
hsa-miR-29a	**0.009**	**-0.7125**
hsa-miR-29b	**0.009**	**-0.7125**
hsa-miR-29c	**0.004**	**-0.7557**
hsa-miR-107	0.037	0.6046
hsa-miR-125b	0.047	-0.5830
hsa-miR-127	0.037	-0.6046
hsa-miR-129	0.013	-0.6909
hsa-miR-132	0.017	-0.6693
hsa-miR-136	0.037	-0.6046
hsa-miR-143	0.023	-0.6478
hsa-miR-154	0.037	-0.6046
hsa-miR-216b	0.013	0.6909
hsa-miR-217	0.047	0.5830
hsa-miR-328	0.023	-0.6478
hsa-miR-338-3p	0.023	-0.6478
hsa-miR-375	0.037	-0.6046
hsa-miR-455	0.037	-0.6046
hsa-miR-485-5p	0.029	-0.6262
hsa-miR-490	0.037	-0.6046
hsa-miR-504	**0.009**	**-0.7125**
hsa-miR-548b-5p	0.047	-0.5830
hsa-miR-653	0.023	-0.6478
hsa-miR-874	0.023	-0.6478
hsa-miR-569	0.013	-0.6909
hsa-miR-634	0.047	-0.5830
hsa-miR-645	0.023	0.6478
hsa-miR-29c*	0.037	-0.6046
hsa-miR-770-5p	0.037	-0.6046
hsa-miR-31*	0.037	0.6046
hsa-miR-130b*	0.029	0.6262
hsa-miR-367*	**0.003**	**-0.7773**
hsa-miR-15b*	**0.003**	**0.7773**
hsa-miR-335*	**0.007**	**0.7341**
hsa-miR-545*	0.023	0.6478
hsa-miR-218-2*	0.047	-0.5830
hsa-miR-513C	**0.007**	**-0.7341**
hsa-miR-1201	**0.003**	**0.7773**
hsa-miR-1292	0.047	0.5830
hsa-miR-1200	0.029	-0.6262
hsa-miR-1248	0.047	0.5830

miR-18a is increasing directly with more aggressive forms of the NE-tumours (from TC – AC – LCNEC – SCLC), showing a 100-fold higher expression in high-grade NE pulmonary tumours than in carcinoids, this association can also be observed for miR-15b* and miR-335*. miR-22 expression decreases significantly more than 10-50 folds from typical to atypical carcinoids and LCNEC (showing an equal expression levels as AC) and 50-100 fold to SCLC. Furthermore, miR-29a, miR-29b and miR-29c expression levels decreases with increasing biological aggressiveness of the given neuroendocrine tumour, all showing the same expression levels in both carcinoids and a clear decrease regarding LCNEC and furthermore in SCLC (figure 10). miR-504 expression seems to be constant and equal in TC, AC and LCNEC, but is totally lost in SCLC. miR-367* shows a similar pattern to miR-22, but showing greater differences (TC/AC: approx. 1000-fold; LCNEC/SCLC: approx. 1000-fold). miR-513C expression can be detected in TC only and is lost or decreases to a minimal level in the remaining entities. miR-1201 shows a stable level in TC and AC and an increased expression in high-grade NELC, and presents with higher expression in LCNEC than in SCLC.

The data are depicted as boxplots in Figure 9.

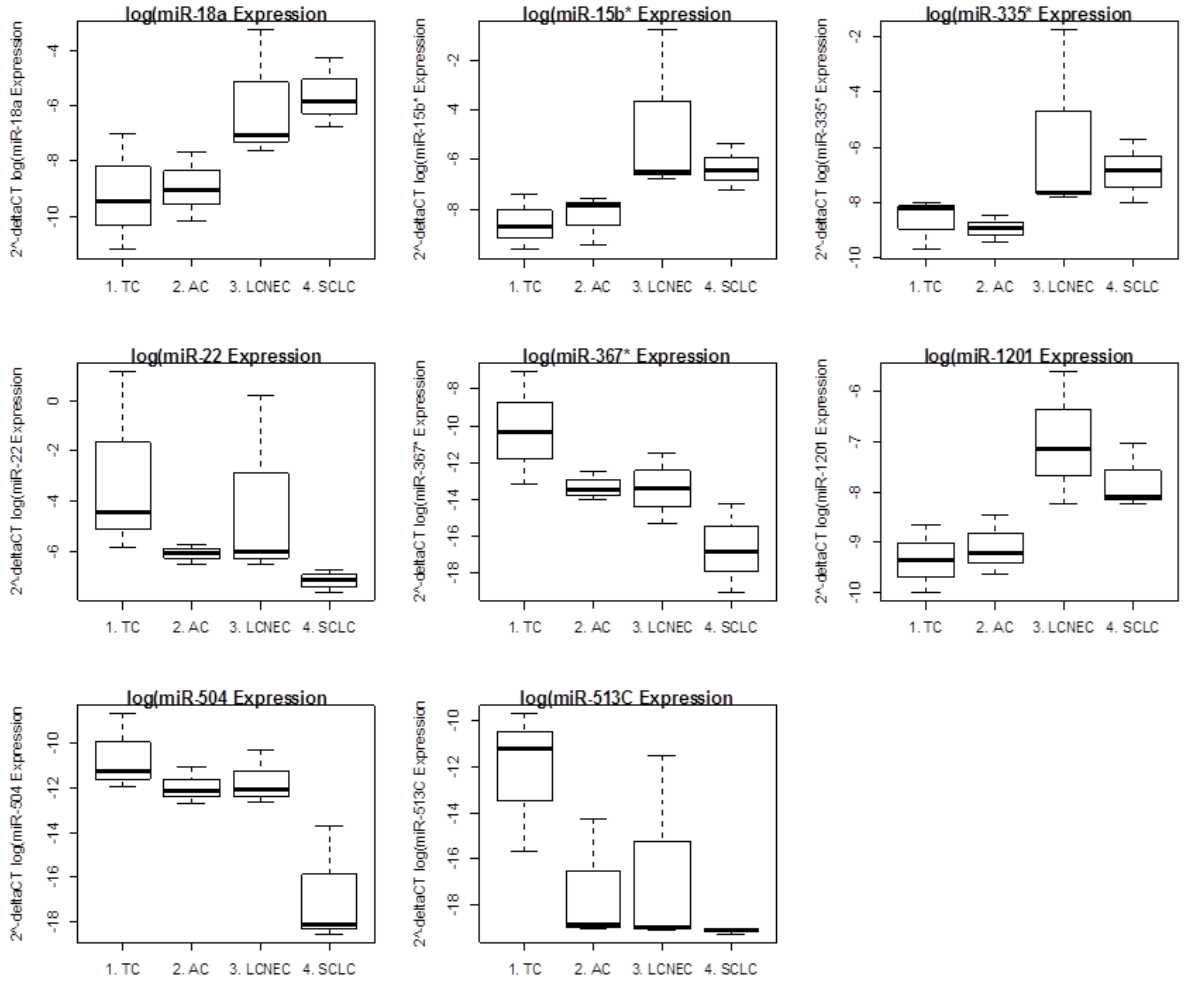

Figure 9 Boxplots depicting significant differences in miRNA expression in neuroendocrine pulmonary tumours. Expression of miR-18a and miR-15b is increasing with increasing malignancy of the tumour. miR-335* and miR-1201 profiles show a decreased expression in carcinoids compared to the neuroendocrine carcinomas. For miR-22 and miR-367* increased malignancy is associated with decreased expression. In SCLC, miR-504 expression is dramatically decreased and for miR-513C, TC show the highest expression.*

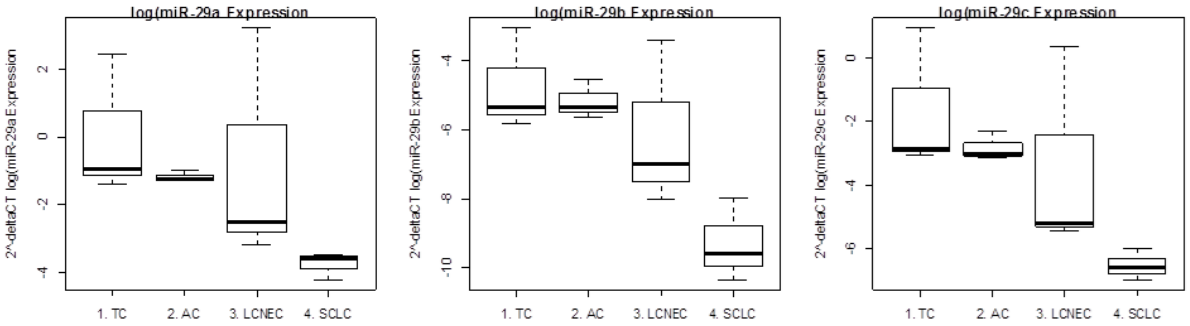

Figure 10 Boxplots showing the expression profiles of the miR-29 family displaying similar patterns between the different tumour entities. Decreasing expression of miR-29a-c correlates with increasing malignancy of the tumour.

For survival analysis, the COXPH-model was used. Three patients (one suffering from LCNEC and two suffering from SCLC) died due to cancer related reasons; none of the carcinoid cases had influenced the survival status of the investigated patients. Absolute survival time including follow-up time of censored patients ranged from less than one month up to more than six years.

We identified 45 micro-RNAs to have a statistically significant impact on survival in our collective, determined by the Likelihood ratio test and Score (logrank) test. Nine of the miRNAs were highly significant in both tests (let-7d; miR-139-5p; miR-197; miR-301; miR-576-5p; miR-582-5p; miR-448; miR-340*; miR-1286), five showed statistical significance when the Wald test was applied (let-7d; miR-19; miR-576-5p; miR-340*; miR-1286). Data are summarised in Table 9.

Table 9 Calculated p-values of miRNA expression regarding OS using COXPH. Highly significant miRNAs are bolded; most significant miRNAs are highlighted grey.

miRNA	Overall Survival p-Value (Likelihood ratio test)	p-Value (Score logrank test)	p-Value (Wald test)
hsa-let-7d	**0.00665**	**0.06477**	**0.00036**
hsa-miR-10b	**0.00668**	**0.02856**	**-**
hsa-miR-17	0.03828	0.04790	-
hsa-miR-19b	0.04567	0.03092	-
hsa-miR-20b	0.04335	0.03399	-
hsa-miR-30c	0.01968	0.01902	-
hsa-miR-95	0.03767	0.01995	-
hsa-miR-106b	0.02492	0.02584	-
hsa-miR-130b	0.04031	0.02232	-
hsa-miR-138	**0.00660**	**0.03985**	**-**
hsa-miR-139-5p	**0.00660**	**0.00628**	**-**
hsa-miR-149	0.02027	0.01258	0.02581
hsa-miR-196b	**0.00660**	**0.03519**	**-**
hsa-miR-197	**0.00689**	**0.00345**	**0.00317**
hsa-miR-216a	0.02496	0.03505	-
hsa-miR-216b	0.02190	0.03537	-
hsa-miR-301	**0.00925**	**0.01598**	**-**
hsa-miR-331	**0.00660**	**0.03736**	**-**
hsa-miR-340	0.03975	0.04009	-
hsa-miR-374	0.02849	0.03736	-
hsa-miR-454	0.02168	0.33980	-
hsa-miR-484	**0.00661**	**0.02801**	**-**
hsa-miR-525-3p	0.02521	0.04496	-
hsa-miR-548d	0.02624	0.01665	-
hsa-miR-576-5p	**0.00828**	**0.01071**	**0.00029**
hsa-miR-582-5p	**0.00660**	**0.00702**	**-**
hsa-miR-448	**0.00660**	**0.00580**	**-**
hsa-miR-30a-5p	**0.00662**	**0.01558**	**-**
hsa-miR-378	**0.00660**	**0.03319**	**-**
hsa-miR-7*	**0.00661**	**0.02938**	**-**
hsa-miR-550	0.03544	0.04218	-
hsa-miR-454*	0.01438	0.02284	-
hsa-miR-130b*	**0.00661**	**0.03563**	**-**
hsa-miR-377*	0.01508	0.03093	-
hsa-miR-936	0.04560	0.03846	-
hsa-miR-340*	**0.00917**	**0.00799**	**0.00198**
hsa-miR-200b*	**0.00669**	**0.03058**	**-**
hsa-miR-10b*	**0.00661**	**0.01125**	**-**
hsa-miR-181a-2*	0.04969	0.03275	-
hsa-miR-106b*	**0.00763**	**0.04640**	**-**
hsa-miR-1286	**0.00668**	**0.00994**	**<0.00001**
hsa-miR-548M	0.02234	0.02838	-
hsa-miR-1271	0.01600	0.04631	-
hsa-miR-1292	**0.00672**	**0.04997**	**-**
hsa-miR-1293	0.04943	0.01999	-

With increasing malignant biological behaviour of pulmonary neuroendocrine tumours, several cellular pathways are upregulated by differential expression of miRNAs. The pathway strongest affected is the ERK-MAPK signalling pathway. Also the PI3K-pathway, involved in different cellular processes, shows significant differences between the four tumour types of pulmonary neuroendocrine tumours. Furthermore, the TGF-beta pathway is becoming activated with increasing metastatic potential, suggesting a causal link between increased angiogenesis and metastasis/malignancy in pulmonary neuroendocrine tumours. In addition, the Wnt-signalling pathway, NFkB pathway, JNK-MAPK signalling network as well as the MTOR-complex associated signalling is differentially regulated via miRNA expression in these tumours (Figure 11).

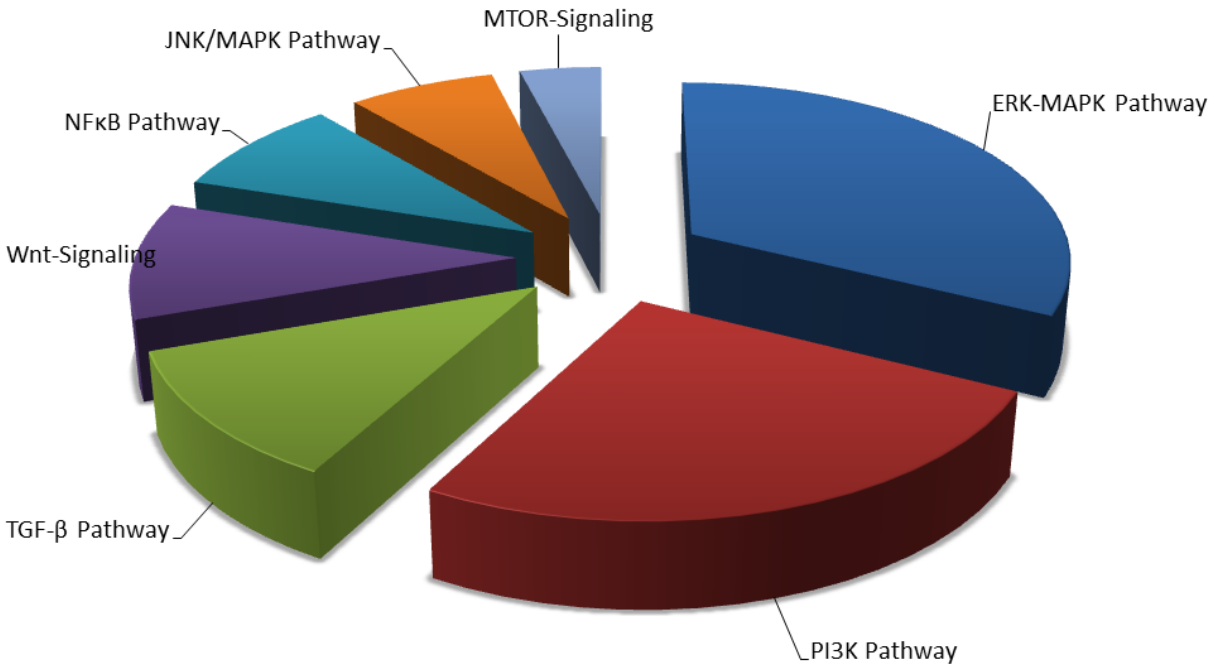

Figure 11 Pie chart showing results of the pathway analysis in pulmonary neuroendocrine tumours: The pathways showing the most prominent alterations by miRNAs were shown to be the MAPK pathway followed by PI3K- and TGF-β-pathway. Aberrations could also be found for Wnt-signalling, NFκB-pathway, JNK-pathway and mTOR-signalling.

The GO-analysis showed 256 hits for regulation of gene expression and transcriptional regulation. The second major differentially regulated cellular processes

were cell cycle regulation (139 hits) followed by development and differentiation of neuronal development (134 hits). In addition, proliferation (125 hits), immune response (105 hits), apoptosis (96 hits) and DNA-damage response (59 hits) are strongly deregulated in this collective of neuroendocrine lung tumours. Furthermore, growth factors as well as growth-factor receptors and their pathways were observed to be affected (53 hits). Less significant, but also differentially regulated were the ion carrier-dependent uptake of compounds as well as angiogenesis (48 and 42 hits, respectively). Moreover, it is of note that a strongly altered regulation of the expression of structural cell compounds (42 hits), especially of collagens (19 hits) was found. The data are illustrated in Figure 12.

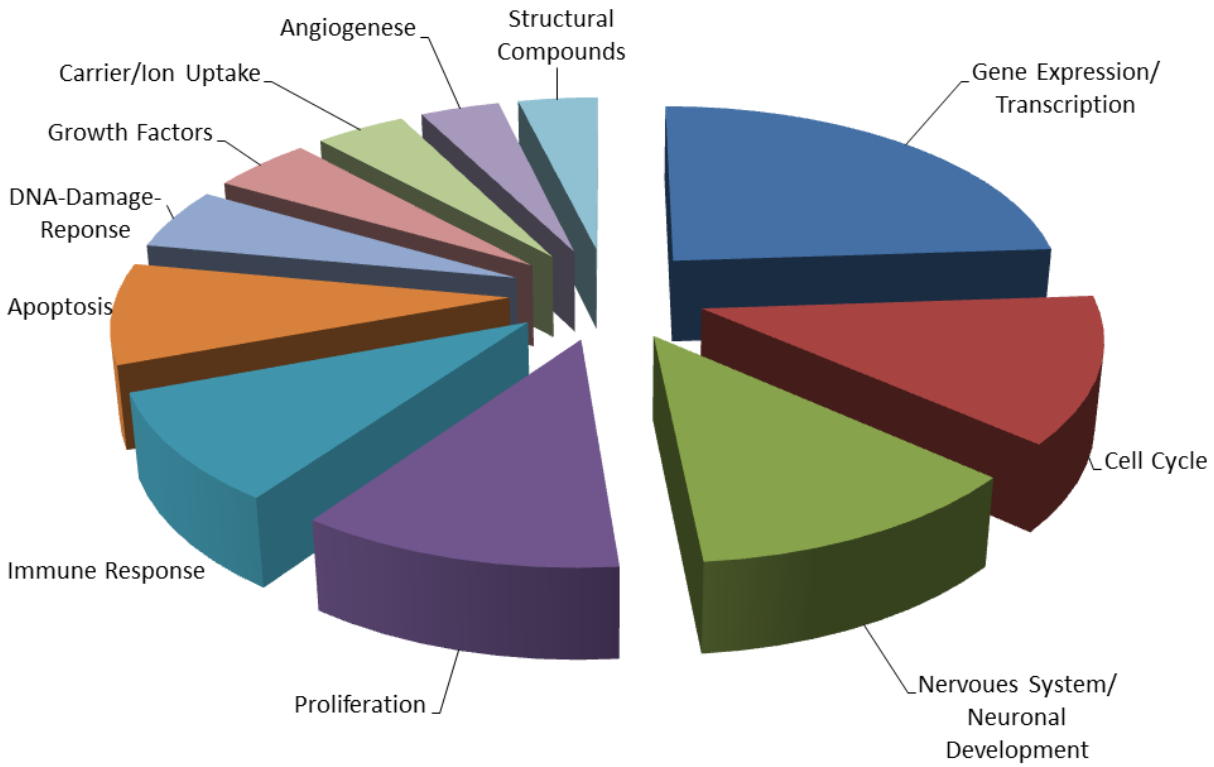

Figure 12 Illustrated results of the GO analysis presenting most hits in gene expression and transcription. Similar hits for cell cycle and nervous system were found. Following, with decreasing impact, also proliferation, immune response, apoptosis, DNA-damage-response, growth factors and signalling, carriers, angiogenesis and expression of structural compounds is affected by differential miRNA expression.

mRNA Expression Profiling Results

The mRNA expression analysis showed 48 significant correlations with tumour type. Sixteen most significant (p≤0.001), 20 highly significant (p≤0.01) and 12 significant (p≤0.05) candidates were identified. Most significant were *BCL2, CDK6, CDKN2A, CHGA, FOLR1, FPGS, GAB1, MAN2C1, MLH1, PAX6, PNN, RTN1, SOX11, SOX4, SYP* and *TYMS*. Highly significant values were found for *ASCL1, CASP8, CAT, CCND1, CCNE1, CDK2, EGFR, ERCC1, FIGF, FLT4, MAN2A1, MSH6, NCAM1, PAX5, RBP1, RICTOR, RPTOR, SEMA3B, STK11* and *UCHL1*. Furthermore, the *BCL2-BAX* ratio was correlated with tumour type and showed a highly significant value (p=0.0064; Chi2 12.3399). The results are summarised in Table 10.

Table 10 Significant p-values of mRNA expression correlating with tumour type calculated by the Kruskal Wallis Rank Sum Test are shown. Highly significant mRNAs are bolded; most significant mRNAs are highlighted grey. Highlighted genes are presented in boxplots in Figure 13.

mRNA vs. type	p-Wert	Chi^2	dF
AKT1	0.01228	10.90060	3
ASCL1	**0.00862**	**11.66480**	**3**
BCL2	**0.00050**	**17.73310**	**3**
CASP8	**0.00279**	**14.08570**	**3**
CAT	**0.00681**	**12.17440**	**3**
CCND1	**0.00179**	**15.02800**	**3**
CCNE1	**0.00452**	**13.05300**	**3**
CDK1	0.01624	10.29250	3
CDK2	**0.00200**	**14.79270**	**3**
CDK6	**0.00004**	**23.18880**	**3**
CDKN1A	0.03464	8.62980	3
CDKN2A	**0.00043**	**18.02390**	**3**
CHGA	**<< 0.00001**	**36.81580**	**3**
EGFR	**0.00437**	**13.12570**	**3**
ERCC1	**0.00210**	**14.69170**	**3**
FGFR1	0.03008	8.94120	3
FIGF	**0.00957**	**11.43970**	**3**
FLT4	**0.00539**	**12.67890**	**3**
FN1	0.02519	9.33160	3
FOLR1	**0.00001**	**27.16270**	**3**
FPGS	**<<0.00001**	**29.24420**	**3**
GAB1	**0.00069**	**17.03900**	**3**
GGT1	0.02889	9.03030	3
MAN2A1	**0.00537**	**12.68520**	**3**
MAN2C1	**0.00051**	**17.67760**	**3**
MLH1	**0.00085**	**16.61270**	**3**
MSH6	**0.00644**	**12.29540**	**3**
NCAM1	**0.00843**	**11.71320**	**3**
NKX21	0.01000	11.34550	3
PAX5	**0.00584**	**12.50620**	**3**
PAX6	**0.00022**	**19.45360**	**3**
PNN	**0.00072**	**16.95160**	**3**
PTEN	0.01641	10.26890	3
RBP1	**0.00567**	**12.56690**	**3**
RHOA	0.02677	9.19820	3
RICTOR	**0.00554**	**12.61750**	**3**
RPTOR	**0.00299**	**13.93940**	**3**
RTN1	**0.00070**	**17.03140**	**3**
SEMA3B	**0.00597**	**12.45920**	**3**
SOD1	0.01321	10.74120	3
SOX11	**<<0.00001**	**28.80580**	**3**
SOX2	0.04982	7.82280	3
SOX4	**0.00021**	**19.51440**	**3**
STK11	**0.00836**	**11.73170**	**3**
SYP	**0.00005**	**22.54800**	**3**
TYMS	**0.00003**	**23.69170**	**3**
UCHL1	**0.00628**	**12.34980**	**3**
XRCC1	0.01312	10.75610	3

Furthermore, 35 significant genes correlated significantly with tumour grade. Seven were most significant, eight were highly significant and 20 showed significant values. The most significant genes were *CDK6, CDKN2A, CHGA, FOLR1, SOX4, SYP* and *TYMS*. As highly significant *BCL2, CDK1, ERCC1, FPGS, GAB1,* MAN2C1, RTN1 and SOX11 were identified. Significant genes are summarised in Table 11.

Table 11 Significant p-values of mRNA expression correlating with tumour grade calculated with the Spearman Test. Highly significant mRNAs are bolded; most significant mRNAs are highlighted grey.

mRNA vs. grade	p-value	rho
ALK	0.02923	-0.3217282
ASCL1	0.03138	0.3177995
BCL2	**0.00584**	**0.4003202**
CASP8	0.03085	0.3187495
CCNE1	0.01449	0.3582982
CDK1	**0.00653**	**0.3954157**
CDK2	0.02292	0.3348748
CDK6	**0.00018**	**-0.525439**
CDKN1A	0.04155	0.3017465
CDKN2A	**0.00001**	**0.600167**
CHGA	**0.00012**	**-0.6890271**
EGFR	0.01393	-0.3602222
ERCC1	**0.00322**	**-0.4252979**
FLT4	0.01031	-0.3746669
FOLR1	**0.00010**	**-0.5412263**
FPGS	**0.00205**	**-0.6358421**
GAB1	**0.00182**	**-0.4475503**
MAN2C1	**0.00231**	**-0.4383885**
MLH1	0.01863	-0.345652
MMP3	0.02327	0.3340618
MST1R	0.04339	0.2992018
NTS	0.05859	0.2809346
PAX5	0.02111	0.3391859
PAX6	0.02668	0.3267251
RTN1	**0.00638**	**-0.3964781**
SEMA3B	0.02573	-0.3286917
SOD1	0.04511	-0.2968973
SOX11	**0.00131**	**0.4598031**
SOX4	**0.00019**	**0.5234697**
STK11	0.01985	-0.3423988
SYP	**0.00083**	**-0.4758176**
TKTL1	0.07582	0.2643776
TYMS	**0.00038**	**0.5022331**
UCHL1	0.05845	-0.2810818
XRCC1	0.03428	-0.31282

Corresponding box plots regarding targets highlighted in Table 10 and Table 11 are shown in Figure 13 to 15.

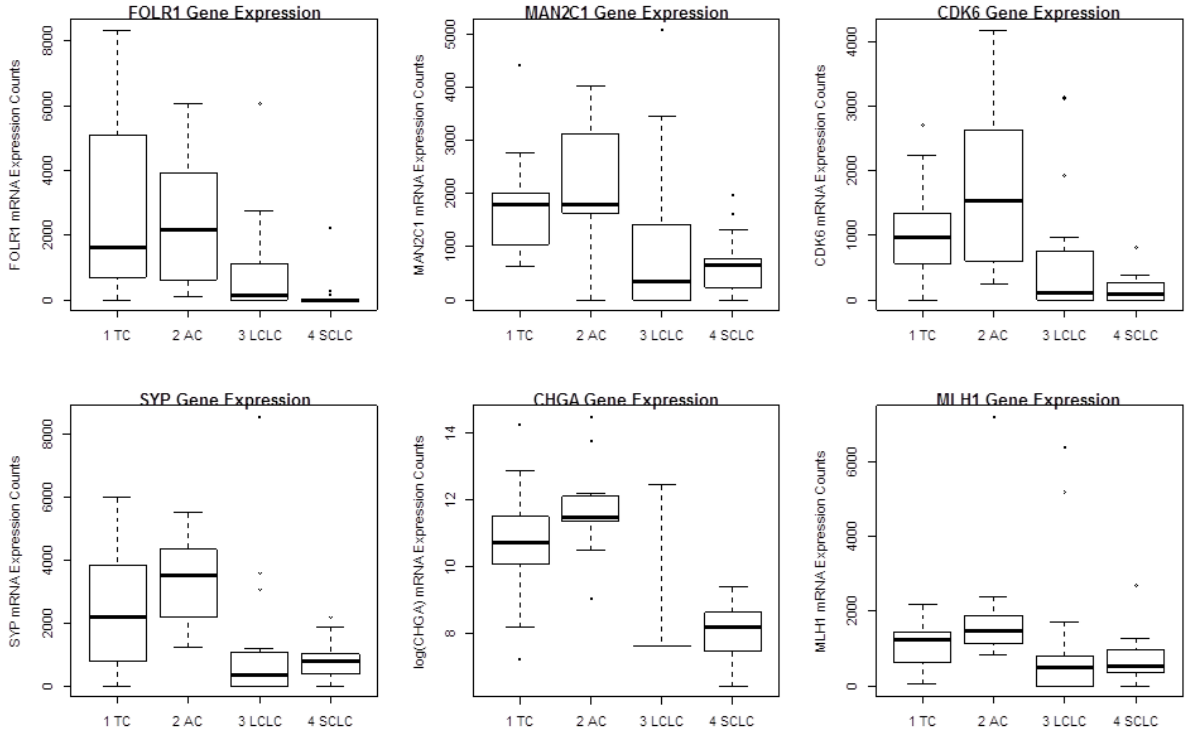

Figure 13 mRNA expression patterns of different genes measured by the NanoString technology. All illustrated genes decrease in their gene expression with increasing malignancy of the NET. FOLR1, CDK6 and SYP show very low median expression levels in NE carcinomas, especially when compared to pulmonary carcinoids. MLH1 is significantly higher in carcinoids then in high-grade tumours, but also carcinomas still have a noteable expression level. CHGA was the strongest expressed gene of all targets. Its y-axis is logarithmically scaled.

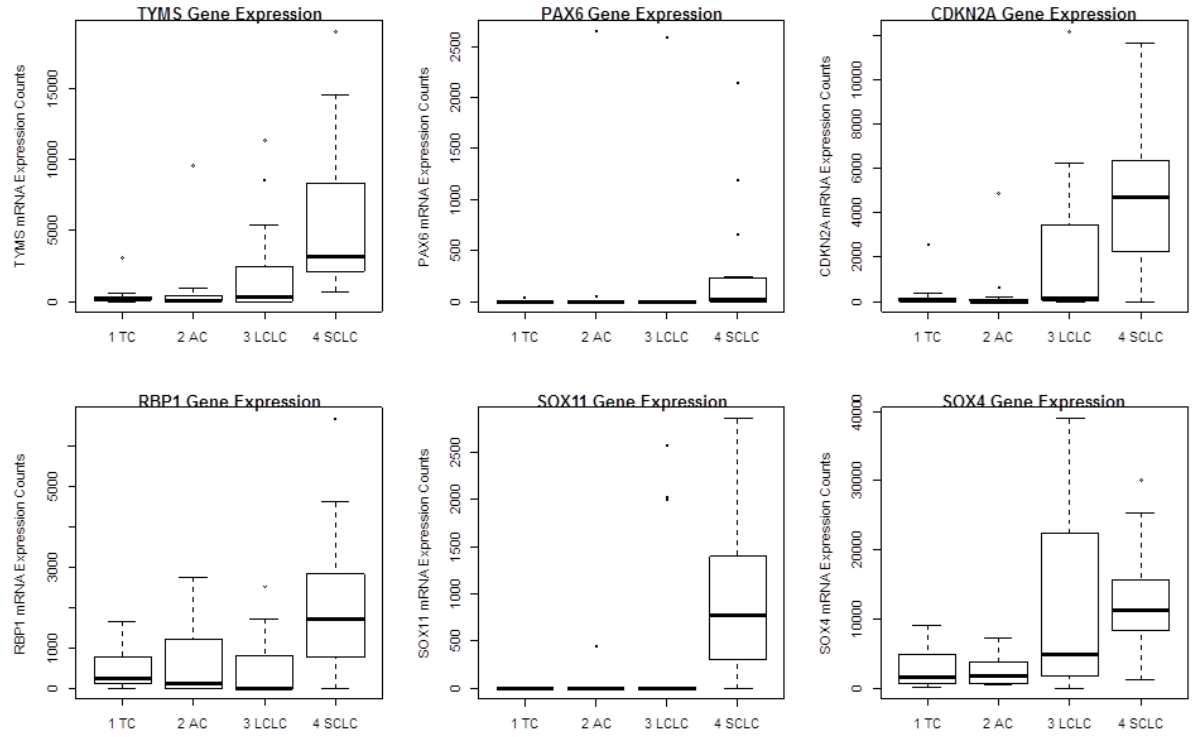

Figure 14 mRNA expression patterns of different genes measured by the NanoString technology are shown. All illustrated genes increase in their expression level with higher aggressiveness of the tumour. TYMS, CDKN2A and SOX4 show nearly no expression in carcinoid tumours but a detectable (LCNEC) to strong (SCLC) expression in high-grade carcinomas. PAX6, RBP1 and SOX11 are absent in carcinoids and LCNEC but expressed in SCLC.

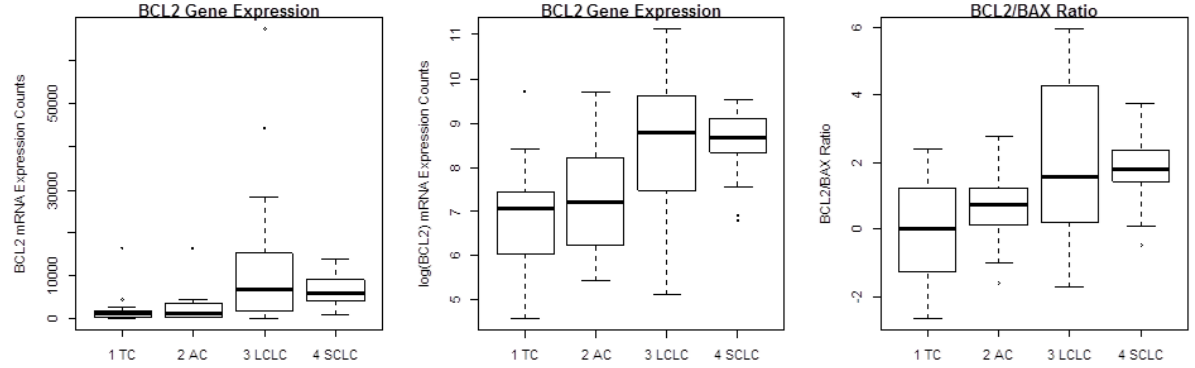

Figure 15 The boxplots present mRNA expression pattern of BCL2 investigated by NanoString nCounter technology and the BCL2/BAX-ratio as marker for evade of apoptosis, respectively. The BCL2 expression increases with increasing malignancy of the tumour entity. Whereas the BCL2/BAX ratio is nearly even in TC, the potential to evade apoptosis increases from AC over LCNEC to the highest value in SCLC.

Moreover, possible correlations with TNM parameters (tumour size, lymph node infiltration and metastasis) and additional parameters including International Association for the Study on Lung Cancer (IASLC)-stage, blood and lymphatic vessel invasion were investigated. With regard to tumour size, CYP1A1 and SOX11 showed

significant correlations. FOLR1 was identified as most significant marker for lymph node invasion. CDKN2A, FPGS, MAN2C1, PAX5, PAX6, SOX11 were highly significant and eight genes were significant for N-status. For metastatic behaviour PAX6 was most significant, followed by SOX11 as highly significant marker. Eight additional genes exhibited significant correlations: For stage FOLR1 was highly significant and six significant genes were found. For blood vessel invasion 13 significant genes were identified. Lymphatic vessel invasion showed highly significant correlations with CHGA and XRCC1 as and also exhibited four additional markers that reached significance. Correlations for gender and expression were also investigated. NKX21 was most significant and FLT4, FOLR1, SYP and UCHL1 were highly significant for gender. Additionally, 17 significant markers were identified correlating with gender. A summary of significant correlations with extended TNM-staging criteria is given in Table 12.

Table 12 P-values of mRNA expression regarding several clinical variables (TNM) using the Spearman Test are shown. Highly significant mRNAs are bolded; most significant mRNAs are highlighted in grey.

mRNA vs. stage	p-value	rho
CHGA	0.03605	-0.3099615
EGFR	0.02803	-0.3240392
ERCC1	0.01472	-0.3575023
FOLR1	**0.00493**	**-0.4076321**
MLH1	0.02144	-0.3383752
SYP	0.03083	-0.3187732
XRCC1	0.02255	-0.3357298
mRNA vs. M-status		
CDK2	0.02908	0.3088549
MSH6	0.03493	0.2989902
PAX6	**0.00023**	**0.4989672**
RBP1	0.01465	0.3433212
SOX11	**0.00125**	**0.4435477**
TYMS	0.02283	0.3214435
mRNA vs. N-status		
BCL2	0.02244	0.3223341
CAT	0.04844	-0.2805598
CCND1	0.03505	-0.2988
CDKN2A	**0.00116**	**0.4464135**
CHGA	0.01808	-0.333135
EGFR	0.01591	-0.3393525
FOLR1	**0.00011**	**-0.5192756**
FPGS	**0.00379**	**-0.402118**
MAN2C1	**0.00457**	**-0.3946589**
MLH1	0.01111	-0.3562231
PAX5	**0.00469**	**0.3935955**
PAX6	**0.00521**	**0.3892678**
SEMA3B	0.02975	-0.3076474
SOX11	**0.00380**	**0.4020669**
SYP	0.02131	-0.3249457

Concerning PFS, nine significant correlations were found. The Score (logrank) test showed the most significant correlation for *OCT4* and significant correlations for *FIGF, FN1, FOLR1, HIF1A, NTS* and *FAS*. The likelihood-ratio test revealed *GABBR2, OCT4* and *PCDHB9* as significant markers.

Kaplan Meier Curves of most important PFS results are shown in Figure 16.

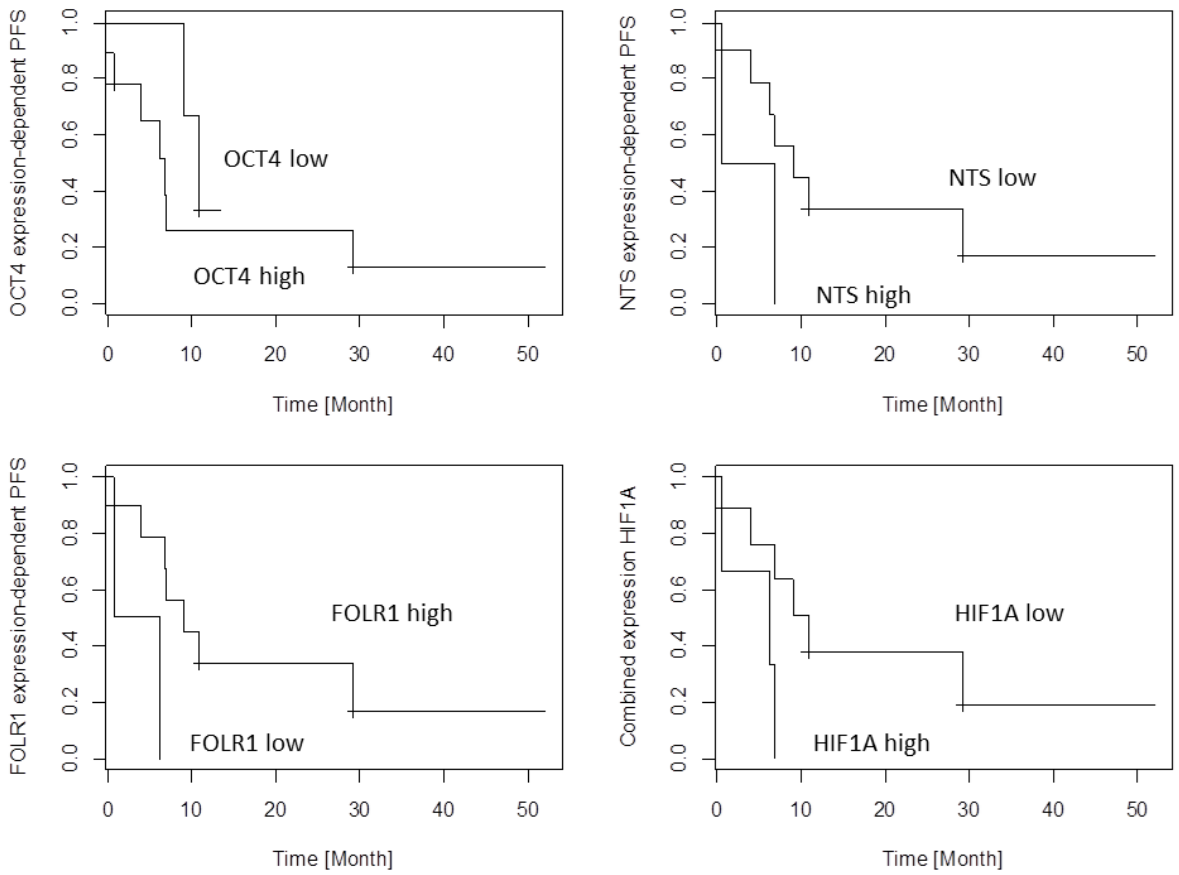

Figure 16 Kaplan-Meier curves for significant results regarding expression-dependent PFS in the group of high-grade pulmonary NET. A high expression level of NTS and HIF1A is associated with shortened time to progression, respectively. Low level expression of FOLR1 leads to an early recurrence of the tumour, whereas in contrast a loss of OCT4 expression is associated with prolonged PFS in this group of tumours.

Overall survival (OS) correlated significantly with nine genes: the Score (logrank) test identified *PAX6* as most significant ($p<0.001$), *OCT4* as highly significant ($p<0.01$) and *CRHR2, FPGS, MAN2B1, SOX11* and *TP53* as significant ($p<0.05$) markers for OS. The likelihood-ratio test identified significant correlations for *CHGA, FOLR1, FPGS, MAN2B1, SOX11* and a highly significant correlation for *PAX6*. Additionally, *OCT4* was identified as significant marker.

Kaplan Meier Curves of most important OS results are shown in Figure 17.

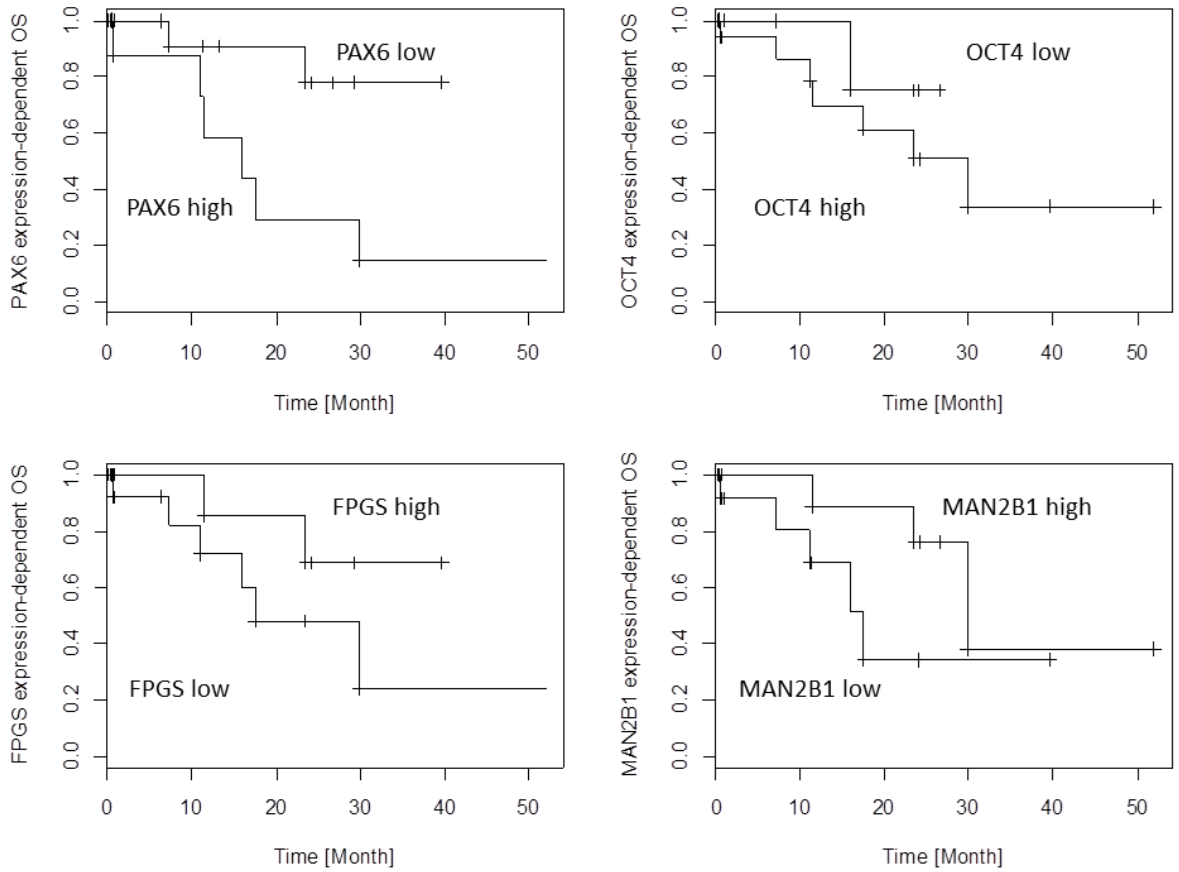

Figure 17 Kaplan-Meier curves for significant results regarding expression-dependent OS. A low PAX6 or OCT4 expression is associated with prolonged, a low FPGS or MAN2B1 expression is associated with shortened overall survival in LCNEC and SCLC, respectively.

Results of Variant Detection

Run Parameters and Determination of Sequencing Quality

Seventy of 74 patients were sequenced within four MiSeq runs, containing 23 or 24 patient samples per run. Samples showing insufficient coverage of some loci (n=23) were re-sequenced with an additional fifth run.

Bridge amplification of the target regions on the flow cell resulted in an average cluster density of 641 K/mm^2 with approximately 80% of the generated clusters passing the quality filter parameters. Altogether, the sequencing runs produced an average of 3.65x10^6 reads and an average output of 1.1 gigabases. The runs showed read quality parameters with average Q30 scores (equals a 0.1% chance of a wrong base call at this position) about 63% in a range of 28%-85%.

Run parameters are summarised in table 13.

Table 13 Overview of the technical run parameters for all five MiSeq runs. In run 5, the 23 samples with the lowest median coverage or insufficient representation of some loci were resequenced.

	Run 1	**Run 2**	**Run 3**	**Run 4**	**Run 5**	**Average**
Samples	23	24	23	24	23	
Panel	TSCP (Illumina)	TSCP (Illumina)	TSCP (Illumina)	TSCP (Illumina)	TSCP (Illumina)	
Amplicons [n]	181	181	181	181	181	181
Cluster Density [K/mm²]	339	1,211	498	454	705	641
Cluster PF	87.59%	56.88%	89.07%	89.64%	72.62%	79.16%
Reads	2.83M	8.66M	4.04M	3.69M	5.43M	4.93M
Reads PF	2.48M	4.93M	3.60M	3.31M	3.95M	3.65M
Total Yield	0.8Gb	1.5Gb	1.1Gb	1.0Gb	1.2Gb	1.1Gb
≥ Q30 Score	75.00%	42.90%	83.70%	85.30%	27.60%	62.9%

TSCP… TruSeq Cancer Panel, PF… passed filter; Q30 Score… 0.1% chance of wrong base call; M… million; Gb… gigabases

After the primary alignment, 25,940 genetic variants could be determined. 7,041 of them were classified as synonymous, leading to no change of the amino acid sequence. 643 of the remaining 18,899 variants detected fulfilled the criteria of more than 10% mutated allelic fraction and more than 25 mutated reads absolute.

An algorithm for variants filtering is illustrated in Figure 18.

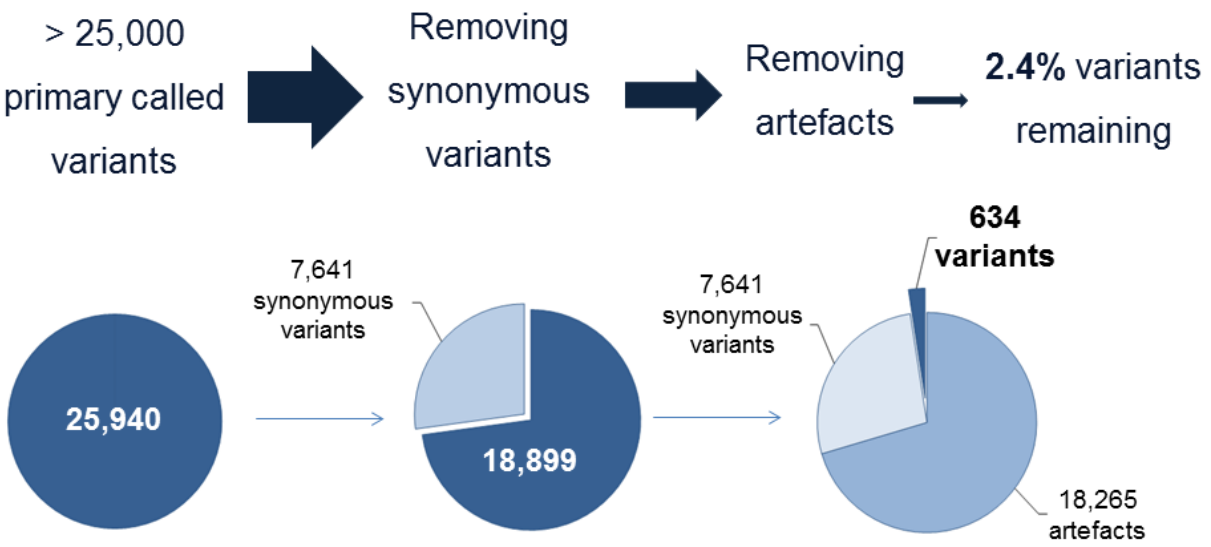

Figure 18 The chart pies summarises the algorithm used for variant filtering. Starting from 25,940 variants detected with the preliminary variant calling, going on with removing of synonymous variants that led to 18,899 variants. After a final filtering of variants below 10% of total reads or less than 25 mutated reads absolute 634 variants were determined.

Approximately 60% of the targets showed coverage between 500 and 2,000 reads (Figure 19).

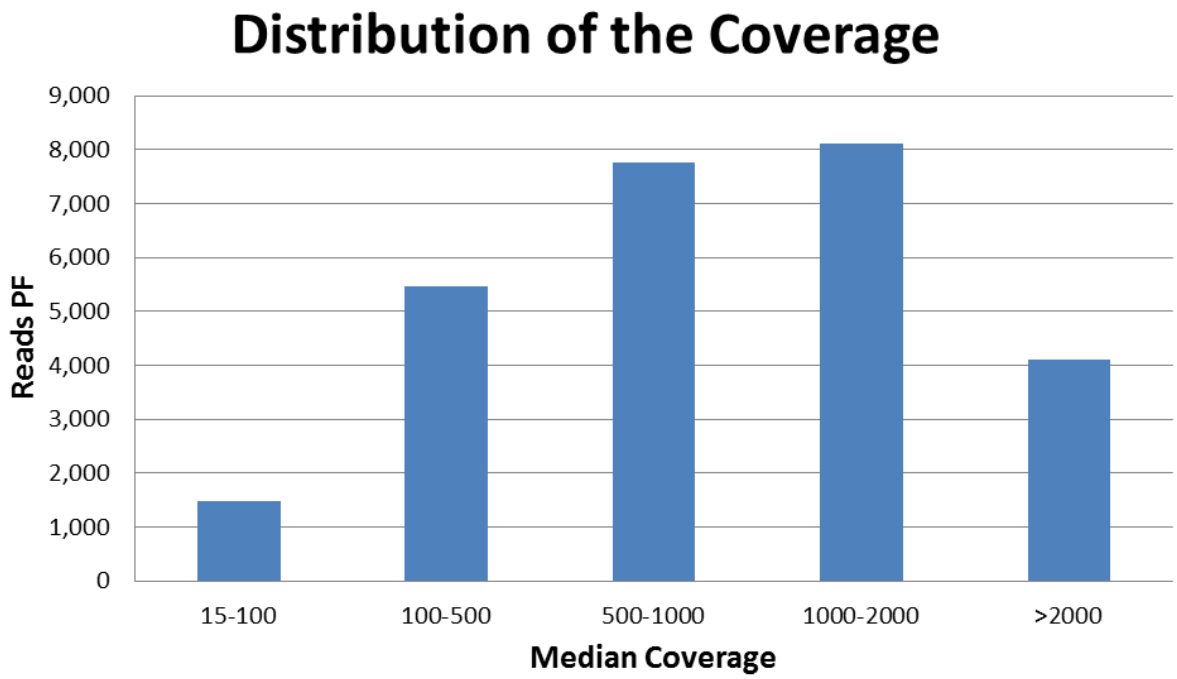

Figure 19 The histogram demonstrates the distribution of the reads past filter (PF) from all targets and runs. The y-axis shows the number of clusters that passed the initial filter process, the x-axis shows the coverage of these loci merged from each sample. Most targets had a median coverage between 500 and 2,000bp.

Variant Calling and Distribution of Detected Mutations

Regarding 643 variants that passed the applied filter processing as described above, 122 variants were related to TC (mean: 7.2 mutation in each sample), 150 were found in AC (mean: 8.8 variants per sample) and 164 were related to LCNEC (mean: 9.6 variants per sample). The final 207 variants were detected in the SCLC samples (mean: 14 variants per sample).

Most frequent alterations were found in *FLT3* (70) followed by *APC* (69) and *TP53* (59).

An overview of the mutation frequency per gene as well as the percentage of samples of each entity showing variants at this locus is summarised in Table 14.

Table 14 The table shows the results of the variant calling. The mutation frequency per gene as well as the percentage of samples of each entity showing at least one mutation at this locus is illustrated.

Gene	Variants (abs.)	Ø TC	Ø AC	Ø LCNEC	Ø SCLC
ABL1	7	11.76%	-	15.79%	6.67%
AKT1	2	-	5.88%	-	6.67%
ALK	2	-	5.88%	5.26%	-
APC	69	35.29%	35.29%	26.32%	40.00%
ATM	22	29.41%	17.65%	15.79%	40.00%
BRAF	3	-	-	10.53%	6.67%
CDH1	1	-	5.88%	-	-
CDKN2A	0	-	-	-	-
CSF1R	0	-	-	-	-
CTNNB1	1	5.88%	-	-	6.67%
EGFR	16	23.53%	23.53%	21.05%	26.67%
ERBB2	35	29.41%	29.41%	31.58%	33.33%
ERBB4	15	17.65%	11.76%	10.53%	20.00%
FBXW7	13	5.88%	29.41%	31.58%	6.67%
FGFR1	2	-	5.88%	5.26%	-
FGFR2	7	17.65%	5.88%	10.53%	-
FGFR3	4	11.76%	5.88%	5.26%	-
FLT3	70	100.00%	88.24%	89.47%	100.00%
GNA11	0	-	-	-	-
GNAQ	0	-	-	-	-
GNAS	2	5.88%	5.88%	-	-
HNF1A	4	-	5.88%	10.53%	6.67%
HRAS	0	-	-	-	-
IDH	6	17.65%	-	-	13.33%
JAK2	0	-	-	-	-
JAK3	5	5.88%	5.88%	10.53%	6.67%
KDR	41	47.06%	41.18%	57.89%	66.67%
KIT	22	35.29%	35.29%	26.32%	20.00%
KRAS	12	5.88%	29.41%	10.53%	20.00%
MET	8	11.76%	11.76%	15.79%	6.67%
MLH1	1	5.88%	-	-	6.67%
MPL	0	-	-	-	-
NOTCH1	0	-	-	-	-
NPM1	0	-	-	-	-
NRAS	3	-	-	-	13.33%
PDGFRA	12	23.53%	-	15.79%	26.67%
PIK3CA	28	17.65%	23.53%	26.32%	40.00%
PTEN	34	23.53%	35.29%	21.05%	26.67%
PTPN11	33	23.53%	35.29%	21.05%	26.67%
RB1	13	11.76%	5.88%	21.05%	20.00%
RET	11	11.76%	23.53%	10.53%	13.33%
SMAD4	33	29.41%	29.41%	26.32%	26.67%
SMARCB1	4	-	5.88%	-	20.00%
SMO	33	17.65%	23.53%	21.05%	13.33%
SRC	0	-	-	-	-
STK11	8	-	11.76%	-	20.00%
TP53	59	29.41%	41.18%	73.68%	93.33%
VHL	2	-	-	-	6.67%

Statistical Analysis

Thirteen statistically significant associations between the mutation frequency per gene and tested variables could be ruled out. Additionally, nine correlations between mutational status of the genes and tested variables were found.

Most conspicuous, all four entities of pulmonary neuroendocrine tumours differ significantly in their genetic profile of *TP53* (p=0.0011, figure 20). Therefore, it seems to be of additional importance when *TP53* shows multiple mutations (p=0.0001).

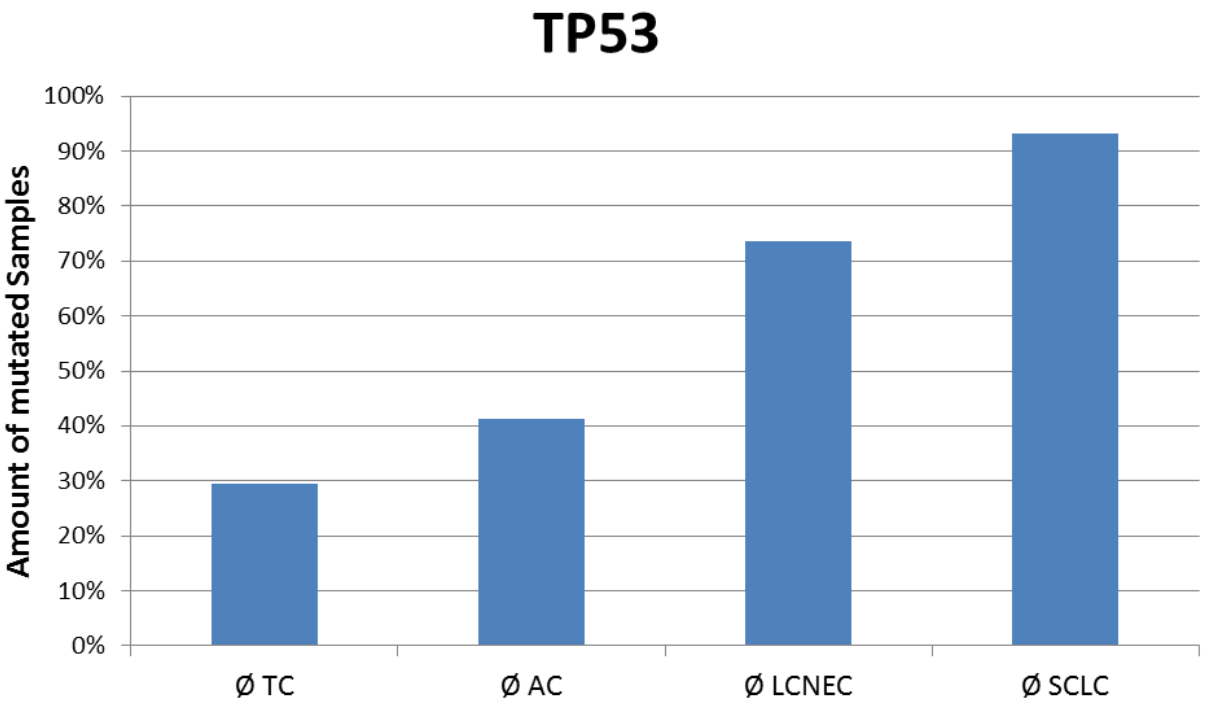

Figure 20 Samples showing at least one TP53 variant regarding the tumour entity. The number of mutated samples increased from TC (below 30%) to SCLC (more than 90%). A sharp edge can be seen between carcinoid tumours (30%-40%) and high-grade carcinomas (75-95%).

TP53 variants significantly correlated with the potential of the tumour to invade lymph nodes (p=0.0061).

In addition, the number of mutations in *APC* (p=0.0433), *BRAF* (p=0.0468) and *STK11* (p=0.0144) were associated with lymph-node invasion. Occurrence of any non-synonymous variant in *APC* (p=0.0262) and *STK11* (p=0.0131) could predict a tendency for lymph vessel infiltration.

However, no correlations between the mutations detected and the occurrence of distant metastases, as well as to gender and size of the tumour detected could be observed.

For progression-free survival analysis, the mutation frequency in *APC*, *ATM*, *MET*, *KRAS*, *PDGFRA*, *PIK3CA* and *RB1* rendered significance in all three tests regarding PFS. The amount of mutations in *FWXB7* correlated significantly with OS.

Analogously, the occurrence of mutations in *ATM*, *FLT3*, *MET*, *KRAS* and *RB1* showed statistical significance to PFS and again *FWXB7* was significant for OS. Important results are illustrated in Figure 21 and Figure 22.

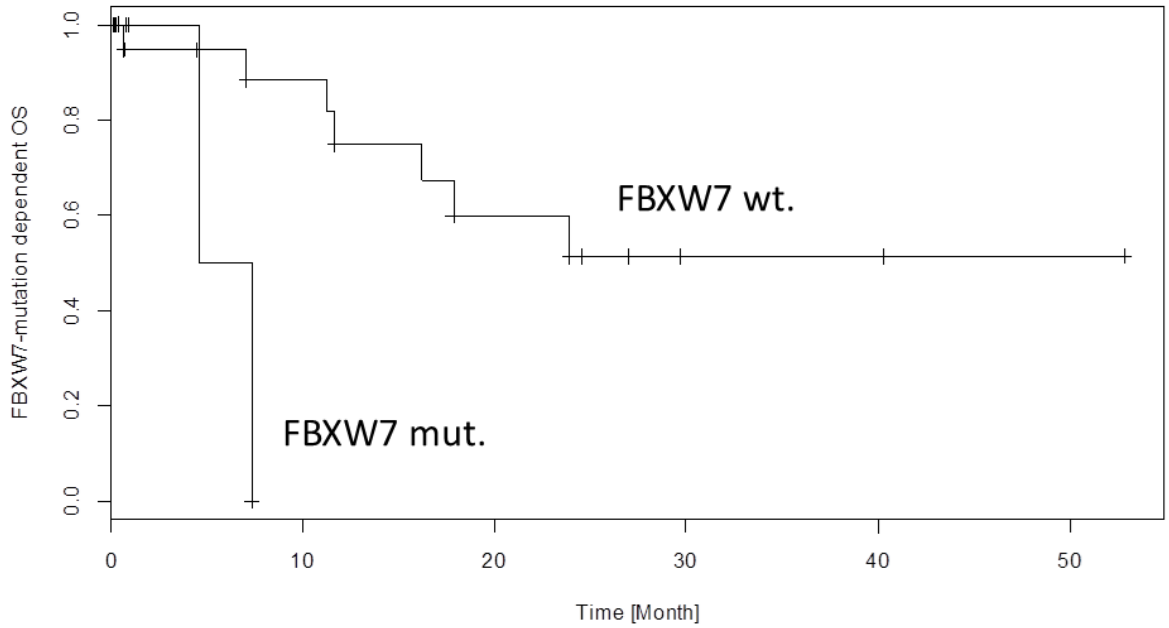

Figure 21 Kaplan-Meier curves of significant results regarding FBXW7. The occurrence of mutations within the coding sequence of FBXW7 is associated with shortened cumulative overall survival.

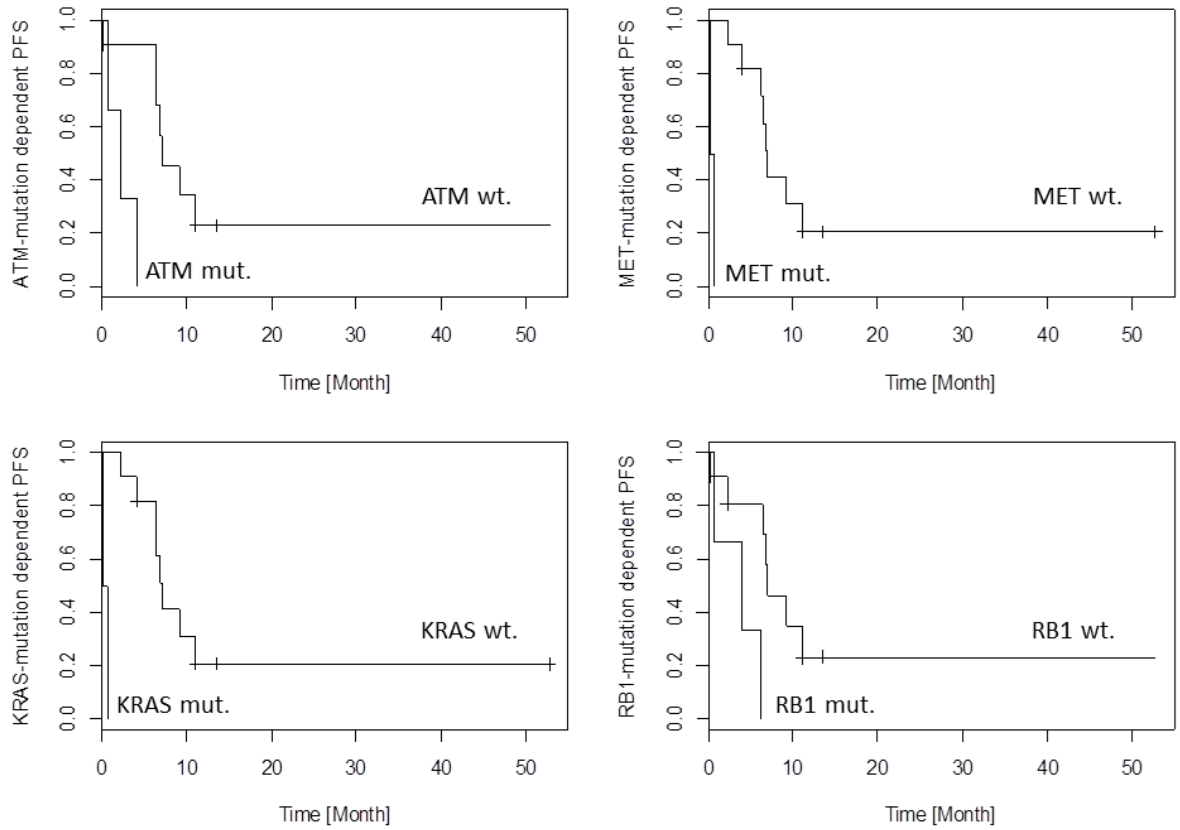

Figure 22 Kaplan-Meier curves of significant results regarding the mutation-dependent PFS analysis. Patients showing mutations in the CDS of either MET or KRAS have a highly significant shortened time to progression of the tumours. Also ATM and RB1 mutations significantly impact to progression of the tumours.

Survival analysis is summarised in Table 15.

Table 15 Summary of significant results regarding the mutation-dependent survival analysis

		Gene	Likelihood ratio Test	Wald test	Score (logrank) Test
Amount of Mutations	OS	FBXW7	0.0500	0.0352	0.0131
	PFS	APC	0.0413	0.0347	0.0101
		ATM	0.0463	0.0379	0.0041
		MET	0.0027	0.9989	0.0001
		KRAS	0.0027	0.9989	0.0001
		PDGFRA	0.0592	0.0490	0.0186
		PIK3CA	0.0452	0.0367	0.0176
		RB1	0.0344	0.0303	0.0110
Mutation Status	OS	FBXW7	0.0500	0.0352	0.0131
	PFS	ATM	0.0120	0.0221	0.0030
		FLT3	0.0216	0.9983	0.0003
		MET	0.0027	0.9989	0.0001
		KRAS	0.0027	0.9989	0.0001
		RB1	0.0424	0.0412	0.0191

Proteasome Expression

Overall Cohort

Five genes of the 26S-proteasome complex coding for proteins of the catalytic domain and two additional reference genes as endogenous controls were tested for their mRNA expression levels using the TaqMan AoD. Efficacies calculated from the standard curves were between 1.89 and 2.01. The standard deviation was lower than 0.4 Ct for any case and assay. None of the non-template controls (NTCs) generated a detectable signal. $2^{-\Delta\Delta Ct}$-values for the 26S-proteasome subunits were as follows: *PSMA1* (3.5E-07 to 53.69; median: 1.35; mean: 2.70), *PSMA5* (7.7E-06 to 901.20; median: 2.27; mean: 136.12), *PSMB4* (1.3E-05 to 77.36; median: 1.61; mean: 3.54) and *PSMD1* (9.9E-07 to 40.38; median: 1.32; mean: 3.78). *GAPDH* was between 0.58 and 1.96 (median: 0.97; mean: 1.31) and *ACTB* was used for normalisation purposes.

The mRNA expression of the 26S-proteasome subunits demonstrated significant correlations to each other ($p \leq 0.003$; rho between 0.338 and 0.598), except *PSMA5* to *PSMB5* (p=0.69; rho=0.047); indicating that any of the 26S-proteasome subunits is equally expressed in these tumours and mRNA of each subunit was reliably detected.

Compared to non-tumorous lung tissue, the gene expression of all 26S-proteasome subunits was significantly increased in any subtypes of pulmonary neuroendocrine tumours (*PSMA1*: p> 0.0001; *PSMA5*: p= 0.0002; *PSMB4*: p> 0.0001; *PSMB5*: p> 0.0001; *PSMD1*: p> 0.0001) (Figure 23, Figure 24). *PSMB4* gene expression was significantly different between the different neuroendocrine tumour subtypes (p=0.043, rho=0.262), showing the highest mRNA levels in LCNEC (Figure 25). All other 26S-proteasome subunit genes investigated did not show statistically significant differences between the different tumour entities. Furthermore, the proliferation index of pulmonary neuroendocrine tumours measured by nuclear expression of Ki-67 showed a significant positive correlation to the mRNA level of *PSMB4* (p=0.0039, rho= 0.301).

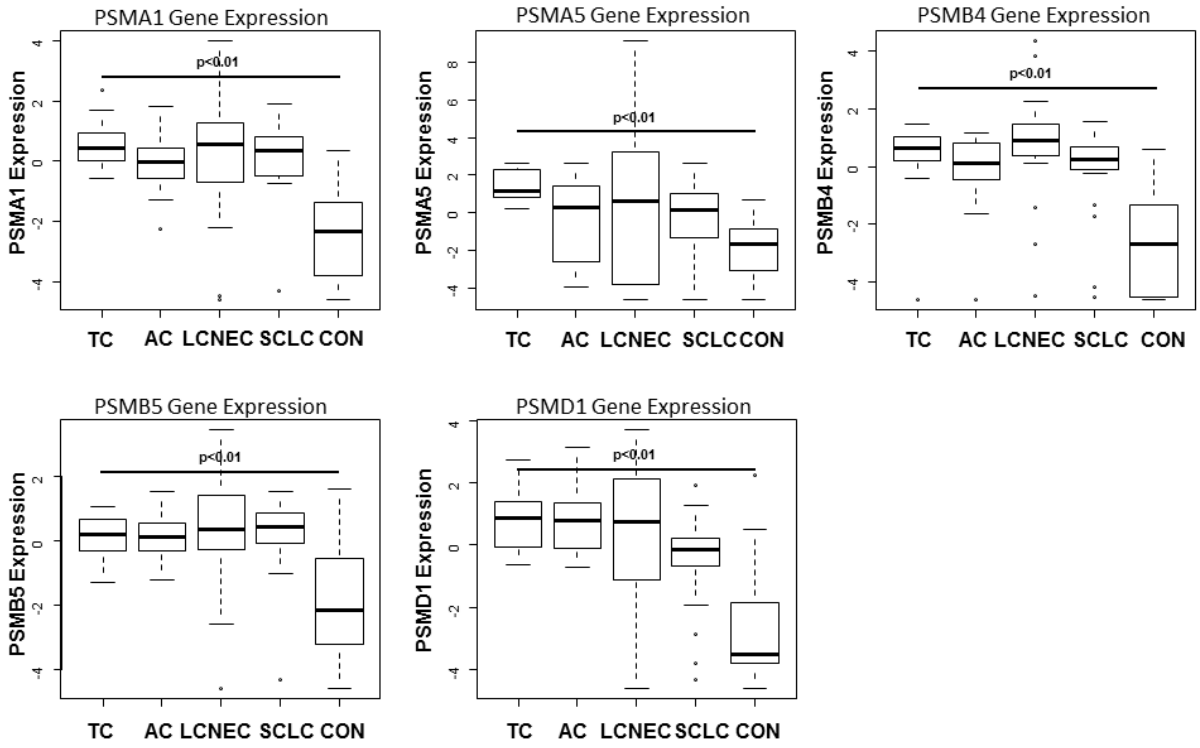

Figure 23 Box plots illustrating significantly upregulated mRNA expression in the different subtypes of pulmonary neuroendocrine tumours are shown. The gene expression measured by TaqMan qPCR is shown using log(2^-dCt) of each target. Horizontal bars indicate significant dependences. Note that any proteasomal subunit mRNA expression is significantly upregulated compared to controls obtained from non-tumorous lung tissue of patients with pneumothorax. Especially PSMB4 and PSMD1 show the strongest upregulation compared to benign lung. LCNEC show the broadest range of proteasomal expression pattern, maybe due to the heterogeneity of this entity. Remarkable is the relatively low PSMA5 expression level when compared to the control.

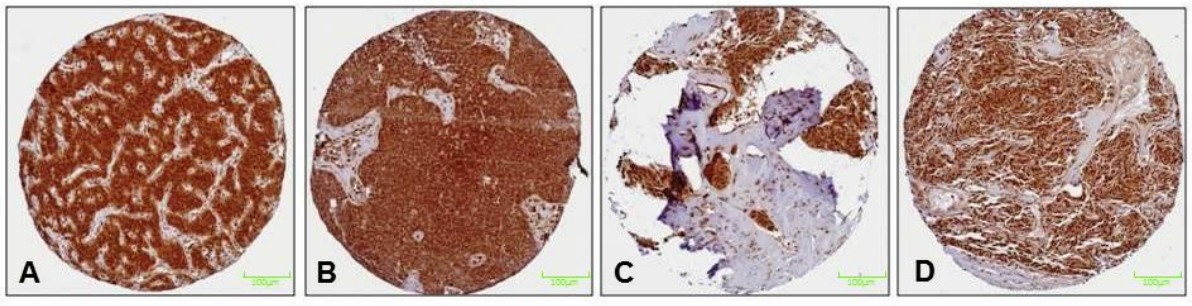

Figure 24 The figure illustrates the results of the immunohistochemical staining of the proteasomal subunit PSMB4 in both, low-grade (A+B) and high-grade (C+D) pulmonary NET. Immunohistochemically, PSMB4 reactivity is strong in any subtypes of pulmonary NET. All NET are silhouetted against the encircling stroma. Immunohistochemical no differences between the four tumour entities could be detected.

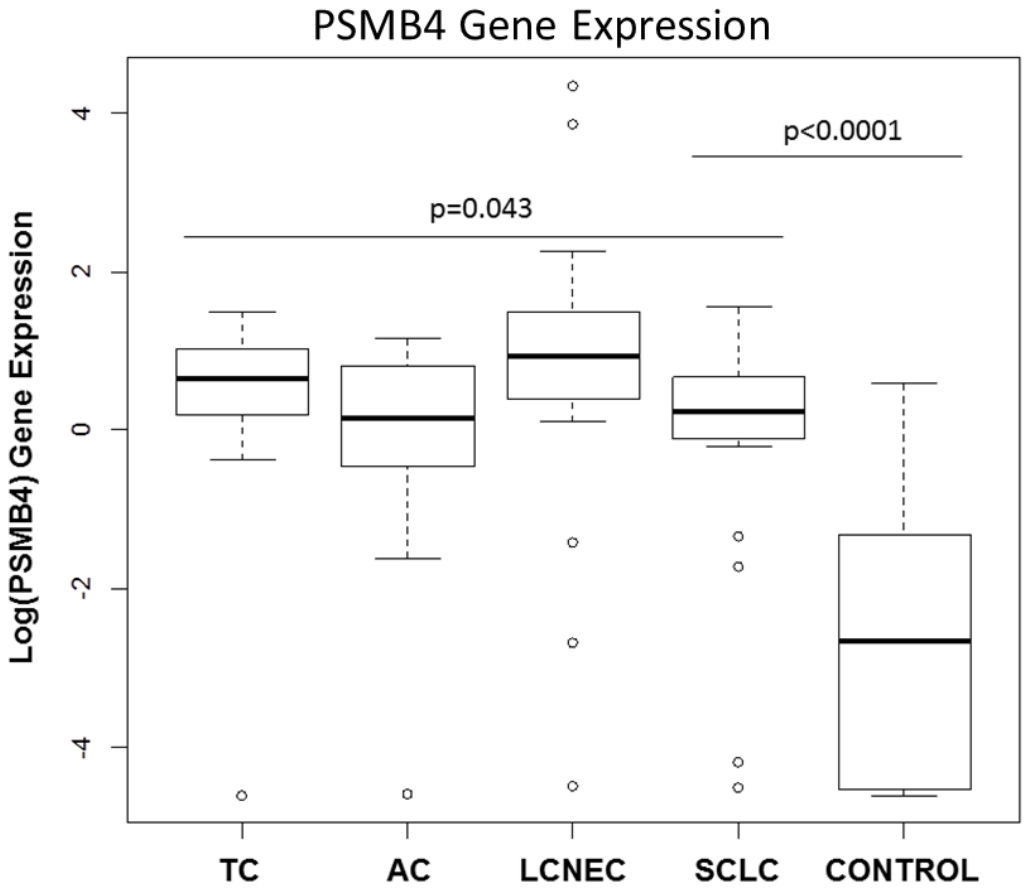

Figure 25 Boxplot of PSMB4 expression levels between the different tumour types. In particular, the PSMB4 mRNA expression is upregulated in pulmonary NET compared to controls and differs significantly among the subtypes of pulmonary NET. PSMB4 shows the highest expression in LCNEC, the lowest expression in AC and SCLC. Nevertheless, immunohistochemically no differences between the four tumour entities could be detected, PSMB4 mRNA expression is higher in LCNEC/SCLC than in TC/AC. The gene expression measured by TaqMan qPCR is shown using log(2^-dCt) of each target. Horizontal bars indicate significant dependences.

Pulmonary Neuroendocrine Carcinomas

As observed in the overall cohort any measured mRNA expression levels of the 26S-proteasome were significantly correlated to each other ($p \leq 0.010$) except *PSMA5*/*PSMB5* (p=0.332; rho=0.159).

PSMB4 gene expression level was significantly higher in LCNEC compared to SCLC (p=0.036) (Figure 26).

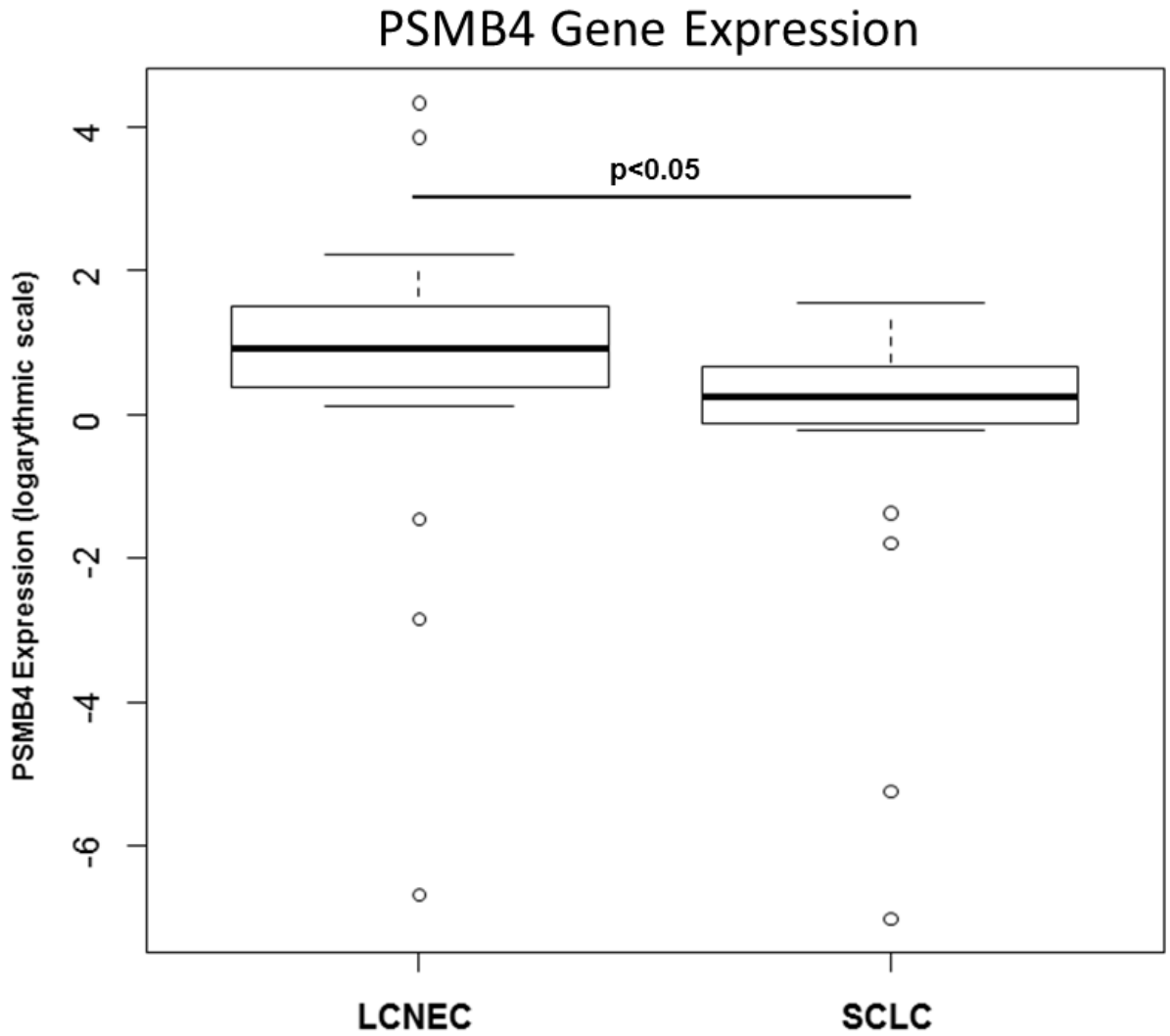

Figure 26 Differential expression of PSMB4 between the two types of high-grade NELC. LCNEC shows a slightly higher expression level then SCLC. The gene expression measured by TaqMan qPCR is shown using log(2^-dCt) of each target. Horizontal bars indicate significant dependences.

Pulmonary Carcinoids Tumours

PSMD1 is associated with Ki-67 expression (p=0.010; rho=-0.484) as well as chromogranin A- immunoexpression (p=0.015; rho=0.440). *PSMB4* also showed a significant correlation to the proliferation index determined by Ki-67 immunoexpression (p=0.046; rho=-0.387).

PSMA1 (p=0.030, rho=-0.372) and *PSMB5* (p=0.035, rho=-0.363) both show a significantly different gene expression between G1 or G2 carcinoid tumours of the lung (Figure 27). Additionally, *PSMA5* (p=0.02389) and *PSMB4* (p=0.050) showed higher expression in TC in comparison to AC.

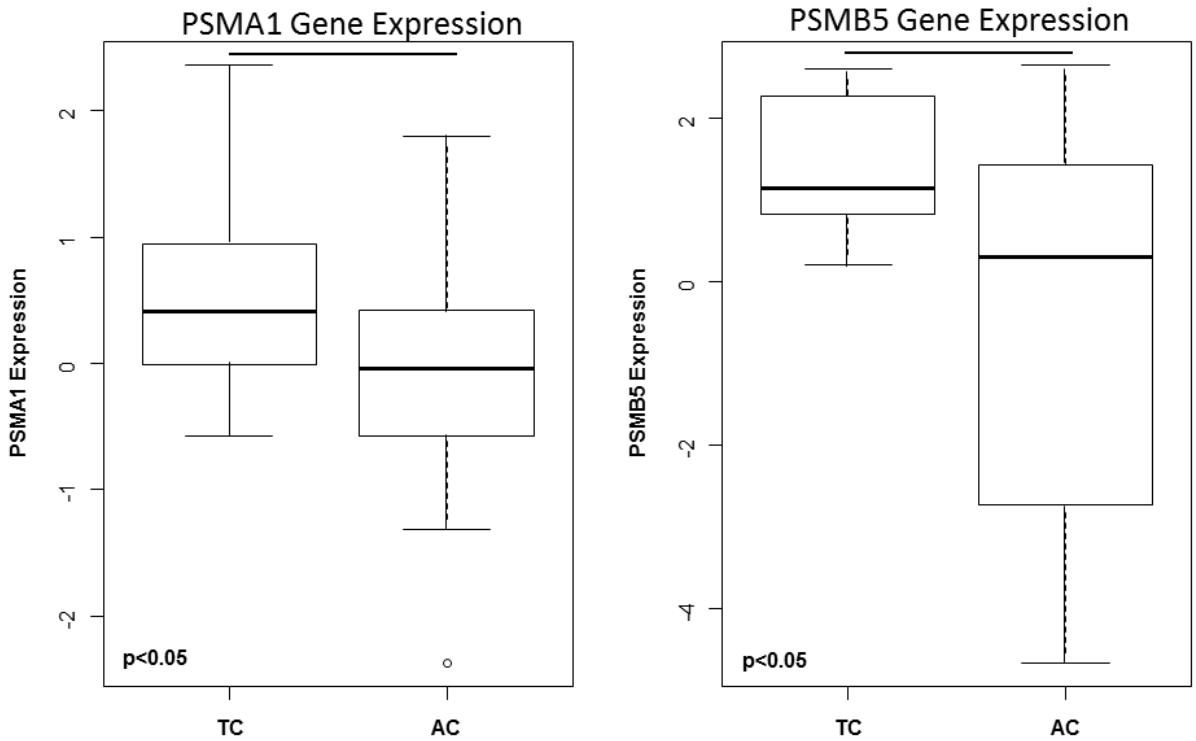

Figure 27 Differential expression pattern of PSMA1 and PSMB5 in low-grade NELC. Among others, the gene expressions of PSMA1 (p= 0.030) and PSMB5 (p= 0.035) are significantly higher in TC compared to AC. The gene expression measured by TaqMan qPCR is shown using log(2^-dCt) of each target. Horizontal bars indicate significant dependences.

Survival Analysis

PSMD1 mRNA expression is significantly associated with OS of all subtypes of pulmonary neuroendocrine tumours (Likelihood ratio test: p=0.019; Score (logrank) test: p=0.020), but no correlation at all could be found for PFS (Likelihood ratio test: p=0.556; Score (logrank) test: p=0.558).

Determination of Protein Expression by Immunohistochemistry

Staining results of the immunohistochemical panel including Pan-Cytokeratin (CK-MNF-116), *NCAM* (CD56), *NKX2-1* (TTF-1), *CHGA* (chromogranin A), cleaved *CASP3* (Casp3), *PSMB4* and *MKI67* (Ki-67), possible correlations to tumour type and survival times (OS/PFS) were calculated.

Three of them, namely CHGA (p=0.0004), Casp3 (p<0.0001) and Ki-67 (p<0.0001) differ significantly between these entities. CHGA is strongly expressed in carcinoid tumours but shows a weak to absent expression in the high-grade group. The proliferation index determined by Ki-67 expression increases as expected with increasing malignancy, showing nearly no proliferative activity in the low grade tumours, a moderate proliferation in LCNEC and a strong activity in SCLCs.

Determination of initiated apoptosis via staining of already cleaved caspase3 shows a moderate to strong appearance in LCNEC and SCLC, a weak to moderate expression in TC and no apoptotic activity in AC. None of the IHC markers show a significant association to PFS or OS.

Boxplots representing the results of the IHC staining are given in Figure 28.

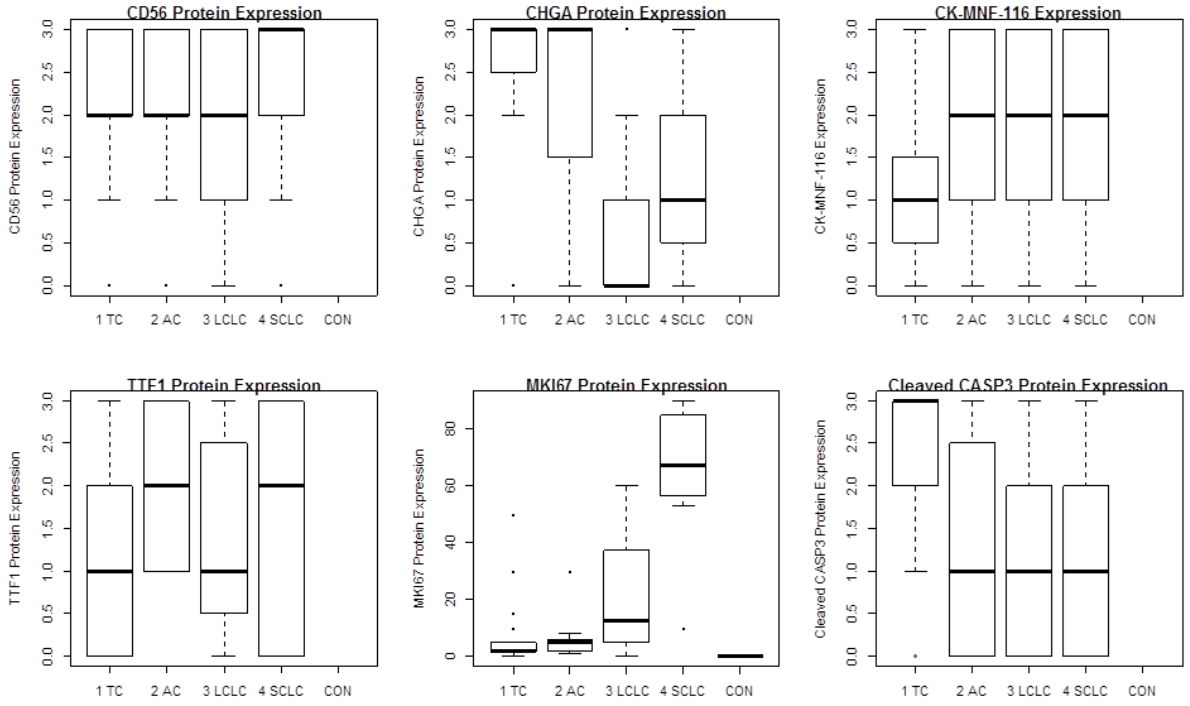

Figure 28 Boxplots illustrating results of the immunohistochemical staining of NELC against the neuroendocrine markers NCAM (CD56) and CHGA, CKMNF-116 and TTF1 as diagnostic standards, Ki67 for proliferation and CASP3 to determine the apoptotic activity fraction.

4. Discussion

In contrast to neuroendocrine tumours of other organ systems (e.g., of gastrointestinal origin), pulmonary neuroendocrine tumours form two distinct, prognostically different groups: the low-grade (LG) carcinoid tumours and the high-grade (HG) carcinomas (Rindi et al. 2014). Both groups can be further divided into subgroups, namely TCs and ACs and LCNECs and SCLCs, respectively.

Both pulmonary carcinoids and SCLCs were previously reported to arise from PNEC (Bensch et al. 1968; Warburton et al. 2000; Swarts et al. 2012). Even though all four subgroups share some morphologic and molecular properties, it is still unclear whether they are different biological entities or a distinct tumour entity showing different grades of differentiation and hence different biological behaviours. The aim of this thesis was to address some aspects of this question. To this end, a broad molecular-biological screening was performed to explore numerous cellular processes on different levels including genetic background, individual expression pattern, transcriptional regulation via miRNAs and cellular protein levels.

Development of a New Model for Lung Tumour Classification

Pulmonary neuroendocrine tumours should be clearly separated from other NSCLCs. These tumours originate from precursor lesions different to pulmonary neuroendocrine tumours and do not share many molecular characteristics with NSCLCs. Thus, the clinical management of LCNEC should move closer to that for SCLC than for NSCLC (Iyoda et al. 2014).

A conclusive proof of our hypothesis can only be achieved through genetic or epigenetic analysis, because gene expression levels can strongly differ and also

depend on environmental influences. The use of formalin-fixed paraffin embedded tissue is standard and crucial in routine molecular diagnostics. As has been known for more than forty years, formalin fixation of tissues can lead to DNA alterations like DNA fragmentation, deamination of cytosine to adenine and cross-linking between protein and DNA (Chalkley and Hunter 1975). It is well known that the formalin fixation process lowers the success of PCR (Chalkley and Hunter 1975), which could therefore lead to an impaired library construction for NGS. The amplification of FFPE DNA can result in the production and amplification of artificial mutations, which ultimately produces many sequencing artefacts. A visual verification of our sequencing data with the alignment-visualizer program integrative genomics viewer (IGV, Broad Institute of MIT and Harvard, Boston, USA) revealed a high background of unspecific variant calls (Figure 29). Due to the high number of sequencing artefacts, leading to a high number of false positive variants, the sequencing results obtained must be treated with caution.

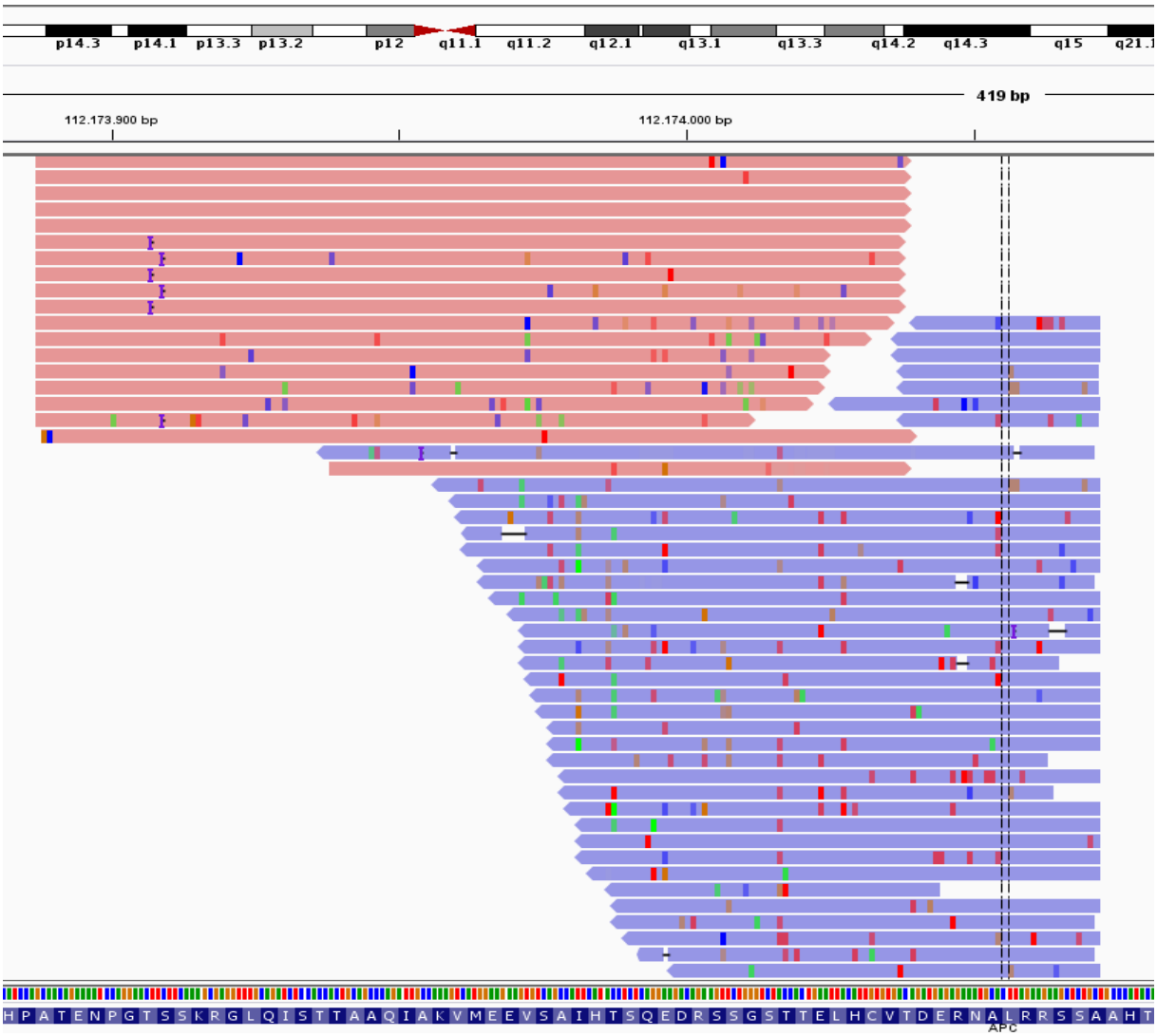

Figure 29 The visual analysis of the next generation sequencing data by integrative genomics viewer shows a high background of false-positive variants for APC exon 14. Pink bars show sequenced forward strand, blue bars show sequenced reverse strands. Colour dots within the strands display discrepancies between the base calls and the hg19 reference build.

Despite these shortcomings, the sequencing data give a clear impression of the genetic background of the different tumour subgroups. The major finding was the different proportion of loss-of-function (LOF) mutations in the *TP53* gene locus, ranging from less than 30% in TCs up to more than 90% in SCLCs. This is in line with previous findings from other studies (Lohmann et al. 1993; Przygodzki et al. 1996; Couce et al. 1999; Leotlela et al. 2003; Swarts et al. 2012). LOF of the p53 protein, considered the “guardian of the genome,” is fundamental to most of the differences between the high-grade and low-grade NELC groups, including the increased genetic

instability of high-grade tumours or the evasion of apoptosis. The epigenetic screening for DNA-methylations is addressed in an ongoing study.

These substantial differences between pulmonary carcinoids and high-grade lung NETs with regard to gene and protein expression levels and mutations of important tumour suppressor genes (especially *TP53*) and oncogenes may simply reflect differences in the exposure to tobacco carcinogens, probably causing further genetic alterations. An improved understanding of the biology of NETs will offer the opportunity for novel approaches in clinical management, resulting in better prognosis and prediction of therapeutic response (Asamura et al. 2006). At present, LCNECs are assigned to the NSCLC group and patients receive clinical management in accordance with NSCLC guidelines. Interestingly, patients with LCNEC receiving an SCLC-based regimen showed a significantly improved overall survival compared to those receiving standard regimes for NSCLC (Rossi et al. 2005; Gridelli et al. 2013).

Figure 30 illustrates our proposal for a classification model of lung tumours.

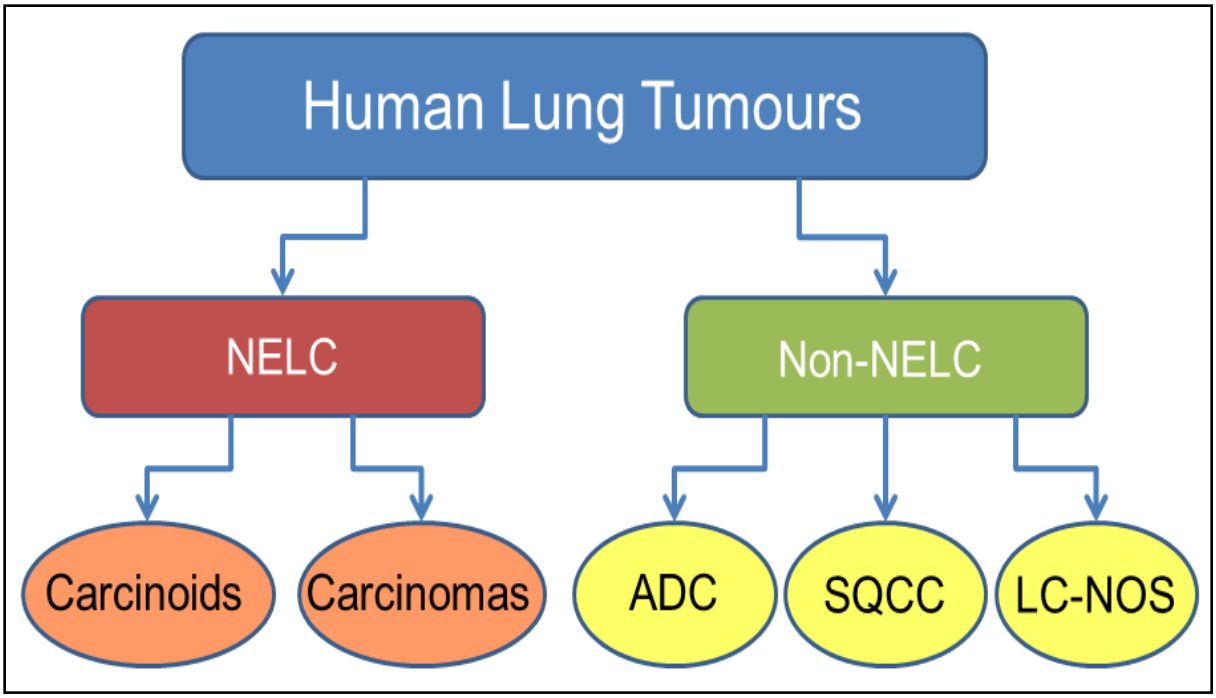

Figure 30 Proposal for a model for classifying lung tumours. Despite the traditional morphologic view and classification into NSCLC and SCLC, which has been undisputed for generations of medical doctors, the family of pulmonary neuroendocrine tumours, although showing different morphological presentation, can be biologically distinguished from all other forms of lung cancers.

miRNA Expression in NET of the Lung and NSCLC

In the past, a small set of miRNAs were identified as distinguishing between different types of lung tumours, playing a driving role in tumourigenesis of lung cancers and/or having a prognostic or predictive impact on these tumours. Unfortunately, the overwhelming majority of these studies focused on NSCLC patients; no joint data for pulmonary neuroendocrine tumours currently exist.

Expression of miR-29 family members correlates with increasing malignancy of the investigated tumour entities. Their expression decreases with increasing aggressiveness of the tumour. It is known for LCNEC that the expression of miR-29 family members is strongly associated with the methylation pattern of the cells by targeting the DNA-methyltransferases 3A and 3B (*DNMT3A*/*DNMT3B*). Its function is required for *de novo* methylation and for establishment of DNA methylation patterns

during development. Therefore a high methylation pattern is present, but inducing expression of miR-29 restores normal pattern and re-expression of silenced tumour suppressor genes like *FHIT* in cell lines (Fabbri et al. 2007). This leads to a reprogramming of the tumour cells to the methylation pattern of a non-tumorous cell, indicating that the miR-29 family (especially miR-29a, miR-29b, miR-29c) are acting as tumour suppressor-miRNAs (Fabbri et al. 2007). Hence, a down-regulation of miR-29 expression is accountable for hypermethylation and frequently induces silencing of tumour suppressor genes. Other targets of the miR-29 family include p85α and *CDC42* (Park et al. 2009). *CDC42* and p85α are negative regulators of p53, which displays apoptotic activity. Lower expression reduces p53 levels, associated with decreased apoptosis, which correlates with increasing malignancy. Although the expression within TC and AC is similar, Figure 10 shows a clear difference between low and high grade lung tumours and between LCLC and SCLC.

miR-34 family members are thought to be associated with the p53 tumour suppressor network, inhibiting inappropriate cell proliferation (He et al. 2007). Nevertheless, the difference between the four tumour types analysed in this study has not shown a correlation to any of them. As reported by Lee et al. (Lee et al. 2011), none of the miR-34 family members can be used as a prognostic marker in neuroendocrine lung cancers, including SCLC.

Members of miRNA family let-7 have been found to be deregulated in human lung cancers, including cancers with neuroendocrine differentiation (Caldas and Brenton 2005; Lee et al. 2012). In contrast to the published data, these miRNAs were unable to discriminate the different entities of neuroendocrine lung cancers in our collective, but let-7d showed a significant correlation with overall survival in these patients,

leading to the assumption that let-7d plays a role in the development of metastasis and progression of these tumours. The miRNAs miR-21 and miR-155, both reported to be overexpressed in neuroendocrine lung cancers (Guan et al. 2012; Lee et al. 2012), showed no statistical significance in our collective, just like miR-210, an miRNA overexpressed in cancer tissue and not in normal lung parenchyma (Guan et al. 2012). miR-21 turned out to be a particularly interesting target, because it is a key regulator of the *MTOR* pathway and is reported to be differently regulated in neuroendocrine tumours (Cingarlini et al. 2012). This also matches the results of our mRNA analysis, as described below. Additionally, miR-96 expression coincides with the methylation pattern of cells and has been shown to be upregulated in NSCLC (Ma et al. 2011), but there is no suggestion that it could be a potential diagnostic marker between the tumour types investigated in this study.

One interesting result in this context is the differential expression of the miR-143 between the different tumour types. miR-143 mainly targets the hexokinase 2 gene, the key regulator of glycolysis, which is activated in a majority of human cancers (Fang et al. 2012). The expression of miR-143 decreases with higher malignant potential of the tumour, leading to increased glycolytic activity (known as the Warburg effect). This result leads to the assumption that the higher proliferative activity of high-grade neuroendocrine cancers requires a higher metabolic activity and depends on the glycolytic utilization of glucose. The dysregulation of members of the glycolytic system, such as *MAN2B1*, also supports this finding.

MAPK Pathway

One of the most promising results yielding the most hits within the pathway analysis is the mitogen-activated protein kinase (*MAPK*) pathway. Recently, West et al. have

shown that nicotine stimulates tumour growth in NSCLC through *AKT*- and *MAPK*-dependent mechanisms, and that modulation of *AKT* signalling pathways may provide a target for directed therapy (West et al. 2003; Castillo et al. 2004; Song et al. 2007).

The *MAPK* pathway is one of the most important intracellular signalling cascades conserved from yeast to mammals (Widmann et al. 1999; Vicent et al. 2004). MAPKs are intracellular serine/threonine kinases that regulate cell survival and proliferation and may play a role in *KIT* signal transduction (Blackhall et al. 2003). Their three main components are the extracellular signal-regulated kinase (*ERK*), c-jun NH2-terminal kinase (*JNK*) and p38 (Cano and Mahadevan 1995; Su and Karin 1996; Vicent et al. 2004). Activation of any of the *MAPK* family members requires phosphorylation of two regulatory residues (a threonine and a tyrosine) by their upstream kinases (Widmann et al. 1999; Vicent et al. 2004). Dephosphorylation of one or both of these regulatory residues induces deactivation of *MAPK* family members (Vicent et al. 2004).

KIT, AKT (also known as PKB) and *MAPK* are expressed in a high percentage of SCLCs, suggesting that *MAPK* is an independent tumour driver in this malignancy (Blackhall et al. 2003). Activation of this pathway caused a dramatic loss of soft agar cloning ability, suppression of growth capacity, associated with cell accumulation in G1 and G2, and S phase depletion in cell line experiments (Ravi et al. 1998; Ravi et al. 1999).

Additionally, within the G protein-coupled receptors signalling to *MAPK*/*ERK* pathway, we found the currently routinely analysed *KRAS* mutations (p.G12D and p.Q61L, respectively) in more than 10% of LCNECs and about 5% of ACs and SCLCs, with about 30% mutated alleles and a good read quality. Interestingly, these findings are contrary to the results published in a recent paper addressing this

question (Przygodzki et al. 1996). Activating *KRAS* mutations are strongly associated with exposure to tobacco smoke; therefore, an accumulation of *KRAS* mutations in these tumours seems expedient.

PI3K Pathway

The phosphoinositide 3-kinase (PI3K)/Akt/mammalian target of the rapamycin (mTOR) signaling pathway shows significant differences between the four types of pulmonary neuroendocrine tumours investigated in this study.

Abberant activation of the PI3K/Akt/mTOR signaling pathway (Burnett et al. 1998) has been widely investigated in the pathogenesis of many cancers (Yamamoto et al. 2008; Liu et al. 2009; Courtney et al. 2010; Wong et al. 2010; Papadimitrakopoulou 2012; Spoerke et al. 2012) and has also been known to be activated during the early phase of lung cancer onset (West et al. 2004; Jeong et al. 2012), thereby causing cell growth, proliferation, angiogenesis and synthesis of various proteins (Janku et al. 2010; Jeong et al. 2012; Reungwetwattana et al. 2012). Constitutive activation of this pathway also leads to upregulated proliferation, evasion of apoptosis and altered metabolism via the Warburg effect (Spoerke et al. 2012). In addition, increased pathway activity has been associated with resistance to anti-cancer therapies (Myers and Cantley 2010; Spoerke et al. 2012). When PI3K and Akt are activated by the stimulation of various growth factors by transmembrane receptor tyrosine kinases (RTKs), including EGFR, HER2, IGFR, VEGFR and PDGFR (Li et al. 2009), they activate mTOR (Jeong et al. 2012). The activated mTOR in turn regulates eukaryotic initiation factor 4E binding protein-1 and 40S ribosomal protein S6 kinase (p70S6K), which are involved in the regulation of protein synthesis (Janku et al. 2010; Jeong et al. 2012; Reungwetwattana et al. 2012).

PI3K-dependent activity is frequently high because of amplification (Shayesteh et al. 1999) or gain of function mutations of the *PIK3CA* gene (Samuels et al. 2004) as well as loss of function of the *PTEN* tumour supressor gene, a critical negative regulator of this pathway (Sansal and Sellers 2004; Spoerke et al. 2012). It has been reported that *PIK3CA* gene mutation and its amplification are observed in approximately 2% and 12-17% of patients with NSCLC, respectively (Kawano et al. 2006; Kawano et al. 2007; Yamamoto et al. 2008; Jeong et al. 2012). In addition, increased pathway activity has been associated with resistance to anti-cancer therapies (Clark et al. 2002; Wallin et al. 2010; Spoerke et al. 2012).

Furthermore, resistance to apoptosis is an important hallmark of tumour cells (Hanahan and Weinberg 2011; Zhu et al. 2012). Apoptosis of tumour cells is known to be regulated by a variety of signalling pathways, including the PI3K/Akt pathway (Zhu et al. 2012). *AKT* has been shown to regulate apoptosis related proteins such as Bcl-2, Bax and caspase-3 (*CASP3*) and is crucially involved in anticancer drug induced apoptosis of cancer cells (Takeuchi et al. 2005; Lee et al. 2006; Li et al. 2009; Bak et al. 2011; Zhu et al. 2012).

The significance of PI3K signalling for tumour survival and proliferation has led to the development of candidate therapeutics designed to inhibit the activity of pathway components such as PI3K, mTOR and Akt (Spoerke et al. 2012).

TGF-β Pathway

Several malignancies have been screened for the presence of transforming growth factor beta (*TGFB1*) and its receptor (*TGFBR1*), but in human lung cancer the data are very sparse (Damstrup et al. 1993). A few studies have demonstrated that *TGFB1* mRNA was expressed only in NSCLC cell lines (Derynck et al. 1985; Bergh 1988; Soderdahl et al. 1988; Damstrup et al. 1993); in another study all of the ten

SCLC cell lines examined were found to be *TGFB1* mRNA negative (Lagadec et al. 1991; Damstrup et al. 1993). The present data suggest a connection between tumourigenesis and TGF-β signalling in neuroendocrine lung tumours.

TGF-β comprises a family of polypeptides which have been shown to be multifunctional regulators of basic cellular functions such as proliferation, differentiation, cell adhesion and interactions with the extracellular matrix (Massague 1990; Moses 1992; Norgaard et al. 1994). Also angiogenesis and response to hypoxia are regulated by TGF-β dependent signalling mechanisms.

Some carcinomas are resistant to the growth inhibitory effect of TGF-β, which in several cases has been ascribed to a lack of type 2 receptor (RII) (Geiser et al. 1992; Inagaki et al. 1993; Norgaard et al. 1994; Park et al. 1994; Hougaard et al. 1999). Recently, it was shown that TGF-β acts as a growth inhibitor of carcinomas *in vivo*, at least during early tumour growth (Cui et al. 1994; Pierce et al. 1995; Hougaard et al. 1999).

Cell Cycle and Proliferation

Genes regulating the cell cycle and proliferation are deregulated in most human malignant tumours, and also in pulmonary neuroendocrine tumours (Russo et al. 1998; Coe et al. 2006; Husain et al. 2012). mRNA expression of ten genes involved in the regulation of cell cycle and proliferation were investigated: *CDKN2A* (p16/INK4) is a cyclin-dependent kinase inhibitor preventing the phosphorylation of retinoblastoma protein 1 (*RB1*), thus functioning as a major cell cycle inhibitor at the G1 checkpoint (Husain et al. 2012). In this study, *CDKN2A* gene expression showed significant correlations with tumour type, grade and lymph node invasiveness. Coe *et al*. reported segmental loss and decreased expression of *CDKN2A* in NSCLC compared to SCLC (Coe et al. 2006). This is consistent with our findings, as we

detected the highest *CDKN2A* expressions in SCLC. *CDKN2A* also interacts with cyclin-dependent kinase 6 (*CDK6*) by forming a complex (Wang et al. 2013). *CKD6* drives cell cycle progression and inactivates *RB1* by phosphorylation (Russo et al. 1998). Additionally, *CDK6* associates with *CCND1* (cyclin D1), another positive regulator of cell cycle progression and *RB1* phosphorylation (Brambilla et al. 1996). Both *CDK6* and *CCND1* have been reported to be involved in tumourigenesis (Brambilla et al. 1996; Russo et al. 1998; Wang et al. 2013). Our data demonstrate that *CDK6* is expressed significantly more in both TCs and ACs than LCNECs and SCLCs, and *CCND1* expression was inversely correlated with the pathological grading of the tumour.

Apoptosis, BCL2-BAX Ratio, P53 and its Regulation

Genetic alterations and inactivation of the tumour suppressor gene *TP53* are known in most human malignant neoplasias (Brambilla et al. 1996). In our study, *TP53* overexpression was significantly associated with decreased OS. Additionally, we evaluated sequencing data of mutation hotspots in the *TP53* gene locus and found LOF mutations in approximately 90% of SCLC samples, decreasing for LCNEC (ca. 75%), AC (ca. 40%) and TC (ca. 30%). Sequencing data indicates that *TP53* has lost its function, but a negative feedback loop seems to lead to overexpression in these patients in order to compensate for that loss. Therefore, *TP53* expression increases with increasing malignancy of the tumour that correlates with a higher number of *TP53* mutated tumours.

FAS is a mediator of extrinsic apoptosis and recruits several other proteins for that purpose (Oh et al. 2012; Aguirre et al. 2013). After associating with other proteins, it also activates initiator-caspases like *CASP8* and downstream caspases (D'Agati and Perzin 1985; Damstrup et al. 1993). In contrast, *FAS* was reported to also be

involved in cell survival and stress response (Oh et al. 2012). Deregulation of proteins involved in apoptosis was reported to contribute to tumour development and maintenance (Oh et al. 2012; Aguirre et al. 2013). We identified overexpression of *FAS* to be a negative marker for PFS. Furthermore, cleaved caspase-3 immunoexpression correlates with increasing malignancy, indicating a higher potential for apoptotic activity in high-grade NETs. It must be remembered that high-grade tumours use multiple ways to evade apoptosis; therefore, the increased availability of activated *CASP3* did not show an association with increased apoptosis in this subgroup. *CASP8* expression was significantly lower in carcinoids than in carcinomas. Kikuchi *et al*. reported that a knockdown of *CASP8* reduced tumour growth and increased cell death (Kikuchi et al. 2012). They suggested that the protease activity of *CASP8* is essential for tumour maintenance (Kikuchi et al. 2012). Additionally, death-inducing signalling complex (DISC) containing *FAS* and *CASP8* was identified as an essential component of embryonic development in mice (Kikuchi et al. 2012). This might indicate that high-grade tumours with elevated proliferation depend on the protease activity of the DISC.

Furthermore, apoptosis is regulated by *BCL2* and *BAX. BAX* is a mediator of apoptosis, whereas *BCL2* acts inversely (Brambilla et al. 1996; Kobayashi et al. 2004). The *BCL2/BAX* ratio is an adequate tool to assess the likelihood that a given cell will undergo apoptosis (Brambilla et al. 1996; Kobayashi et al. 2004). Higher *BCL2* expression was reported in LCNEC and SCLC in contrast to AC and TC, where higher *BAX* expression was found (Brambilla et al. 1996; Kobayashi et al. 2004). Also in our study, the *BCL2/BAX* ratio increased with tumour type. Carcinoids showed a ratio of nearly 1, whereas carcinomas showed a ratio of ≥1. A ratio close to 1 indicates that apoptosis and proliferation are balanced, whereas elevated ratios indicate a skew towards proliferation. Additionally, *BCL2* was reported as a

prognostic marker in several solid and hematopoietic malignancies (Srivastava and Grizzle 2010). In our study, *BCL2* and *BAX* exhibited no significant correlation with prognosis, but *BCL2* was inversely correlated with the grade of differentiation.

Angiogenesis

Angiogenesis and lymphangiogenesis are important characteristics of aggressive tumours, resulting in the formation of metastases (Harris et al. 2011; Yu et al. 2013). Yu *et al*. reported that increased expression of *VEGFA* and *KDR* (VEGFR(-2)) correlated with progression of the tumour (Yu et al. 2013). In our study, an absence of *KDR* expression was significantly associated with blood vessel invasion, and its expression was only found in tumours without an infiltration of blood vessels. An association of *FIGF* (VEGFD) and *HIF1A* overexpression with disease progression was noted. Yu et al. also identified HIF1A, a transcription factor that regulates genes that respond to hypoxia, as being overexpressed in lung cancer. They proposed that this might be due to the hypoxic environment of a tumour and that this might trigger angiogenesis (Yu et al. 2013). In our study, *HIF1A* was identified as a significant marker for blood vessel invasion. The highest *HIF1A* expression was found in N0-tumours. *FIGF* is an activator of *KDR* and *FLT4* (VEGFR-3) and induces angiogenesis and lymphangiogenesis (Harris et al. 2011). In our study, *FIGF* and *FLT4* correlated significantly with tumour type, and higher expression was more frequent in carcinoids than in carcinomas. Expression constantly decreased with poorer differentiation.

Neuroendocrine Markers

Routine immunohistochemistry analysis of neuroendocrine tumours relies on the detection of specific molecules, e.g., *NCAM1* (CD56), *SYP* and chromogranin A

(*CHGA*) (Kashiwagi et al. 2012). *CHGA* and *SYP* correlated most significantly with grade of differentiation and tumour type. Both showed higher expression in carcinoids than in carcinomas, which is in line with our findings of a stronger immunoexpression of *CHGA* in TC/AC compared to neuroendocrine carcinomas. Similar results were also reported by Jensen *et al*. (Jensen et al. 1990). *SYP* showed a significantly higher expression in women than men. Additionally, low grade tumours showed increased expression of *SYP* and *CHGA*. High *CHGA* expression correlated with improved survival and with low lymphatic metastasis potential.

Significant correlations regarding tumour type and grade were also observed for *RTN1*. *RTN1* is involved in neuronal and neuroendocrine differentiation in tumours and normal tissue (Di Sano et al. 2007). It was reported that *RTN1* may act as a pro-apoptotic protein, but the function of this process is poorly understood (Pinton et al. 2001; Di Sano et al. 2003). Our results indicate that *RTN1* expression decreases with lower grade of differentiation, and a higher expression was observed in carcinoids compared to carcinomas. Fenretinide is a chemotherapeutical agent that induces apoptosis in tumours with *RTN1* overexpression (Di Sano et al. 2007). It might enter further clinical development and may be proposed as a future drug for carcinoids with elevated *RTN1* expression.

Elevated expression of the neurotensin receptor 1 (*NTSR1*) and *NTS* were correlated with poorer survival rates and progression of the disease in stage I lung adenocarcinomas (Alifano et al. 2010). In our study, high *NTS* expression was associated with shortened PFS.

Low *GABBR2* expression correlated with poor response to treatment and worse PFS. Several studies addressed the function of this receptor for GABA and its role in synaptic transmission in the nervous system (Balasubramanian et al. 2007; Hannan

et al. 2011), but few studies investigated the role of *GABBR2* in cancerogenesis (Stein et al. 2010).

SEMA3B is a potential tumour suppressor in lung and breast cancer, involved in apoptosis induction (Castro-Rivera et al. 2008). It is frequently silenced (allelic loss and/or epigenetic silencing) in NSCLC, ovarian and breast cancer (Castro-Rivera et al. 2008). In our study, *SEMA3B* expression was detected in all pulmonary neuroendocrine tumours. Notably, a higher expression was found in carcinoids than in carcinomas.

NCAM1 showed similar results to *SEMA3B* for expression and tumour type; these relations were found on both an mRNA and protein level. *NCAM1* was reported to be expressed in all neuroendocrine tumours and is used as a routine marker for IHC (Kashiwagi et al. 2012). Additionally, Iqbal *et al.* suggested that elevated *SOX4* expression might induce *NCAM1* expression in human myeloma (Iqbal et al. 2010). In our study, *NCAM1* and *SOX4* mRNA expression showed an inverted correlation with each other.

Transcription Factors and Transcriptional Regulation

OCT4 (*POU5F1*) is a transcription factor that is necessary to maintain and initiate the pluripotent state of stem cells. OCT4 and *SOX2* (as well as *KLF4* and *MYC*) are also essential for reprogramming fibroblasts to obtain induced pluripotent stem cells (Yamanaka and Blau 2010). OCT4 was identified as a tumorigenic factor in several cancer types, but its function in tumourigenesis is not fully understood (Ikushima et al. 2011). We found associations between OCT4 expression and both OS and PFS. High OCT4 expression correlated with reduced progression-free survival time and lower survival rates. These results fit well with a study proving that a knockdown in OCT4 increased sensitivity to chemotherapy (Ikushima et al. 2011).

SOX4 expression correlates with *NCAM1* (CD56) expression and is a proto-oncogene in a variety of tumours, including lung cancer (Castillo et al. 2012; Vervoort et al. 2012). It was linked to tumour development and progression by inhibiting apoptosis, promoting cell survival and facilitating the development of metastases (Castillo et al. 2012; Vervoort et al. 2012). In our study, *SOX4* was most significant for grade of differentiation and tumour type, which were in line with reported results.

SOX11 shares structural and functional characteristics with SOX4 and was also reported to be overexpressed in tumours (Dy et al. 2008). We noted significant associations between *SOX11* expression and decreased OS. However, detectable expression was only found in SCLC.

PAX6 is a transcription factor which plays a crucial role during organ development, being involved in crucial biological processes such as proliferation, apoptosis and differentiation, as well as in tumourigenesis (Mascarenhas et al. 2009; Zong et al. 2011). In bladder cancer and prostate cancer, *PAX6* was reported as a potential tumour suppressor (Hellwinkel et al. 2008; Shyr et al. 2010). It is supposed that *PAX6* plays an ambiguous role depending on the cancer type and development status of the tumour (Hellwinkel et al. 2008; Mascarenhas et al. 2009; Shyr et al. 2010; Zong et al. 2011). In our study, increased *PAX6* expression correlated with tumour type, grade of differentiation, increased metastatic potential of the tumour, infiltration of lymph nodes and decreased OS.

PAX5 is a transcription factor involved in the development of B cells, organs, differentiation of tissue and tumourigenesis (Song et al. 2010; Li et al. 2012). In our study, elevated expression of *PAX5* correlated significantly with poorly differentiated tumours and lymphatic metastasis. Furthermore, *PAX5* and *PAX6* regulate the expression of *MET* (Mascarenhas et al. 2009; Song et al. 2010). Importantly, two

markers (*PAX6*, *SOX11*) were found to distinguish SCLCs from other neuroendocrine tumours.

Additional Growth Factor Receptors

In addition to *VEGFR*s and *KDR* (discussed above), *EGFR* is also a receptor tyrosine kinase involved in proliferation and cell survival (Takeda et al. 2013). For *EGFR*-inhibition, several tyrosine kinase inhibitors (TKIs) exist (Johnson et al. 2013; Takeda et al. 2013). In our study, mRNA expression analysis of *EGFR* showed higher expression in carcinoids than in carcinomas. Reduced expression was observed in more aggressive tumours based on grade of differentiation, stage, invasion into lymph nodes and blood vessels. Elevated expression was also more common in female than male patients. *FGFR1* is a tyrosine kinase that contributes to cell development. Alterations in this gene were reported in several cancer types (Weiss et al. 2010; Dutt et al. 2011). In addition, potential TKIs exist for *FGFR1* (Weiss et al. 2010; Dutt et al. 2011). In our study, *FGFR1* was expressed significantly more in carcinoids than carcinomas.

ALK is another receptor tyrosine kinase mediating neuronal development and differentiation (Dirks et al. 2002). Chromosomal translocations of the *ALK* gene into the loci of housekeeping genes can lead to constant expression due to the reference gene promoter and reportedly contributes to tumourigenesis (Dirks et al. 2002; Camidge et al. 2012). In our study, significantly elevated *ALK* mRNA expression was found in low-grade tumours, whereas high-grade tumours lacked *ALK* expression. Potent inhibitors exist for *ALK* inhibition (Camidge et al. 2012), which in this context could be considered for the treatment of chemoresistent low-grade neuroendocrine tumours.

Growth Factor Signalling via AKT/MTOR

MTOR is a kinase involved in crucial cellular processes like cell growth, proliferation and differentiation by regulating downstream kinases like *AKT* and *S6K* (Zoncu et al. 2011; Agrawal et al. 2012). *RICTOR* and *RPTOR* form complexes with *MTOR*, known as MTORC2 and MTORC1, respectively. MTORC1 is involved in translation, transcription, stress response and other important cell functions (Zoncu et al. 2011). MTORC2 is an important protein for actin regulation (Jacinto et al. 2004). MTORC1/2 are involved in cancer development and maintenance (Zoncu et al. 2011). In our study, expression of *RICTOR* and *RPTOR* was reduced in LCNEC compared to the other entities. Additionally, *RICTOR* exhibited elevated expression in TCs. In conclusion, the investigation of the accessory proteins of each MTOR-complex can reveal more useful information than the investigation of MTOR alone for lung tumours with neuroendocrine features. Additionally, MTORC1 is sensitive to rapamycin treatment, whereas MTORC2 showed insensitivity to this inhibition (Jacinto et al. 2004; Zoncu et al. 2011; Agrawal et al. 2012).

Genes in the *MET*-pathway are overexpressed and active as oncogenes in several types of cancer (Mascarenhas et al. 2009; Zong et al. 2011). G*AB1* is a mediator for cell survival, motility and morphogenesis and acts as an anti-apoptotic regulator when it has caspase-cleaved *GAB1* status (Le Goff et al. 2012). In our study, *GAB1* showed higher expression in low-grade than in high-grade tumours.

MET itself showed no differential expression in the investigated tumour types, which is in accordance with another study (Song et al. 2010).

Folate Metabolism

The folate metabolism is mandatory for normal cell proliferation and replication. Some antifolates such as fluoropyrimidines or pemetrexed inhibit thymidylate

synthetase (*TYMS)*, ultimately resulting in cell cycle arrest (Ceppi et al. 2012; Wilson et al. 2012). In our study, *TYMS* expression was correlated with poorer differentiation. *FPGS* adds glutamate residues to folates and antifolates, thereby retaining them inside the cell (Odin et al. 2003; Mairinger et al. 2013). Loss of *FPGS* activity was reported to contribute to chemotherapy resistance in a variety of human malignancies (Liani et al. 2003; Stark et al. 2009; Christoph et al. 2012; Mairinger et al. 2013; Mairinger et al. 2013). In our study, *FPGS* expression was higher in carcinoids than in carcinomas and lymph node metastasis correlated inversely with its expression. Therefore, *FPGS* expression is a potential marker to distinguish metastasizing carcinoids from carcinoids that will not metastasize. Additionally, elevated *FPGS* expression is a marker for good prognosis.

FOLR1 is a glycoprotein which transports folates through the cell membrane. This receptor is upregulated in several cancer types (Parker et al. 2005; Nunez et al. 2012). Early and locally advanced adenocarcinomas, large cell carcinomas and carcinoid tumours express this receptor, but its expression in squamous cell carcinomas and SCLCs has rarely been observed (Franklin et al. 1994; Nunez et al. 2012; O'Shannessy et al. 2012). In our study, expression in carcinoids was elevated compared to carcinomas and the expression in SCLC was at a minimum. Furthermore, decreasing *FOLR1* expression correlated significantly with aggressiveness of the tumour in terms of lymph node metastasis. *FOLR1* expression also exhibited prognostic and predictive value. Elevated expression was a marker for progression, whereas it was a good marker for prolonged survival.

DNA Repair Mechanisms

DNA mismatch repair is a crucial cell feature for maintaining accurate DNA replication during cell division (Kouso et al. 2008; Bischoff et al. 2012). Loss of

function of mismatch repair genes results in various aberrations like genomic instability, increased DNA mutations and microsatellite instability (Kouso et al. 2008; Bischoff et al. 2012).

As we were able to show in malignant pleural mesothelioma, *ERCC1* is an important member of this DNA repair machinery, removing cisplatin-induced DNA damages (de Jong et al. 2012; Ting et al. 2013). *ERCC1* mRNA expression was higher in the carcinoid group than in high-grade carcinomas.

MLH1 and *MSH6* are further mismatch repair genes, which were found altered in several tumour types (de Jong et al. 2012; Ting et al. 2013). In our study, *MLH1* expression was elevated in carcinoids compared to carcinomas and *MSH6* showed the highest expression in SCLC.

XRCC1 is an important key protein in the base-excision repair pathway and mediates repair of single-strand breaks (Della-Maria et al. 2012; Erculj et al. 2012). *XRCC1* mRNA expression was significant for tumour type, grade of differentiation and lowered expression correlated with lymphatic vessel invasion. That is consistent with a report by Erčulj *et al*. (Erculj et al. 2012).

Expression and Activity of the 26S-Proteasome

Upregulation of the proteasomal subunits *PSMA6, PSMB4, PSMC2* and *PSMD12* was demonstrated in hepatocellular carcinomas of p21-HBx transgenic mice by using MALDI-TOF analysis (Cui et al. 2006). By applying small interfering (si) RNA screening in human glioblastoma cells, Thaker et al. were able to identify 55 survival genes encoding proteases, kinases and transferases, of which twelve were subunits of the 26S-proteasome, including *PSMB4* (Thaker et al. 2009), suggesting a role for different gene expression of proteasomal subunits in the development of various malignant tumours. Our study demonstrates that gene expression of proteasomal

subunits is generally increased in pulmonary neuroendocrine tumours compared to non-tumorous lung tissue. In particular, *PSMB4* is associated with the potential for proliferation in these neoplasias and differs significantly between the different subgroups of pulmonary NET. *PSMB4* expression levels interfere with numerous cellular processes involved in malignant transformations, such as cell cycle regulation, proliferation and apoptosis, promoting further malignant transformation along with EMT. Present studies identified increased proteasome and especially *PSMB4* expression in different malignant tumours, suggesting it may be a survival gene in cancer (Kumatori et al. 1990; Kanayama et al. 1991; Choi 2001; Cui et al. 2006; Thaker et al. 2009). In particular, the ubiquitin-proteasome system has been shown to play a complex role in the regulation of apoptosis, in which inhibition of the system has both pro-apoptotic and anti-apoptotic effects (Naujokat and Hoffmann 2002). The activation of NFκB by proteasomes through degradation of IκB induces the expression of anti-apoptotic members of the Bcl-2 family (Catz and Johnson 2001). Additionally, proteasomes degrade pro-apoptotic proteins, including *BAX* and *BID* (Breitschopf et al. 2000; Li and Dou 2000).

A study into the inhibition of neuroendocrine lung tumours with bortezomib (Velcade®), the first and currently only FDA-approved proteasome inhibition, has recently begun in our laboratory.

Conclusion

To summarize the data generated for this doctoral thesis and reviewing the literature, we hypothesise that there is adequate evidence that neuroendocrine tumours should be viewed as an overall biological family of neoplasms. Despite the currently undisputed traditional morphological view and classification into carcinoids, LCNECs and SCLCs, our results will hopefully spur a re-evaluation of the current distinction

between SCLCs and NSCLCs by complementing it with a more biologically driven classification. The family of pulmonary neuroendocrine tumours, although showing different morphological presentation, age of onset and clinical outcome, can be biologically well distinguished from all other forms of lung cancers. Grouping LCNECs with SCLCs may allow for a more tumour adapted oncological management of those conditions. Notably, carcinoids should be separated from pulmonary neuroendocrine carcinomas, forming a different subgroup of NE tumours. Nevertheless, both subtypes of pulmonary neuroendocrine tumours cluster together and can be clearly separated from other forms of lung neoplasia. A more profound biological understanding of both carcinoids and neuroendocrine lung carcinomas might increase the chance of finding novel therapeutic targets, thereby leading to a more personalized therapeutic concept for this group of malignancies.

5. Results at a Glance

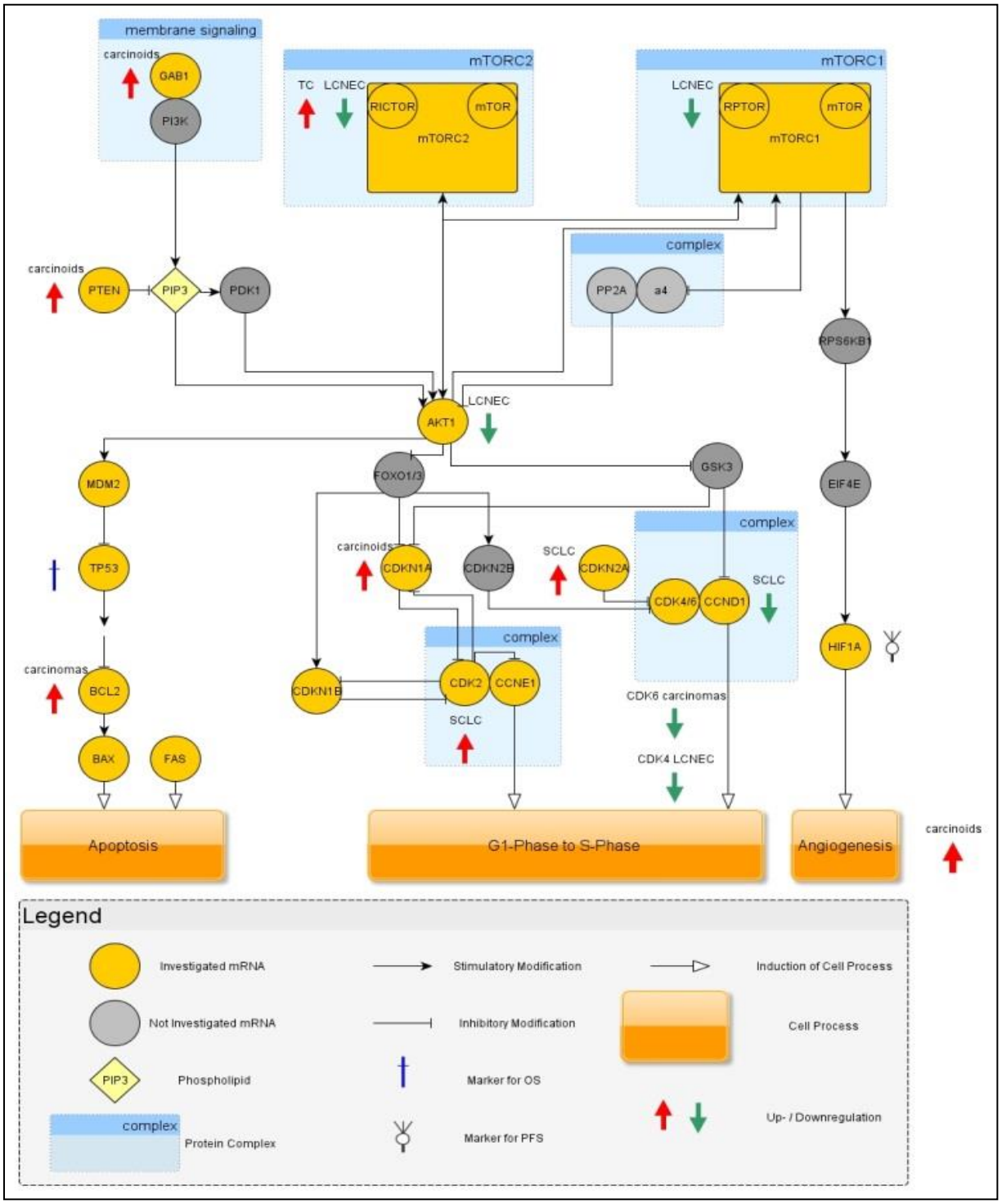

Figure 31 Overview of differences in signalling pathways and cellular processes between pulmonary neuroendocrine lung tumours. Red arrows indicate activation, green arrows downregulation of different key players for important cellular pathways. Also markers important for prognosis (OS/PFS) are highlighted. Of note are the different entries into the cell cycle between carcinoids and carcinomas and the strong activation of angiogenesis in pulmonary carcinoid tumours.

6. Synopsis

Lung cancer is the leading cause of cancer-related deaths worldwide, accounting for more than 40,000 deaths each year in Germany. Twenty-five percent of all lung tumours belong to the group of neuroendocrine tumours, encompassing typical (TC) and atypical carcinoids (AC), large-cell neuroendocrine carcinoma (LCNEC) and small-cell lung cancer (SCLC). Even though all four subgroups share some morphological and molecular properties, it is still unclear whether they are different biological entities or form one distinct tumour entity displaying different grades of differentiation. They were previously reported to arise from serotonin producing pulmonary neuroendocrine cells (PNEC). It is suggested that LCNEC and SCLC originate from the same or similar precursor cells. However, it remains unclear how carcinoids can be integrated into this scheme.

In order to address this question, 74 representative tumour specimens were used for sequencing analysis performed on a MiSeq instrument covering the 221 most important mutation hotspots related to human neoplasias. Additionally, mRNA-expression profiles of 80 tumour samples were determined for 91 selected genes using NanoString nCounter technology. Furthermore, three unequivocal samples of each tumour entity were chosen to be tested for their miRNA signature via 384 well TaqMan low-density array real-time qPCR for the expression of 768 unique miRNAs. Finally, the pulmonary neuroendocrine tumour samples were analysed via TaqMan qPCR and immunohistochemistry for expression of the five most important subunits of the 26S proteasome.

44 miRNAs were identified which showed a significantly different miRNA expression between the subtypes of pulmonary neuroendocrine tumours. For 12 miRNAs, the difference was highly significant ($p<0.01$). Eight of these were negatively correlated with the grade of tumour biology, the other four were positively correlated. Six miRNAs are significantly associated with survival. The mRNA expression analysis showed 48 significant correlations with tumour type. Sixteen most significant ($p\leq0.001$), 20 highly significant ($p\leq0.01$) and 12 significant ($p\leq0.05$) candidates were identified. Nine significant correlations with progression-free survival were found. Overall survival correlated significantly with nine genes. Of the 643 variants that passed the applied filter processing as described above, 122 variants were related to TC, 150 to AC, 164 to LCNEC and the final 207 variants were detected in the SCLC samples. We found a number of molecular features associated with pulmonary neuroendocrine tumours.

In summary, we hypothesise that there is adequate evidence that neuroendocrine tumours should be considered an overall biological family of neoplasms. The family of pulmonary neuroendocrine tumours can be biologically well distinguished from all other forms of lung cancers. Additionally, better biological understanding of carcinoids and neuroendocrine lung carcinomas will increase the chance of finding new drug targets, maybe resulting in a more personalized therapeutic concept for this group of malignancies.

7. References

1. Jett, J. R. and D. E. Midthun (2004). "Screening for lung cancer: current status and future directions: Thomas A. Neff lecture." Chest 125(5 Suppl): 158S-162S.
2. Eramo, A., F. Lotti, G. Sette, E. Pilozzi, M. Biffoni, A. Di Virgilio, C. Conticello, L. Ruco, C. Peschle and R. De Maria (2008). "Identification and expansion of the tumorigenic lung cancer stem cell population." Cell Death Differ 15(3): 504-514.
3. Mallick, R., S. K. Patnaik and S. Yendamuri (2010). "MicroRNAs and lung cancer: Biology and applications in diagnosis and prognosis." J Carcinog 9.
4. Brambilla, C., F. Fievet, M. Jeanmart, F. de Fraipont, S. Lantuejoul, V. Frappat, G. Ferretti, P. Y. Brichon and D. Moro-Sibilot (2003). "Early detection of lung cancer: role of biomarkers." Eur Respir J Suppl 39: 36s-44s.
5. Boyle, P., Lewin, B. (2008). World Cancer Report 2008. Lyon, International Agency for research on cancer.
6. Rekhtman, N. (2010). "Neuroendocrine tumors of the lung: an update." Arch Pathol Lab Med 134(11): 1628-1638.
7. Takei, H., H. Asamura, A. Maeshima, K. Suzuki, H. Kondo, T. Niki, T. Yamada, R. Tsuchiya and Y. Matsuno (2002). "Large cell neuroendocrine carcinoma of the lung: a clinicopathologic study of eighty-seven cases." J Thorac Cardiovasc Surg 124(2): 285-292.
8. Swarts, D. R., F. C. Ramaekers and E. J. Speel (2012). "Molecular and cellular biology of neuroendocrine lung tumors: evidence for separate biological entities." Biochim Biophys Acta 1826(2): 255-271.
9. Travis, W. D., W. Rush, D. B. Flieder, R. Falk, M. V. Fleming, A. A. Gal and M. N. Koss (1998). "Survival analysis of 200 pulmonary neuroendocrine tumors with clarification of criteria for atypical carcinoid and its separation from typical carcinoid." Am J Surg Pathol 22(8): 934-944.
10. Beasley, M. B., F. B. Thunnissen, E. Brambilla, P. Hasleton, R. Steele, S. P. Hammar, T. V. Colby, M. Sheppard, Y. Shimosato, M. N. Koss, R. Falk and W. D. Travis (2000). "Pulmonary atypical carcinoid: predictors of survival in 106 cases." Hum Pathol 31(10): 1255-1265.
11. Fink, G., T. Krelbaum, A. Yellin, D. Bendayan, M. Saute, M. Glazer and M. R. Kramer (2001). "Pulmonary carcinoid: presentation, diagnosis, and outcome in 142 cases in Israel and review of 640 cases from the literature." Chest 119(6): 1647-1651.
12. Thomas, C. F., Jr., H. D. Tazelaar and J. R. Jett (2001). "Typical and atypical pulmonary carcinoids : outcome in patients presenting with regional lymph node involvement." Chest 119(4): 1143-1150.
13. Cardillo, G., F. Sera, M. Di Martino, P. Graziano, R. Giunti, L. Carbone, F. Facciolo and M. Martelli (2004). "Bronchial carcinoid tumors: nodal status and long-term survival after resection." Ann Thorac Surg 77(5): 1781-1785.
14. Pelosi, G., A. Scarpa, G. Puppa, G. Veronesi, L. Spaggiari, F. Pasini, P. Maisonneuve, A. Iannucci, G. Arrigoni and G. Viale (2005). "Alteration of the E-cadherin/beta-catenin cell adhesion system is common in pulmonary neuroendocrine tumors and is an independent predictor of lymph node metastasis in atypical carcinoids." Cancer 103(6): 1154-1164.
15. Asamura, H., T. Kameya, Y. Matsuno, M. Noguchi, H. Tada, Y. Ishikawa, T. Yokose, S. X. Jiang, T. Inoue, K. Nakagawa, K. Tajima and K. Nagai (2006). "Neuroendocrine neoplasms of the lung: a prognostic spectrum." J Clin Oncol 24(1): 70-76.
16. Garcia-Yuste, M., J. M. Matilla, A. Cueto, J. M. Paniagua, G. Ramos, M. A. Canizares and I. Muguruza (2007). "Typical and atypical carcinoid tumours: analysis of the experience of the Spanish Multi-centric Study of Neuroendocrine Tumours of the Lung." Eur J Cardiothorac Surg 31(2): 192-197.

17. Rea, F., G. Rizzardi, A. Zuin, G. Marulli, S. Nicotra, R. Bulf, M. Schiavon and F. Sartori (2007). "Outcome and surgical strategy in bronchial carcinoid tumors: single institution experience with 252 patients." Eur J Cardiothorac Surg 31(2): 186-191.
18. Travis, W. D. (2009). "Lung tumours with neuroendocrine differentiation." Eur J Cancer 45 Suppl 1: 251-266.
19. Scott, W. J. (2003). "Surgical treatment of other bronchial tumors." Chest Surg Clin N Am 13(1): 111-128.
20. Travis, W. D., World Health Organization., International Agency for Research on Cancer., International Association for the Study of Lung Cancer. and International Academy of Pathology. (2004). Pathology and genetics of tumours of the lung, pleura, thymus and heart. Lyon
21. Oxford, IARC Press
22. Oxford University Press (distributor).
23. Govindan, R., N. Page, D. Morgensztern, W. Read, R. Tierney, A. Vlahiotis, E. L. Spitznagel and J. Piccirillo (2006). "Changing epidemiology of small-cell lung cancer in the United States over the last 30 years: analysis of the surveillance, epidemiologic, and end results database." J Clin Oncol 24(28): 4539-4544.
24. Zhu, C. Q., W. Shih, C. H. Ling and M. S. Tsao (2006). "Immunohistochemical markers of prognosis in non-small cell lung cancer: a review and proposal for a multiphase approach to marker evaluation." J Clin Pathol 59(8): 790-800.
25. Bensch, K. G., B. Corrin, R. Pariente and H. Spencer (1968). "Oat-cell carcinoma of the lung. Its origin and relationship to bronchial carcinoid." Cancer 22(6): 1163-1172.
26. Warburton, D., M. Schwarz, D. Tefft, G. Flores-Delgado, K. D. Anderson and W. V. Cardoso (2000). "The molecular basis of lung morphogenesis." Mech Dev 92(1): 55-81.
27. Boers, J. E., J. L. den Brok, J. Koudstaal, J. W. Arends and F. B. Thunnissen (1996). "Number and proliferation of neuroendocrine cells in normal human airway epithelium." Am J Respir Crit Care Med 154(3 Pt 1): 758-763.
28. Linnoila, R. I. (2006). "Functional facets of the pulmonary neuroendocrine system." Lab Invest 86(5): 425-444.
29. Cutz, E. and A. Jackson (1999). "Neuroepithelial bodies as airway oxygen sensors." Respir Physiol 115(2): 201-214.
30. Jones, M. H., C. Virtanen, D. Honjoh, T. Miyoshi, Y. Satoh, S. Okumura, K. Nakagawa, H. Nomura and Y. Ishikawa (2004). "Two prognostically significant subtypes of high-grade lung neuroendocrine tumours independent of small-cell and large-cell neuroendocrine carcinomas identified by gene expression profiles." Lancet 363(9411): 775-781.
31. Finkelstein, S. D., T. Hasegawa, T. Colby and S. A. Yousem (1999). "11q13 allelic imbalance discriminates pulmonary carcinoids from tumorlets. A microdissection-based genotyping approach useful in clinical practice." Am J Pathol 155(2): 633-640.
32. D'Agati, V. D. and K. H. Perzin (1985). "Carcinoid tumorlets of the lung with metastasis to a peribronchial lymph node. Report of a case and review of the literature." Cancer 55(10): 2472-2476.
33. Arioglu, E., J. Doppman, M. Gomes, D. Kleiner, D. Mauro, C. Barlow and D. A. Papanicolaou (1998). "Cushing's syndrome caused by corticotropin secretion by pulmonary tumorlets." N Engl J Med 339(13): 883-886.
34. Liu, S. M., H. H. Wu, C. J. Wu, C. L. Kuo and L. R. Mo (2003). "Adrenocorticotropin-producing pulmonary tumorlets with lymph node metastasis." Pathol Int 53(12): 883-886.
35. Lantuejoul, S., D. Salameire, C. Salon and E. Brambilla (2009). "Pulmonary preneoplasia--sequential molecular carcinogenetic events." Histopathology 54(1): 43-54.
36. Gosney, J. R., I. J. Williams, A. R. Dodson and C. S. Foster (2011). "Morphology and antigen expression profile of pulmonary neuroendocrine cells in reactive proliferations and diffuse idiopathic pulmonary neuroendocrine cell hyperplasia (DIPNECH)." Histopathology 59(4): 751-762.

37. Toyooka, S., K. O. Toyooka, R. Maruyama, A. K. Virmani, L. Girard, K. Miyajima, K. Harada, Y. Ariyoshi, T. Takahashi, K. Sugio, E. Brambilla, M. Gilcrease, J. D. Minna and A. F. Gazdar (2001). "DNA methylation profiles of lung tumors." Mol Cancer Ther 1(1): 61-67.
38. Granberg, D., E. Wilander, K. Oberg and B. Skogseid (1999). "Decreased survival in patients with CD44-negative typical bronchial carcinoid tumors." Int J Cancer 84(5): 484-488.
39. Gorgoulis, V. G., L. V. Vassiliou, P. Karakaidos, P. Zacharatos, A. Kotsinas, T. Liloglou, M. Venere, R. A. Ditullio, Jr., N. G. Kastrinakis, B. Levy, D. Kletsas, A. Yoneta, M. Herlyn, C. Kittas and T. D. Halazonetis (2005). "Activation of the DNA damage checkpoint and genomic instability in human precancerous lesions." Nature 434(7035): 907-913.
40. Brambilla, E., S. Gazzeri, S. Lantuejoul, J. L. Coll, D. Moro, A. Negoescu and C. Brambilla (1998). "p53 mutant immunophenotype and deregulation of p53 transcription pathway (Bcl2, Bax, and Waf1) in precursor bronchial lesions of lung cancer." Clin Cancer Res 4(7): 1609-1618.
41. Wong, A. J., J. M. Ruppert, J. Eggleston, S. R. Hamilton, S. B. Baylin and B. Vogelstein (1986). "Gene amplification of c-myc and N-myc in small cell carcinoma of the lung." Science 233(4762): 461-464.
42. Takahashi, T., Y. Obata, Y. Sekido, T. Hida, R. Ueda, H. Watanabe, Y. Ariyoshi and T. Sugiura (1989). "Expression and amplification of myc gene family in small cell lung cancer and its relation to biological characteristics." Cancer Res 49(10): 2683-2688.
43. Travis, W. D., B. E., M.-H. H. K. and H. C. C. (2004). World Health Organization International Histological Classification of Tumours. Pathology and Genetics of Tumours of the Lung, Pleura, Thymus and Heart. Lyon, IARC Press.
44. Travis, W. D., R. I. Linnoila, M. G. Tsokos, C. L. Hitchcock, G. B. Cutler, Jr., L. Nieman, G. Chrousos, H. Pass and J. Doppman (1991). "Neuroendocrine tumors of the lung with proposed criteria for large-cell neuroendocrine carcinoma. An ultrastructural, immunohistochemical, and flow cytometric study of 35 cases." Am J Surg Pathol 15(6): 529-553.
45. Hirsch, F. R., M. J. Matthews and R. Yesner (1982). "Histopathologic classification of small cell carcinoma of the lung: comments based on an interobserver examination." Cancer 50(7): 1360-1366.
46. Jagoe, R., J. H. Steel, V. Vucicevic, N. Alexander, S. Van Noorden, R. Wootton and J. M. Polak (1991). "Observer variation in quantification of immunocytochemistry by image analysis." Histochem J 23(11-12): 541-547.
47. Jarlov, A. E. (2000). "Observer variation in the diagnosis of thyroid disorders. Criteria for and impact on diagnostic decision-making." Dan Med Bull 47(5): 328-339.
48. Travis, W. D., A. A. Gal, T. V. Colby, D. S. Klimstra, R. Falk and M. N. Koss (1998). "Reproducibility of neuroendocrine lung tumor classification." Hum Pathol 29(3): 272-279.
49. den Bakker, M. A., S. Willemsen, K. Grunberg, L. A. Noorduijn, M. F. van Oosterhout, R. J. van Suylen, W. Timens, B. Vrugt, A. Wiersma-van Tilburg and F. B. Thunnissen (2010). "Small cell carcinoma of the lung and large cell neuroendocrine carcinoma interobserver variability." Histopathology 56(3): 356-363.
50. Meert, A. P., B. Martin, P. Delmotte, T. Berghmans, J. J. Lafitte, C. Mascaux, M. Paesmans, E. Steels, J. M. Verdebout and J. P. Sculier (2002). "The role of EGF-R expression on patient survival in lung cancer: a systematic review with meta-analysis." Eur Respir J 20(4): 975-981.
51. Mascaux, C., N. Iannino, B. Martin, M. Paesmans, T. Berghmans, M. Dusart, A. Haller, P. Lothaire, A. P. Meert, S. Noel, J. J. Lafitte and J. P. Sculier (2005). "The role of RAS oncogene in survival of patients with lung cancer: a systematic review of the literature with meta-analysis." Br J Cancer 92(1): 131-139.
52. Nakamura, H., N. Kawasaki, M. Taguchi and K. Kabasawa (2005). "Association of HER-2 overexpression with prognosis in nonsmall cell lung carcinoma: a metaanalysis." Cancer 103(9): 1865-1873.

53. Steels, E., M. Paesmans, T. Berghmans, F. Branle, F. Lemaitre, C. Mascaux, A. P. Meert, F. Vallot, J. J. Lafitte and J. P. Sculier (2001). "Role of p53 as a prognostic factor for survival in lung cancer: a systematic review of the literature with a meta-analysis." Eur Respir J 18(4): 705-719.
54. Martin, B., M. Paesmans, C. Mascaux, T. Berghmans, P. Lothaire, A. P. Meert, J. J. Lafitte and J. P. Sculier (2004). "Ki-67 expression and patients survival in lung cancer: systematic review of the literature with meta-analysis." Br J Cancer 91(12): 2018-2025.
55. Martin, B., M. Paesmans, T. Berghmans, F. Branle, L. Ghisdal, C. Mascaux, A. P. Meert, E. Steels, F. Vallot, J. M. Verdebout, J. J. Lafitte and J. P. Sculier (2003). "Role of Bcl-2 as a prognostic factor for survival in lung cancer: a systematic review of the literature with meta-analysis." Br J Cancer 89(1): 55-64.
56. Gridelli, C., A. Rossi, G. Airoma, R. Bianco, R. Costanzo, B. Daniele, G. D. Chiara, G. Grimaldi, L. Irtelli, P. Maione, A. Morabito, F. V. Piantedosi and F. Riccardi (2012). "Treatment of pulmonary neuroendocrine tumours: State of the art and future developments." Cancer Treat Rev.
57. Gridelli, C., A. Rossi, G. Airoma, R. Bianco, R. Costanzo, B. Daniele, G. D. Chiara, G. Grimaldi, L. Irtelli, P. Maione, A. Morabito, F. V. Piantedosi and F. Riccardi (2013). "Treatment of pulmonary neuroendocrine tumours: State of the art and future developments." Cancer Treat Rev 39(5): 466-472.
58. Ducrocq, X., P. Thomas, G. Massard, P. Barsotti, R. Giudicelli, P. Fuentes and J. M. Wihlm (1998). "Operative risk and prognostic factors of typical bronchial carcinoid tumors." Ann Thorac Surg 65(5): 1410-1414.
59. Luckraz, H., K. Amer, L. Thomas, A. Gibbs and E. G. Butchart (2006). "Long-term outcome of bronchoscopically resected endobronchial typical carcinoid tumors." J Thorac Cardiovasc Surg 132(1): 113-115.
60. Brokx, H. A., E. K. Risse, M. A. Paul, K. Grunberg, R. P. Golding, P. W. Kunst, J. P. Eerenberg, J. C. van Mourik, P. E. Postmus, W. J. Mooi and T. G. Sutedja (2007). "Initial bronchoscopic treatment for patients with intraluminal bronchial carcinoids." J Thorac Cardiovasc Surg 133(4): 973-978.
61. Mackley, H. B. and G. M. Videtic (2006). "Primary carcinoid tumors of the lung: a role for radiotherapy." Oncology (Williston Park) 20(12): 1537-1543; discussion 1544-1535, 1549.
62. Rossi, G., A. Cavazza, A. Marchioni, L. Longo, M. Migaldi, G. Sartori, N. Bigiani, L. Schirosi, C. Casali, U. Morandi, N. Facciolongo, A. Maiorana, M. Bavieri, L. M. Fabbri and E. Brambilla (2005). "Role of chemotherapy and the receptor tyrosine kinases KIT, PDGFRalpha, PDGFRbeta, and Met in large-cell neuroendocrine carcinoma of the lung." J Clin Oncol 23(34): 8774-8785.
63. Zacharias, J., A. G. Nicholson, G. P. Ladas and P. Goldstraw (2003). "Large cell neuroendocrine carcinoma and large cell carcinomas with neuroendocrine morphology of the lung: prognosis after complete resection and systematic nodal dissection." Ann Thorac Surg 75(2): 348-352.
64. Rinaldi, M., C. Cauchi and C. Gridelli (2006). "First line chemotherapy in advanced or metastatic NSCLC." Ann Oncol 17 Suppl 5: v64-67.
65. Vansteenkiste, J., D. De Ruysscher, W. E. Eberhardt, E. Lim, S. Senan, E. Felip and S. Peters (2013). "Early and locally advanced non-small-cell lung cancer (NSCLC): ESMO Clinical Practice Guidelines for diagnosis, treatment and follow-up." Ann Oncol 24 Suppl 6: vi89-98.
66. Filosso, P. L., E. Ruffini, A. Oliaro, E. Papalia, G. Donati and O. Rena (2002). "Long-term survival of atypical bronchial carcinoids with liver metastases, treated with octreotide." Eur J Cardiothorac Surg 21(5): 913-917.
67. Waldherr, C., M. Pless, H. R. Maecke, T. Schumacher, A. Crazzolara, E. U. Nitzsche, A. Haldemann and J. Mueller-Brand (2002). "Tumor response and clinical benefit in neuroendocrine tumors after 7.4 GBq (90)Y-DOTATOC." J Nucl Med 43(5): 610-616.
68. Srirajaskanthan, R., C. Toumpanakis, A. Karpathakis, L. Marelli, A. M. Quigley, M. Dusmet, T. Meyer and M. E. Caplin (2009). "Surgical management and palliative treatment in bronchial neuroendocrine tumours: a clinical study of 45 patients." Lung Cancer 65(1): 68-73.

69. Bushnell, D. L., Jr., T. M. O'Dorisio, M. S. O'Dorisio, Y. Menda, R. J. Hicks, E. Van Cutsem, J. L. Baulieu, F. Borson-Chazot, L. Anthony, A. B. Benson, K. Oberg, A. B. Grossman, M. Connolly, H. Bouterfa, Y. Li, K. A. Kacena, N. LaFrance and S. A. Pauwels (2010). "90Y-edotreotide for metastatic carcinoid refractory to octreotide." J Clin Oncol 28(10): 1652-1659.
70. Oberg, K., P. Hellman, D. Kwekkeboom and S. Jelic (2010). "Neuroendocrine bronchial and thymic tumours: ESMO Clinical Practice Guidelines for diagnosis, treatment and follow-up." Ann Oncol 21 Suppl 5: v220-222.
71. O'Reilly, K. E., F. Rojo, Q. B. She, D. Solit, G. B. Mills, D. Smith, H. Lane, F. Hofmann, D. J. Hicklin, D. L. Ludwig, J. Baselga and N. Rosen (2006). "mTOR inhibition induces upstream receptor tyrosine kinase signaling and activates Akt." Cancer Res 66(3): 1500-1508.
72. Pollak, M. N., C. Polychronakos and H. Guyda (1989). "Somatostatin analogue SMS 201-995 reduces serum IGF-I levels in patients with neoplasms potentially dependent on IGF-I." Anticancer Res 9(4): 889-891.
73. La Rosa, S., S. Uccella, G. Finzi, L. Albarello, F. Sessa and C. Capella (2003). "Localization of vascular endothelial growth factor and its receptors in digestive endocrine tumors: correlation with microvessel density and clinicopathologic features." Hum Pathol 34(1): 18-27.
74. Chaudhry, A., V. Papanicolaou, K. Oberg, C. H. Heldin and K. Funa (1992). "Expression of platelet-derived growth factor and its receptors in neuroendocrine tumors of the digestive system." Cancer Res 52(4): 1006-1012.
75. Mendel, D. B., A. D. Laird, X. Xin, S. G. Louie, J. G. Christensen, G. Li, R. E. Schreck, T. J. Abrams, T. J. Ngai, L. B. Lee, L. J. Murray, J. Carver, E. Chan, K. G. Moss, J. O. Haznedar, J. Sukbuntherng, R. A. Blake, L. Sun, C. Tang, T. Miller, S. Shirazian, G. McMahon and J. M. Cherrington (2003). "In vivo antitumor activity of SU11248, a novel tyrosine kinase inhibitor targeting vascular endothelial growth factor and platelet-derived growth factor receptors: determination of a pharmacokinetic/pharmacodynamic relationship." Clin Cancer Res 9(1): 327-337.
76. Rickman, O. B., P. K. Vohra, B. Sanyal, J. A. Vrana, M. C. Aubry, D. A. Wigle and C. F. Thomas, Jr. (2009). "Analysis of ErbB receptors in pulmonary carcinoid tumors." Clin Cancer Res 15(10): 3315-3324.
77. Shinohara, E. T., A. Gonzalez, P. P. Massion, S. J. Olson, J. M. Albert, Y. Shyr, D. P. Carbone, D. H. Johnson, D. E. Hallahan and B. Lu (2007). "PDGFR-beta expression in small cell lung cancer patients." Int J Radiat Oncol Biol Phys 67(2): 431-437.
78. Krystal, G. W., S. Honsawek, J. Litz and E. Buchdunger (2000). "The selective tyrosine kinase inhibitor STI571 inhibits small cell lung cancer growth." Clin Cancer Res 6(8): 3319-3326.
79. Watkins, D. N., D. M. Berman, S. G. Burkholder, B. Wang, P. A. Beachy and S. B. Baylin (2003). "Hedgehog signalling within airway epithelial progenitors and in small-cell lung cancer." Nature 422(6929): 313-317.
80. Park, K. S., L. G. Martelotto, M. Peifer, M. L. Sos, A. N. Karnezis, M. R. Mahjoub, K. Bernard, J. F. Conklin, A. Szczepny, J. Yuan, R. Guo, B. Ospina, J. Falzon, S. Bennett, T. J. Brown, A. Markovic, W. L. Devereux, C. A. Ocasio, J. K. Chen, T. Stearns, R. K. Thomas, M. Dorsch, S. Buonamici, D. N. Watkins, C. D. Peacock and J. Sage (2011). "A crucial requirement for Hedgehog signaling in small cell lung cancer." Nat Med 17(11): 1504-1508.
81. Walch, A. K., H. F. Zitzelsberger, M. M. Aubele, A. E. Mattis, M. Bauchinger, S. Candidus, H. W. Prauer, M. Werner and H. Hofler (1998). "Typical and atypical carcinoid tumors of the lung are characterized by 11q deletions as detected by comparative genomic hybridization." Am J Pathol 153(4): 1089-1098.
82. Zhao, J., R. R. de Krijger, D. Meier, E. J. Speel, P. Saremaslani, S. Muletta-Feurer, C. Matter, J. Roth, P. U. Heitz and P. Komminoth (2000). "Genomic alterations in well-differentiated gastrointestinal and bronchial neuroendocrine tumors (carcinoids): marked differences indicating diversity in molecular pathogenesis." Am J Pathol 157(5): 1431-1438.
83. Leotlela, P. D., A. Jauch, H. Holtgreve-Grez and R. V. Thakker (2003). "Genetics of neuroendocrine and carcinoid tumours." Endocr Relat Cancer 10(4): 437-450.

84. Petzmann, S., R. Ullmann, I. Halbwedl and H. H. Popper (2004). "Analysis of chromosome-11 aberrations in pulmonary and gastrointestinal carcinoids: an array comparative genomic hybridization-based study." Virchows Arch 445(2): 151-159.
85. Petersen, I., H. Langreck, G. Wolf, A. Schwendel, R. Psille, P. Vogt, M. B. Reichel, T. Ried and M. Dietel (1997). "Small-cell lung cancer is characterized by a high incidence of deletions on chromosomes 3p, 4q, 5q, 10q, 13q and 17p." Br J Cancer 75(1): 79-86.
86. Michelland, S., S. Gazzeri, E. Brambilla and M. Robert-Nicoud (1999). "Comparison of chromosomal imbalances in neuroendocrine and non-small-cell lung carcinomas." Cancer Genet Cytogenet 114(1): 22-30.
87. Ullmann, R., S. Petzmann, A. Sharma, P. T. Cagle and H. H. Popper (2001). "Chromosomal aberrations in a series of large-cell neuroendocrine carcinomas: unexpected divergence from small-cell carcinoma of the lung." Hum Pathol 32(10): 1059-1063.
88. Peng, W. X., T. Shibata, H. Katoh, A. Kokubu, Y. Matsuno, H. Asamura, R. Tsuchiya, Y. Kanai, F. Hosoda, T. Sakiyama, M. Ohki, I. Imoto, J. Inazawa and S. Hirohashi (2005). "Array-based comparative genomic hybridization analysis of high-grade neuroendocrine tumors of the lung." Cancer Sci 96(10): 661-667.
89. Wistuba, II, C. Behrens, S. Milchgrub, D. Bryant, J. Hung, J. D. Minna and A. F. Gazdar (1999). "Sequential molecular abnormalities are involved in the multistage development of squamous cell lung carcinoma." Oncogene 18(3): 643-650.
90. Zienolddiny, S., D. Ryberg, M. O. Arab, V. Skaug and A. Haugen (2001). "Loss of heterozygosity is related to p53 mutations and smoking in lung cancer." Br J Cancer 84(2): 226-231.
91. Wistuba, II and A. F. Gazdar (2006). "Lung cancer preneoplasia." Annu Rev Pathol 1: 331-348.
92. Swarts, D. R., S. M. Claessen, Y. M. Jonkers, R. J. van Suylen, A. M. Dingemans, W. W. de Herder, R. R. de Krijger, E. F. Smit, F. B. Thunnissen, C. A. Seldenrijk, A. Vink, A. Perren, F. C. Ramaekers and E. J. Speel (2011). "Deletions of 11q22.3-q25 are associated with atypical lung carcinoids and poor clinical outcome." Am J Pathol 179(3): 1129-1137.
93. Koreth, J., C. J. Bakkenist and J. O. McGee (1999). "Chromosomes, 11Q and cancer: a review." J Pathol 187(1): 28-38.
94. Sachithanandan, N., R. A. Harle and J. R. Burgess (2005). "Bronchopulmonary carcinoid in multiple endocrine neoplasia type 1." Cancer 103(3): 509-515.
95. Debelenko, L. V., J. I. Swalwell, M. J. Kelley, E. Brambilla, P. Manickam, G. Baibakov, S. K. Agarwal, A. M. Spiegel, S. J. Marx, S. C. Chandrasekharappa, F. S. Collins, W. D. Travis and M. R. Emmert-Buck (2000). "MEN1 gene mutation analysis of high-grade neuroendocrine lung carcinoma." Genes Chromosomes Cancer 28(1): 58-65.
96. Anbazhagan, R., T. Tihan, D. M. Bornman, J. C. Johnston, J. H. Saltz, A. Weigering, S. Piantadosi and E. Gabrielson (1999). "Classification of small cell lung cancer and pulmonary carcinoid by gene expression profiles." Cancer Res 59(20): 5119-5122.
97. Bhattacharjee, A., W. G. Richards, J. Staunton, C. Li, S. Monti, P. Vasa, C. Ladd, J. Beheshti, R. Bueno, M. Gillette, M. Loda, G. Weber, E. J. Mark, E. S. Lander, W. Wong, B. E. Johnson, T. R. Golub, D. J. Sugarbaker and M. Meyerson (2001). "Classification of human lung carcinomas by mRNA expression profiling reveals distinct adenocarcinoma subclasses." Proc Natl Acad Sci U S A 98(24): 13790-13795.
98. Virtanen, C., Y. Ishikawa, D. Honjoh, M. Kimura, M. Shimane, T. Miyoshi, H. Nomura and M. H. Jones (2002). "Integrated classification of lung tumors and cell lines by expression profiling." Proc Natl Acad Sci U S A 99(19): 12357-12362.
99. He, P., L. Varticovski, E. D. Bowman, J. Fukuoka, J. A. Welsh, K. Miura, J. Jen, E. Gabrielson, E. Brambilla, W. D. Travis and C. C. Harris (2004). "Identification of carboxypeptidase E and gamma-glutamyl hydrolase as biomarkers for pulmonary neuroendocrine tumors by cDNA microarray." Hum Pathol 35(10): 1196-1209.

100. Jiang, S. X., T. Kameya, H. Asamura, A. Umezawa, Y. Sato, J. Shinada, Y. Kawakubo, T. Igarashi, K. Nagai and I. Okayasu (2004). "hASH1 expression is closely correlated with endocrine phenotype and differentiation extent in pulmonary neuroendocrine tumors." Mod Pathol 17(2): 222-229.
101. Lantuejoul, S., D. Moro, R. J. Michalides, C. Brambilla and E. Brambilla (1998). "Neural cell adhesion molecules (NCAM) and NCAM-PSA expression in neuroendocrine lung tumors." Am J Surg Pathol 22(10): 1267-1276.
102. Kibbelaar, R. E., C. E. Moolenaar, R. J. Michalides, D. Bitter-Suermann, B. J. Addis and W. J. Mooi (1989). "Expression of the embryonal neural cell adhesion molecule N-CAM in lung carcinoma. Diagnostic usefulness of monoclonal antibody 735 for the distinction between small cell lung cancer and non-small cell lung cancer." J Pathol 159(1): 23-28.
103. Komminoth, P., J. Roth, P. M. Lackie, D. Bitter-Suermann and P. U. Heitz (1991). "Polysialic acid of the neural cell adhesion molecule distinguishes small cell lung carcinoma from carcinoids." Am J Pathol 139(2): 297-304.
104. Michalides, R., B. Kwa, D. Springall, N. van Zandwijk, J. Koopman, J. Hilkens and W. Mooi (1994). "NCAM and lung cancer." Int J Cancer Suppl 8: 34-37.
105. Patriarca, C., G. Pruneri, R. M. Alfano, N. Carboni, L. Ermellino, F. Guddo, R. Buffa, A. G. Siccardi and G. Coggi (1997). "Polysialylated N-CAM, chromogranin A and B, and secretogranin II in neuroendocrine tumours of the lung." Virchows Arch 430(6): 455-460.
106. Lohmann, D. R., B. Fesseler, B. Putz, U. Reich, J. Bohm, H. Prauer, P. H. Wunsch and H. Hofler (1993). "Infrequent mutations of the p53 gene in pulmonary carcinoid tumors." Cancer Res 53(23): 5797-5801.
107. Przygodzki, R. M., S. D. Finkelstein, J. C. Langer, P. A. Swalsky, N. Fishback, A. Bakker, D. G. Guinee, M. Koss and W. D. Travis (1996). "Analysis of p53, K-ras-2, and C-raf-1 in pulmonary neuroendocrine tumors. Correlation with histological subtype and clinical outcome." Am J Pathol 148(5): 1531-1541.
108. Couce, M. E., D. Bautista, J. Costa and D. Carter (1999). "Analysis of K-ras, N-ras, H-ras, and p53 in lung neuroendocrine neoplasms." Diagn Mol Pathol 8(2): 71-79.
109. Onuki, N., Wistuba, II, W. D. Travis, A. K. Virmani, K. Yashima, E. Brambilla, P. Hasleton and A. F. Gazdar (1999). "Genetic changes in the spectrum of neuroendocrine lung tumors." Cancer 85(3): 600-607.
110. Brambilla, E., A. Negoescu, S. Gazzeri, S. Lantuejoul, D. Moro, C. Brambilla and J. L. Coll (1996). "Apoptosis-related factors p53, Bcl2, and Bax in neuroendocrine lung tumors." Am J Pathol 149(6): 1941-1952.
111. Eymin, B., S. Gazzeri, C. Brambilla and E. Brambilla (2002). "Mdm2 overexpression and p14(ARF) inactivation are two mutually exclusive events in primary human lung tumors." Oncogene 21(17): 2750-2761.
112. Salon, C., D. Moro, S. Lantuejoul, P. Brichon Py, H. Drabkin, C. Brambilla and E. Brambilla (2004). "E-cadherin-beta-catenin adhesion complex in neuroendocrine tumors of the lung: a suggested role upon local invasion and metastasis." Hum Pathol 35(9): 1148-1155.
113. Ibusuki, M., P. Fu, S. Yamamoto, S. Fujiwara, Y. Yamamoto, Y. Honda, K. I. Iyama and H. Iwase (2011). "Establishment of a standardized gene-expression analysis system using formalin-fixed, paraffin-embedded, breast cancer specimens." Breast Cancer.
114. von Ahlfen, S., A. Missel, K. Bendrat and M. Schlumpberger (2007). "Determinants of RNA quality from FFPE samples." PLoS One 2(12): e1261.
115. Ludyga, N., B. Grunwald, O. Azimzadeh, S. Englert, H. Hofler, S. Tapio and M. Aubele (2012). "Nucleic acids from long-term preserved FFPE tissues are suitable for downstream analyses." Virchows Arch 460(2): 131-140.
116. Walter, R. F., F. D. Mairinger, J. Wohlschlaeger, K. Worm, S. Ting, C. Vollbrecht, S. Kurt Werner and T. Hager (2013). "FFPE tissue as a feasible source for gene expression analysis--a comparison of three reference genes and one tumor marker." Pathol Res Pract 209(12): 784-789.

117. Geiss, G. K., R. E. Bumgarner, B. Birditt, T. Dahl, N. Dowidar, D. L. Dunaway, H. P. Fell, S. Ferree, R. D. George, T. Grogan, J. J. James, M. Maysuria, J. D. Mitton, P. Oliveri, J. L. Osborn, T. Peng, A. L. Ratcliffe, P. J. Webster, E. H. Davidson, L. Hood and K. Dimitrov (2008). "Direct multiplexed measurement of gene expression with color-coded probe pairs." Nat Biotechnol 26(3): 317-325.
118. Northcott, P. A., D. J. Shih, M. Remke, Y. J. Cho, M. Kool, C. Hawkins, C. G. Eberhart, A. Dubuc, T. Guettouche, Y. Cardentey, E. Bouffet, S. L. Pomeroy, M. Marra, D. Malkin, J. T. Rutka, A. Korshunov, S. Pfister and M. D. Taylor (2012). "Rapid, reliable, and reproducible molecular sub-grouping of clinical medulloblastoma samples." Acta Neuropathol 123(4): 615-626.
119. Vollbrecht, C., K. Konig, L. Heukamp, R. Buttner and M. Odenthal (2013). "[Molecular pathology of the lungs. New perspectives by next generation sequencing]." Pathologe 34(1): 16-24.
120. Mairinger, F. D., C. Vollbrecht, A. Streubel, A. Roth, O. Landt, H. F. Walter, J. Kollmeier and T. Mairinger (2014). "The "COLD-PCR approach" for early and cost-effective detection of tyrosine kinase inhibitor resistance mutations in EGFR-positive non-small cell lung cancer." Appl Immunohistochem Mol Morphol 22(2): 114-118.
121. Mairinger FD, W. R., Vollbrecht C, Hager H, Worm K, Ting S, Zarogoulidis P, Zarogoulidis K, Schmid KW, Wohlschlaeger J (2014). "Isothermal multiple displacement amplification: a methodical approach enhancing molecular routine diagnostics of microcarcinomas and small biopsies." OncoTargets and Therapy accepted 29.03.2014.
122. Travis, W. D. (2010). "Advances in neuroendocrine lung tumors." Ann Oncol 21 Suppl 7: vii65-71.
123. Bustin, S. A., V. Benes, J. A. Garson, J. Hellemans, J. Huggett, M. Kubista, R. Mueller, T. Nolan, M. W. Pfaffl, G. L. Shipley, J. Vandesompele and C. T. Wittwer (2009). "The MIQE guidelines: minimum information for publication of quantitative real-time PCR experiments." Clin Chem 55(4): 611-622.
124. Rindi, G., G. Petrone and F. Inzani (2014). "The 2010 WHO Classification of Digestive Neuroendocrine Neoplasms: a Critical Appraisal four years after Its Introduction." Endocr Pathol.
125. Iyoda, A., T. Makino, S. Koezuka, H. Otsuka and Y. Hata (2014). "Treatment options for patients with large cell neuroendocrine carcinoma of the lung." Gen Thorac Cardiovasc Surg.
126. Chalkley, R. and C. Hunter (1975). "Histone-histone propinquity by aldehyde fixation of chromatin." Proc Natl Acad Sci U S A 72(4): 1304-1308.
127. Fabbri, M., R. Garzon, A. Cimmino, Z. Liu, N. Zanesi, E. Callegari, S. Liu, H. Alder, S. Costinean, C. Fernandez-Cymering, S. Volinia, G. Guler, C. D. Morrison, K. K. Chan, G. Marcucci, G. A. Calin, K. Huebner and C. M. Croce (2007). "MicroRNA-29 family reverts aberrant methylation in lung cancer by targeting DNA methyltransferases 3A and 3B." Proc Natl Acad Sci U S A 104(40): 15805-15810.
128. Park, S. Y., J. H. Lee, M. Ha, J. W. Nam and V. N. Kim (2009). "miR-29 miRNAs activate p53 by targeting p85 alpha and CDC42." Nat Struct Mol Biol 16(1): 23-29.
129. He, L., X. He, L. P. Lim, E. de Stanchina, Z. Xuan, Y. Liang, W. Xue, L. Zender, J. Magnus, D. Ridzon, A. L. Jackson, P. S. Linsley, C. Chen, S. W. Lowe, M. A. Cleary and G. J. Hannon (2007). "A microRNA component of the p53 tumour suppressor network." Nature 447(7148): 1130-1134.
130. Lee, J. H., J. Voortman, A. M. Dingemans, D. M. Voeller, T. Pham, Y. Wang and G. Giaccone (2011). "MicroRNA expression and clinical outcome of small cell lung cancer." PLoS One 6(6): e21300.
131. Caldas, C. and J. D. Brenton (2005). "Sizing up miRNAs as cancer genes." Nat Med 11(7): 712-714.
132. Lee, H. W., E. H. Lee, S. Y. Ha, C. H. Lee, H. K. Chang, S. Chang, K. Y. Kwon, I. S. Hwang, M. S. Roh and J. W. Seo (2012). "Altered expression of microRNA miR-21, miR-155, and let-7a and their roles in pulmonary neuroendocrine tumors." Pathol Int 62(9): 583-591.

133. Guan, P., Z. Yin, X. Li, W. Wu and B. Zhou (2012). "Meta-analysis of human lung cancer microRNA expression profiling studies comparing cancer tissues with normal tissues." J Exp Clin Cancer Res 31: 54.
134. Cingarlini, S., M. Bonomi, V. Corbo, A. Scarpa and G. Tortora (2012). "Profiling mTOR pathway in neuroendocrine tumors." Target Oncol 7(3): 183-188.
135. Ma, L., Y. Huang, W. Zhu, S. Zhou, J. Zhou, F. Zeng, X. Liu, Y. Zhang and J. Yu (2011). "An integrated analysis of miRNA and mRNA expressions in non-small cell lung cancers." PLoS One 6(10): e26502.
136. Fang, R., T. Xiao, Z. Fang, Y. Sun, F. Li, Y. Gao, Y. Feng, L. Li, Y. Wang, X. Liu, H. Chen, X. Y. Liu and H. Ji (2012). "MicroRNA-143 (miR-143) regulates cancer glycolysis via targeting hexokinase 2 gene." J Biol Chem 287(27): 23227-23235.
137. West, K. A., J. Brognard, A. S. Clark, I. R. Linnoila, X. Yang, S. M. Swain, C. Harris, S. Belinsky and P. A. Dennis (2003). "Rapid Akt activation by nicotine and a tobacco carcinogen modulates the phenotype of normal human airway epithelial cells." J Clin Invest 111(1): 81-90.
138. Castillo, S. S., J. Brognard, P. A. Petukhov, C. Zhang, J. Tsurutani, C. A. Granville, M. Li, M. Jung, K. A. West, J. G. Gills, A. P. Kozikowski and P. A. Dennis (2004). "Preferential inhibition of Akt and killing of Akt-dependent cancer cells by rationally designed phosphatidylinositol ether lipid analogues." Cancer Res 64(8): 2782-2792.
139. Song, P., H. S. Sekhon, A. Lu, J. Arredondo, D. Sauer, C. Gravett, G. P. Mark, S. A. Grando and E. R. Spindel (2007). "M3 muscarinic receptor antagonists inhibit small cell lung carcinoma growth and mitogen-activated protein kinase phosphorylation induced by acetylcholine secretion." Cancer Res 67(8): 3936-3944.
140. Widmann, C., S. Gibson, M. B. Jarpe and G. L. Johnson (1999). "Mitogen-activated protein kinase: conservation of a three-kinase module from yeast to human." Physiol Rev 79(1): 143-180.
141. Vicent, S., M. Garayoa, J. M. Lopez-Picazo, M. D. Lozano, G. Toledo, F. B. Thunnissen, R. G. Manzano and L. M. Montuenga (2004). "Mitogen-activated protein kinase phosphatase-1 is overexpressed in non-small cell lung cancer and is an independent predictor of outcome in patients." Clin Cancer Res 10(11): 3639-3649.
142. Blackhall, F. H., M. Pintilie, M. Michael, N. Leighl, R. Feld, M. S. Tsao and F. A. Shepherd (2003). "Expression and prognostic significance of kit, protein kinase B, and mitogen-activated protein kinase in patients with small cell lung cancer." Clin Cancer Res 9(6): 2241-2247.
143. Cano, E. and L. C. Mahadevan (1995). "Parallel signal processing among mammalian MAPKs." Trends Biochem Sci 20(3): 117-122.
144. Su, B. and M. Karin (1996). "Mitogen-activated protein kinase cascades and regulation of gene expression." Curr Opin Immunol 8(3): 402-411.
145. Ravi, R. K., E. Weber, M. McMahon, J. R. Williams, S. Baylin, A. Mal, M. L. Harter, L. E. Dillehay, P. P. Claudio, A. Giordano, B. D. Nelkin and M. Mabry (1998). "Activated Raf-1 causes growth arrest in human small cell lung cancer cells." J Clin Invest 101(1): 153-159.
146. Ravi, R. K., A. Thiagalingam, E. Weber, M. McMahon, B. D. Nelkin and M. Mabry (1999). "Raf-1 causes growth suppression and alteration of neuroendocrine markers in DMS53 human small-cell lung cancer cells." Am J Respir Cell Mol Biol 20(4): 543-549.
147. Burnett, P. E., R. K. Barrow, N. A. Cohen, S. H. Snyder and D. M. Sabatini (1998). "RAFT1 phosphorylation of the translational regulators p70 S6 kinase and 4E-BP1." Proc Natl Acad Sci U S A 95(4): 1432-1437.
148. Yamamoto, H., H. Shigematsu, M. Nomura, W. W. Lockwood, M. Sato, N. Okumura, J. Soh, M. Suzuki, Wistuba, II, K. M. Fong, H. Lee, S. Toyooka, H. Date, W. L. Lam, J. D. Minna and A. F. Gazdar (2008). "PIK3CA mutations and copy number gains in human lung cancers." Cancer Res 68(17): 6913-6921.
149. Liu, P., H. Cheng, T. M. Roberts and J. J. Zhao (2009). "Targeting the phosphoinositide 3-kinase pathway in cancer." Nat Rev Drug Discov 8(8): 627-644.

150. Courtney, K. D., R. B. Corcoran and J. A. Engelman (2010). "The PI3K pathway as drug target in human cancer." J Clin Oncol 28(6): 1075-1083.
151. Wong, K. K., J. A. Engelman and L. C. Cantley (2010). "Targeting the PI3K signaling pathway in cancer." Curr Opin Genet Dev 20(1): 87-90.
152. Papadimitrakopoulou, V. (2012). "Development of PI3K/AKT/mTOR pathway inhibitors and their application in personalized therapy for non-small-cell lung cancer." J Thorac Oncol 7(8): 1315-1326.
153. Spoerke, J. M., C. O'Brien, L. Huw, H. Koeppen, J. Fridlyand, R. K. Brachmann, P. M. Haverty, A. Pandita, S. Mohan, D. Sampath, L. S. Friedman, L. Ross, G. M. Hampton, L. C. Amler, D. S. Shames and M. R. Lackner (2012). "Phosphoinositide 3-kinase (PI3K) pathway alterations are associated with histologic subtypes and are predictive of sensitivity to PI3K inhibitors in lung cancer preclinical models." Clin Cancer Res 18(24): 6771-6783.
154. West, K. A., I. R. Linnoila, S. A. Belinsky, C. C. Harris and P. A. Dennis (2004). "Tobacco carcinogen-induced cellular transformation increases activation of the phosphatidylinositol 3'-kinase/Akt pathway in vitro and in vivo." Cancer Res 64(2): 446-451.
155. Jeong, E. H., H. S. Choi, T. G. Lee, H. R. Kim and C. H. Kim (2012). "Dual Inhibition of PI3K/Akt/mTOR Pathway and Role of Autophagy in Non-Small Cell Lung Cancer Cells." Tuberc Respir Dis (Seoul) 72(4): 343-351.
156. Janku, F., D. J. Stewart and R. Kurzrock (2010). "Targeted therapy in non-small-cell lung cancer--is it becoming a reality?" Nat Rev Clin Oncol 7(7): 401-414.
157. Reungwetwattana, T., S. J. Weroha and J. R. Molina (2012). "Oncogenic pathways, molecularly targeted therapies, and highlighted clinical trials in non-small-cell lung cancer (NSCLC)." Clin Lung Cancer 13(4): 252-266.
158. Myers, A. P. and L. C. Cantley (2010). "Targeting a common collaborator in cancer development." Sci Transl Med 2(48): 48ps45.
159. Li, D., X. Qu, K. Hou, Y. Zhang, Q. Dong, Y. Teng, J. Zhang and Y. Liu (2009). "PI3K/Akt is involved in bufalin-induced apoptosis in gastric cancer cells." Anticancer Drugs 20(1): 59-64.
160. Shayesteh, L., Y. Lu, W. L. Kuo, R. Baldocchi, T. Godfrey, C. Collins, D. Pinkel, B. Powell, G. B. Mills and J. W. Gray (1999). "PIK3CA is implicated as an oncogene in ovarian cancer." Nat Genet 21(1): 99-102.
161. Samuels, Y., Z. Wang, A. Bardelli, N. Silliman, J. Ptak, S. Szabo, H. Yan, A. Gazdar, S. M. Powell, G. J. Riggins, J. K. Willson, S. Markowitz, K. W. Kinzler, B. Vogelstein and V. E. Velculescu (2004). "High frequency of mutations of the PIK3CA gene in human cancers." Science 304(5670): 554.
162. Sansal, I. and W. R. Sellers (2004). "The biology and clinical relevance of the PTEN tumor suppressor pathway." J Clin Oncol 22(14): 2954-2963.
163. Kawano, O., H. Sasaki, K. Endo, E. Suzuki, H. Haneda, H. Yukiue, Y. Kobayashi, M. Yano and Y. Fujii (2006). "PIK3CA mutation status in Japanese lung cancer patients." Lung Cancer 54(2): 209-215.
164. Kawano, O., H. Sasaki, K. Okuda, H. Yukiue, T. Yokoyama, M. Yano and Y. Fujii (2007). "PIK3CA gene amplification in Japanese non-small cell lung cancer." Lung Cancer 58(1): 159-160.
165. Clark, A. S., K. West, S. Streicher and P. A. Dennis (2002). "Constitutive and inducible Akt activity promotes resistance to chemotherapy, trastuzumab, or tamoxifen in breast cancer cells." Mol Cancer Ther 1(9): 707-717.
166. Wallin, J. J., J. Guan, W. W. Prior, K. A. Edgar, R. Kassees, D. Sampath, M. Belvin and L. S. Friedman (2010). "Nuclear phospho-Akt increase predicts synergy of PI3K inhibition and doxorubicin in breast and ovarian cancer." Sci Transl Med 2(48): 48ra66.
167. Hanahan, D. and R. A. Weinberg (2011). "Hallmarks of cancer: the next generation." Cell 144(5): 646-674.
168. Zhu, Z., H. Sun, G. Ma, Z. Wang, E. Li and Y. Liu (2012). "Bufalin Induces Lung Cancer Cell Apoptosis via the Inhibition of PI3K/Akt Pathway." Int J Mol Sci 13(2): 2025-2035.

169. Takeuchi, H., J. Kim, A. Fujimoto, N. Umetani, T. Mori, A. Bilchik, R. Turner, A. Tran, C. Kuo and D. S. Hoon (2005). "X-Linked inhibitor of apoptosis protein expression level in colorectal cancer is regulated by hepatocyte growth factor/C-met pathway via Akt signaling." Clin Cancer Res 11(21): 7621-7628.
170. Lee, S. M., C. T. Lee, Y. W. Kim, S. K. Han, Y. S. Shim and C. G. Yoo (2006). "Hypoxia confers protection against apoptosis via PI3K/Akt and ERK pathways in lung cancer cells." Cancer Lett 242(2): 231-238.
171. Bak, Y., H. Kim, J. W. Kang, D. H. Lee, M. S. Kim, Y. S. Park, J. H. Kim, K. Y. Jung, Y. Lim, J. Hong and D. Y. Yoon (2011). "A synthetic naringenin derivative, 5-hydroxy-7,4'-diacetyloxyflavanone-N-phenyl hydrazone (N101-43), induces apoptosis through up-regulation of Fas/FasL expression and inhibition of PI3K/Akt signaling pathways in non-small-cell lung cancer cells." J Agric Food Chem 59(18): 10286-10297.
172. Damstrup, L., K. Rygaard, M. Spang-Thomsen and H. Skovgaard Poulsen (1993). "Expression of transforming growth factor beta (TGF beta) receptors and expression of TGF beta 1, TGF beta 2 and TGF beta 3 in human small cell lung cancer cell lines." Br J Cancer 67(5): 1015-1021.
173. Derynck, R., J. A. Jarrett, E. Y. Chen, D. H. Eaton, J. R. Bell, R. K. Assoian, A. B. Roberts, M. B. Sporn and D. V. Goeddel (1985). "Human transforming growth factor-beta complementary DNA sequence and expression in normal and transformed cells." Nature 316(6030): 701-705.
174. Bergh, J. (1988). "The expression of the platelet-derived and transforming growth factor genes in human nonsmall lung cancer cell lines is related to tumor stroma formation in nude mice tumors." Am J Pathol 133(3): 434-439.
175. Soderdahl, G., C. Betsholtz, A. Johansson, K. Nilsson and J. Bergh (1988). "Differential expression of platelet-derived growth factor and transforming growth factor genes in small- and non-small-cell human lung carcinoma lines." Int J Cancer 41(4): 636-641.
176. Lagadec, P. F., K. A. Saraya and F. R. Balkwill (1991). "Human small-cell lung-cancer cells are cytokine-resistant but NK/LAK-sensitive." Int J Cancer 48(2): 311-317.
177. Massague, J. (1990). "The transforming growth factor-beta family." Annu Rev Cell Biol 6: 597-641.
178. Moses, H. L. (1992). "TGF-beta regulation of epithelial cell proliferation." Mol Reprod Dev 32(2): 179-184.
179. Norgaard, P., L. Damstrup, K. Rygaard, M. Spang-Thomsen and H. Skovgaard Poulsen (1994). "Growth suppression by transforming growth factor beta 1 of human small-cell lung cancer cell lines is associated with expression of the type II receptor." Br J Cancer 69(5): 802-808.
180. Geiser, A. G., J. K. Burmester, R. Webbink, A. B. Roberts and M. B. Sporn (1992). "Inhibition of growth by transforming growth factor-beta following fusion of two nonresponsive human carcinoma cell lines. Implication of the type II receptor in growth inhibitory responses." J Biol Chem 267(4): 2588-2593.
181. Inagaki, M., A. Moustakas, H. Y. Lin, H. F. Lodish and B. I. Carr (1993). "Growth inhibition by transforming growth factor beta (TGF-beta) type I is restored in TGF-beta-resistant hepatoma cells after expression of TGF-beta receptor type II cDNA." Proc Natl Acad Sci U S A 90(11): 5359-5363.
182. Park, K., S. J. Kim, Y. J. Bang, J. G. Park, N. K. Kim, A. B. Roberts and M. B. Sporn (1994). "Genetic changes in the transforming growth factor beta (TGF-beta) type II receptor gene in human gastric cancer cells: correlation with sensitivity to growth inhibition by TGF-beta." Proc Natl Acad Sci U S A 91(19): 8772-8776.
183. Hougaard, S., P. Norgaard, N. Abrahamsen, H. L. Moses, M. Spang-Thomsen and H. Skovgaard Poulsen (1999). "Inactivation of the transforming growth factor beta type II receptor in human small cell lung cancer cell lines." Br J Cancer 79(7-8): 1005-1011.
184. Cui, W., C. J. Kemp, E. Duffie, A. Balmain and R. J. Akhurst (1994). "Lack of transforming growth factor-beta 1 expression in benign skin tumors of p53null mice is prognostic for a high risk of malignant conversion." Cancer Res 54(22): 5831-5836.

185. Pierce, D. F., Jr., A. E. Gorska, A. Chytil, K. S. Meise, D. L. Page, R. J. Coffey, Jr. and H. L. Moses (1995). "Mammary tumor suppression by transforming growth factor beta 1 transgene expression." Proc Natl Acad Sci U S A 92(10): 4254-4258.
186. Russo, A. A., L. Tong, J. O. Lee, P. D. Jeffrey and N. P. Pavletich (1998). "Structural basis for inhibition of the cyclin-dependent kinase Cdk6 by the tumour suppressor p16INK4a." Nature 395(6699): 237-243.
187. Coe, B. P., W. W. Lockwood, L. Girard, R. Chari, C. Macaulay, S. Lam, A. F. Gazdar, J. D. Minna and W. L. Lam (2006). "Differential disruption of cell cycle pathways in small cell and non-small cell lung cancer." Br J Cancer 94(12): 1927-1935.
188. Husain, H., A. Psyrri, A. Markovic, T. Rampias, E. Pectasides, H. Wang, R. Slebos, W. G. Yarbrough, B. Burtness and C. H. Chung (2012). "Nuclear epidermal growth factor receptor and p16 expression in head and neck squamous cell carcinoma." Laryngoscope 122(12): 2762-2768.
189. Wang, J., Y. Zhao, Y. Wang and J. Huang (2013). "Molecular dynamics simulations and statistical coupling analysis reveal functional coevolution network of oncogenic mutations in the CDKN2A-CDK6 complex." FEBS Lett 587(2): 136-141.
190. Oh, J., S. H. Kim, S. Ahn and C. E. Lee (2012). "Suppressors of cytokine signaling promote Fas-induced apoptosis through downregulation of NF-kappaB and mitochondrial Bfl-1 in leukemic T cells." J Immunol 189(12): 5561-5571.
191. Aguirre, A., K. F. Shoji, J. C. Saez, M. Henriquez and A. F. Quest (2013). "FasL-triggered death of Jurkat cells requires caspase 8-induced, ATP-dependent cross-talk between Fas and the purinergic receptor P2X(7)." J Cell Physiol 228(2): 485-493.
192. Kikuchi, M., S. Kuroki, M. Kayama, S. Sakaguchi, K. K. Lee and S. Yonehara (2012). "Protease activity of procaspase-8 is essential for cell survival by inhibiting both apoptotic and nonapoptotic cell death dependent on receptor-interacting protein kinase 1 (RIP1) and RIP3." J Biol Chem 287(49): 41165-41173.
193. Kobayashi, Y., Y. Tokuchi, T. Hashimoto, M. Hayashi, H. Nishimura, Y. Ishikawa, K. Nakagawa, Y. Sato, A. Takahashi and E. Tsuchiya (2004). "Molecular markers for reinforcement of histological subclassification of neuroendocrine lung tumors." Cancer Sci 95(4): 334-341.
194. Srivastava, S. and W. E. Grizzle (2010). "Biomarkers and the genetics of early neoplastic lesions." Cancer Biomark 9(1-6): 41-64.
195. Harris, N. C., K. Paavonen, N. Davydova, S. Roufail, T. Sato, Y. F. Zhang, T. Karnezis, S. A. Stacker and M. G. Achen (2011). "Proteolytic processing of vascular endothelial growth factor-D is essential for its capacity to promote the growth and spread of cancer." Faseb Journal 25(8): 2615-2625.
196. Yu, S., J. Sun, J. Zhang, X. Xu, H. Li, B. Shan, T. Tian, H. Wang, D. Ma and C. Ji (2013). "Aberrant expression and association of VEGF and Dll4/Notch pathway molecules under hypoxia in patients with lung cancer." Histol Histopathol 28(2): 277-284.
197. Kashiwagi, K., J. Ishii, M. Sakaeda, Y. Arimasu, H. Shimoyamada, H. Sato, C. Miyata, H. Kamma, I. Aoki and T. Yazawa (2012). "Differences of molecular expression mechanisms among neural cell adhesion molecule 1, synaptophysin, and chromogranin A in lung cancer cells." Pathol Int 62(4): 232-245.
198. Jensen, S. M., A. F. Gazdar, F. Cuttitta, E. K. Russell and R. I. Linnoila (1990). "A comparison of synaptophysin, chromogranin, and L-dopa decarboxylase as markers for neuroendocrine differentiation in lung cancer cell lines." Cancer Res 50(18): 6068-6074.
199. Di Sano, F., B. Fazi, R. Tufi, R. Nardacci and M. Piacentini (2007). "Reticulon-1C acts as a molecular switch between endoplasmic reticulum stress and genotoxic cell death pathway in human neuroblastoma cells." J Neurochem 102(2): 345-353.
200. Pinton, P., D. Ferrari, E. Rapizzi, F. Di Virgilio, T. Pozzan and R. Rizzuto (2001). "The Ca2+ concentration of the endoplasmic reticulum is a key determinant of ceramide-induced apoptosis: significance for the molecular mechanism of Bcl-2 action." EMBO J 20(11): 2690-2701.

201. Di Sano, F., B. Fazi, G. Citro, P. E. Lovat, G. Cesareni and M. Piacentini (2003). "Glucosylceramide synthase and its functional interaction with RTN-1C regulate chemotherapeutic-induced apoptosis in neuroepithelioma cells." Cancer Res 63(14): 3860-3865.
202. Alifano, M., F. Souaze, S. Dupouy, S. Camilleri-Broet, M. Younes, S. M. Ahmed-Zaid, T. Takahashi, A. Cancellieri, S. Damiani, M. Boaron, P. Broet, L. D. Miller, C. Gespach, J. F. Regnard and P. Forgez (2010). "Neurotensin receptor 1 determines the outcome of non-small cell lung cancer." Clin Cancer Res 16(17): 4401-4410.
203. Balasubramanian, S., S. R. Fam and R. A. Hall (2007). "GABAB receptor association with the PDZ scaffold Mupp1 alters receptor stability and function." J Biol Chem 282(6): 4162-4171.
204. Hannan, S., M. E. Wilkins, E. Dehghani-Tafti, P. Thomas, S. M. Baddeley and T. G. Smart (2011). "Gamma-aminobutyric acid type B (GABA(B)) receptor internalization is regulated by the R2 subunit." J Biol Chem 286(27): 24324-24335.
205. Stein, L., J. Rothschild, J. Luce, J. K. Cowell, G. Thomas, T. I. Bogdanova, M. D. Tronko and L. Hawthorn (2010). "Copy number and gene expression alterations in radiation-induced papillary thyroid carcinoma from chernobyl pediatric patients." Thyroid 20(5): 475-487.
206. Castro-Rivera, E., S. Ran, R. A. Brekken and J. D. Minna (2008). "Semaphorin 3B inhibits the phosphatidylinositol 3-kinase/Akt pathway through neuropilin-1 in lung and breast cancer cells." Cancer Res 68(20): 8295-8303.
207. Iqbal, M. S., K. Otsuyama, K. Shamsasenjan, H. Asaoku and M. M. Kawano (2010). "CD56 expression in human myeloma cells derived from the neurogenic gene expression: possible role of the SRY-HMG box gene, SOX4." Int J Hematol 91(2): 267-275.
208. Yamanaka, S. and H. M. Blau (2010). "Nuclear reprogramming to a pluripotent state by three approaches." Nature 465(7299): 704-712.
209. Ikushima, H., T. Todo, Y. Ino, M. Takahashi, N. Saito, K. Miyazawa and K. Miyazono (2011). "Glioma-initiating cells retain their tumorigenicity through integration of the Sox axis and Oct4 protein." J Biol Chem 286(48): 41434-41441.
210. Castillo, S. D., A. Matheu, N. Mariani, J. Carretero, F. Lopez-Rios, R. Lovell-Badge and M. Sanchez-Cespedes (2012). "Novel transcriptional targets of the SRY-HMG box transcription factor SOX4 link its expression to the development of small cell lung cancer." Cancer Res 72(1): 176-186.
211. Vervoort, S. J., R. van Boxtel and P. J. Coffer (2012). "The role of SRY-related HMG box transcription factor 4 (SOX4) in tumorigenesis and metastasis: friend or foe?" Oncogene.
212. Dy, P., A. Penzo-Mendez, H. Wang, C. E. Pedraza, W. B. Macklin and V. Lefebvre (2008). "The three SoxC proteins--Sox4, Sox11 and Sox12--exhibit overlapping expression patterns and molecular properties." Nucleic Acids Res 36(9): 3101-3117.
213. Mascarenhas, J. B., K. P. Young, E. L. Littlejohn, B. K. Yoo, R. Salgia and D. Lang (2009). "PAX6 is expressed in pancreatic cancer and actively participates in cancer progression through activation of the MET tyrosine kinase receptor gene." J Biol Chem 284(40): 27524-27532.
214. Zong, X., H. Yang, Y. Yu, D. Zou, Z. Ling, X. He and X. Meng (2011). "Possible role of Pax-6 in promoting breast cancer cell proliferation and tumorigenesis." BMB Rep 44(9): 595-600.
215. Hellwinkel, O. J., M. Kedia, H. Isbarn, L. Budaus and M. G. Friedrich (2008). "Methylation of the TPEF- and PAX6-promoters is increased in early bladder cancer and in normal mucosa adjacent to pTa tumours." BJU Int 101(6): 753-757.
216. Shyr, C. R., M. Y. Tsai, S. Yeh, H. Y. Kang, Y. C. Chang, P. L. Wong, C. C. Huang, K. E. Huang and C. Chang (2010). "Tumor suppressor PAX6 functions as androgen receptor co-repressor to inhibit prostate cancer growth." Prostate 70(2): 190-199.
217. Song, J., M. Li, M. Tretiakova, R. Salgia, P. T. Cagle and A. N. Husain (2010). "Expression patterns of PAX5, c-Met, and paxillin in neuroendocrine tumors of the lung." Arch Pathol Lab Med 134(11): 1702-1705.

218. Li, X., K. F. Cheung, X. Ma, L. Tian, J. Zhao, M. Y. Go, B. Shen, A. S. Cheng, J. Ying, Q. Tao, J. J. Sung, H. F. Kung and J. Yu (2012). "Epigenetic inactivation of paired box gene 5, a novel tumor suppressor gene, through direct upregulation of p53 is associated with prognosis in gastric cancer patients." Oncogene 31(29): 3419-3430.
219. Takeda, H., N. Takigawa, K. Ohashi, D. Minami, I. Kataoka, E. Ichihara, N. Ochi, M. Tanimoto and K. Kiura (2013). "Vandetanib is effective in EGFR-mutant lung cancer cells with PTEN deficiency." Exp Cell Res 319(4): 417-423.
220. Johnson, M. L., C. S. Sima, J. Chaft, P. K. Paik, W. Pao, M. G. Kris, M. Ladanyi and G. J. Riely (2013). "Association of KRAS and EGFR mutations with survival in patients with advanced lung adenocarcinomas." Cancer 119(2): 356-362.
221. Weiss, J., M. L. Sos, D. Seidel, M. Peifer, T. Zander, J. M. Heuckmann, R. T. Ullrich, R. Menon, S. Maier, A. Soltermann, H. Moch, P. Wagener, F. Fischer, S. Heynck, M. Koker, J. Schottle, F. Leenders, F. Gabler, I. Dabow, S. Querings, L. C. Heukamp, H. Balke-Want, S. Ansen, D. Rauh, I. Baessmann, J. Altmuller, Z. Wainer, M. Conron, G. Wright, P. Russell, B. Solomon, E. Brambilla, C. Brambilla, P. Lorimier, S. Sollberg, O. T. Brustugun, W. Engel-Riedel, C. Ludwig, I. Petersen, J. Sanger, J. Clement, H. Groen, W. Timens, H. Sietsma, E. Thunnissen, E. Smit, D. Heideman, F. Cappuzzo, C. Ligorio, S. Damiani, M. Hallek, R. Beroukhim, W. Pao, B. Klebl, M. Baumann, R. Buettner, K. Ernestus, E. Stoelben, J. Wolf, P. Nurnberg, S. Perner and R. K. Thomas (2010). "Frequent and focal FGFR1 amplification associates with therapeutically tractable FGFR1 dependency in squamous cell lung cancer." Sci Transl Med 2(62): 62ra93.
222. Dutt, A., A. H. Ramos, P. S. Hammerman, C. Mermel, J. Cho, T. Sharifnia, A. Chande, K. E. Tanaka, N. Stransky, H. Greulich, N. S. Gray and M. Meyerson (2011). "Inhibitor-sensitive FGFR1 amplification in human non-small cell lung cancer." PLoS One 6(6): e20351.
223. Dirks, W. G., S. Fahnrich, Y. Lis, E. Becker, R. A. MacLeod and H. G. Drexler (2002). "Expression and functional analysis of the anaplastic lymphoma kinase (ALK) gene in tumor cell lines." Int J Cancer 100(1): 49-56.
224. Camidge, D. R., Y. J. Bang, E. L. Kwak, A. J. Iafrate, M. Varella-Garcia, S. B. Fox, G. J. Riely, B. Solomon, S. H. Ou, D. W. Kim, R. Salgia, P. Fidias, J. A. Engelman, L. Gandhi, P. A. Janne, D. B. Costa, G. I. Shapiro, P. Lorusso, K. Ruffner, P. Stephenson, Y. Tang, K. Wilner, J. W. Clark and A. T. Shaw (2012). "Activity and safety of crizotinib in patients with ALK-positive non-small-cell lung cancer: updated results from a phase 1 study." Lancet Oncol 13(10): 1011-1019.
225. Zoncu, R., A. Efeyan and D. M. Sabatini (2011). "mTOR: from growth signal integration to cancer, diabetes and ageing." Nat Rev Mol Cell Biol 12(1): 21-35.
226. Agrawal, P., Y. T. Chen, B. Schilling, B. W. Gibson and R. E. Hughes (2012). "Ubiquitin-specific peptidase 9, X-linked (USP9X) modulates activity of mammalian target of rapamycin (mTOR)." J Biol Chem 287(25): 21164-21175.
227. Jacinto, E., R. Loewith, A. Schmidt, S. Lin, M. A. Ruegg, A. Hall and M. N. Hall (2004). "Mammalian TOR complex 2 controls the actin cytoskeleton and is rapamycin insensitive." Nat Cell Biol 6(11): 1122-1128.
228. Le Goff, A., Z. Ji, B. Leclercq, R. P. Bourette, A. Mougel, C. Guerardel, Y. de Launoit, J. Vicogne, G. Goormachtigh and V. Fafeur (2012). "Anti-apoptotic role of caspase-cleaved GAB1 adaptor protein in hepatocyte growth factor/scatter factor-MET receptor protein signaling." J Biol Chem 287(42): 35382-35396.
229. Ceppi, P., I. Rapa, M. Lo Iacono, L. Righi, J. Giorcelli, M. Pautasso, A. Bille, F. Ardissone, M. Papotti and G. V. Scagliotti (2012). "Expression and pharmacological inhibition of thymidylate synthase and Src kinase in nonsmall cell lung cancer." Int J Cancer 130(8): 1777-1786.
230. Wilson, P. M., M. J. LaBonte, H. J. Lenz, P. C. Mack and R. D. Ladner (2012). "Inhibition of dUTPase induces synthetic lethality with thymidylate synthase-targeted therapies in non-small cell lung cancer." Mol Cancer Ther 11(3): 616-628.
231. Odin, E., Y. Wettergren, S. Nilsson, R. Willen, G. Carlsson, C. P. Spears, L. Larsson and B. Gustavsson (2003). "Altered gene expression of folate enzymes in adjacent mucosa is associated with outcome of colorectal cancer patients." Clin Cancer Res 9(16 Pt 1): 6012-6019.

232. Mairinger, F., C. Vollbrecht, I. Halbwedl, M. Hatz, E. Stacher, C. Gully, F. Quehenberger, S. Stephan-Falkenau, J. Kollmeier, A. Roth, T. Mairinger and H. Popper (2013). "Reduced folate carrier and folylpolyglutamate synthetase, but not thymidylate synthase predict survival in pemetrexed-treated patients suffering from malignant pleural mesothelioma." J Thorac Oncol 8(5): 644-653.
233. Liani, E., L. Rothem, M. A. Bunni, C. A. Smith, G. Jansen and Y. G. Assaraf (2003). "Loss of folylpoly-gamma-glutamate synthetase activity is a dominant mechanism of resistance to polyglutamylation-dependent novel antifolates in multiple human leukemia sublines." Int J Cancer 103(5): 587-599.
234. Stark, M., C. Wichman, I. Avivi and Y. G. Assaraf (2009). "Aberrant splicing of folylpolyglutamate synthetase as a novel mechanism of antifolate resistance in leukemia." Blood 113(18): 4362-4369.
235. Christoph, D. C., B. R. Asuncion, C. Mascaux, C. Tran, X. Lu, M. W. Wynes, T. C. Gauler, J. Wohlschlaeger, D. Theegarten, V. Neumann, R. Hepp, S. Welter, G. Stamatis, A. Tannapfel, M. Schuler, W. E. Eberhardt and F. R. Hirsch (2012). "Folylpoly-glutamate synthetase expression is associated with tumor response and outcome from pemetrexed-based chemotherapy in malignant pleural mesothelioma." J Thorac Oncol 7(9): 1440-1448.
236. Mairinger, F., C. Vollbrecht, T. Mairinger and H. Popper (2013). "The issue of studies evaluating biomarkers which predict outcome after pemetrexed-based chemotherapy in malignant pleural mesothelioma." J Thorac Oncol 8(8): e80-82.
237. Parker, N., M. J. Turk, E. Westrick, J. D. Lewis, P. S. Low and C. P. Leamon (2005). "Folate receptor expression in carcinomas and normal tissues determined by a quantitative radioligand binding assay." Anal Biochem 338(2): 284-293.
238. Nunez, M. I., C. Behrens, D. M. Woods, H. Lin, M. Suraokar, H. Kadara, W. Hofstetter, N. Kalhor, J. J. Lee, W. Franklin, D. J. Stewart and Wistuba, II (2012). "High expression of folate receptor alpha in lung cancer correlates with adenocarcinoma histology and EGFR [corrected] mutation." J Thorac Oncol 7(5): 833-840.
239. Franklin, W. A., M. Waintrub, D. Edwards, K. Christensen, P. Prendegrast, J. Woods, P. A. Bunn and J. F. Kolhouse (1994). "New anti-lung-cancer antibody cluster 12 reacts with human folate receptors present on adenocarcinoma." Int J Cancer Suppl 8: 89-95.
240. O'Shannessy, D. J., G. Yu, R. Smale, Y. S. Fu, S. Singhal, R. P. Thiel, E. B. Somers and A. Vachani (2012). "Folate receptor alpha expression in lung cancer: diagnostic and prognostic significance." Oncotarget 3(4): 414-425.
241. Kouso, H., I. Yoshino, N. Miura, T. Takenaka, T. Ohba, T. Yohena, A. Osoegawa, F. Shoji and Y. Maehara (2008). "Expression of mismatch repair proteins, hMLH1/hMSH2, in non-small cell lung cancer tissues and its clinical significance." J Surg Oncol 98(5): 377-383.
242. Bischoff, J., A. Ignatov, A. Semczuk, C. Schwarzenau, T. Ignatov, T. Krebs, D. Kuster, D. Przadka-Rabaniuk, A. Roessner, S. D. Costa and R. Schneider-Stock (2012). "hMLH1 promoter hypermethylation and MSI status in human endometrial carcinomas with and without metastases." Clin Exp Metastasis 29(8): 889-900.
243. de Jong, R. A., A. Boerma, H. M. Boezen, M. J. Mourits, H. Hollema and H. W. Nijman (2012). "Loss of HLA class I and mismatch repair protein expression in sporadic endometrioid endometrial carcinomas." Int J Cancer 131(8): 1828-1836.
244. Ting, S., F. D. Mairinger, T. Hager, S. Welter, W. E. Eberhardt, J. Wohlschlaeger, K. W. Schmid and D. C. Christoph (2013). "ERCC1, MLH1, MSH2, MSH6, and betaIII-tubulin: resistance proteins associated with response and outcome to platinum-based chemotherapy in malignant pleural mesothelioma." Clin Lung Cancer 14(5): 558-567 e553.
245. Della-Maria, J., M. L. Hegde, D. R. McNeill, Y. Matsumoto, M. S. Tsai, T. Ellenberger, D. M. Wilson, 3rd, S. Mitra and A. E. Tomkinson (2012). "The interaction between polynucleotide kinase phosphatase and the DNA repair protein XRCC1 is critical for repair of DNA alkylation damage and stable association at DNA damage sites." J Biol Chem 287(46): 39233-39244.

246. Erculj, N., V. Kovac, J. Hmeljak, A. Franko, M. Dodic-Fikfak and V. Dolzan (2012). "DNA repair polymorphisms and treatment outcomes of patients with malignant mesothelioma treated with gemcitabine-platinum combination chemotherapy." J Thorac Oncol 7(10): 1609-1617.
247. Cui, F., Y. Wang, J. Wang, K. Wei, J. Hu, F. Liu, H. Wang, X. Zhao, X. Zhang and X. Yang (2006). "The up-regulation of proteasome subunits and lysosomal proteases in hepatocellular carcinomas of the HBx gene knockin transgenic mice." Proteomics 6(2): 498-504.
248. Thaker, N. G., F. Zhang, P. R. McDonald, T. Y. Shun, M. D. Lewen, I. F. Pollack and J. S. Lazo (2009). "Identification of survival genes in human glioblastoma cells by small interfering RNA screening." Mol Pharmacol 76(6): 1246-1255.
249. Kumatori, A., K. Tanaka, N. Inamura, S. Sone, T. Ogura, T. Matsumoto, T. Tachikawa, S. Shin and A. Ichihara (1990). "Abnormally high expression of proteasomes in human leukemic cells." Proc Natl Acad Sci U S A 87(18): 7071-7075.
250. Kanayama, H., K. Tanaka, M. Aki, S. Kagawa, H. Miyaji, M. Satoh, F. Okada, S. Sato, N. Shimbara and A. Ichihara (1991). "Changes in expressions of proteasome and ubiquitin genes in human renal cancer cells." Cancer Res 51(24): 6677-6685.
251. Choi, Y. H. (2001). "Proteasome-mediated degradation of BRCA1 protein in MCF-7 human breast cancer cells." Int J Oncol 19(4): 687-693.
252. Naujokat, C. and S. Hoffmann (2002). "Role and function of the 26S proteasome in proliferation and apoptosis." Lab Invest 82(8): 965-980.
253. Catz, S. D. and J. L. Johnson (2001). "Transcriptional regulation of bcl-2 by nuclear factor kappa B and its significance in prostate cancer." Oncogene 20(50): 7342-7351.
254. Breitschopf, K., A. M. Zeiher and S. Dimmeler (2000). "Ubiquitin-mediated degradation of the proapoptotic active form of bid. A functional consequence on apoptosis induction." J Biol Chem 275(28): 21648-21652.
255. Li, B. and Q. P. Dou (2000). "Bax degradation by the ubiquitin/proteasome-dependent pathway: involvement in tumor survival and progression." Proc Natl Acad Sci U S A 97(8): 3850-3855.

8. List of Abbreviations Used

Abbreviation	Full Name
AAH	Atypical adenomatous hyperplasia
AC	Atypical carcinoid
ADC	Adenocarcinomas
ASCO	American Society of Clinical Oncology
BAC	Bronchoalveolar carcinoma in situ
BASC	Bronchoalveolar stem cell
BLAST	Basic Local Alignment Search Tool
CC	Cell cycle
CDS	Coding sequence
CGH	Comparative genomic hybridisation
CNV	Copy number variation
COLD-PCR	Co-amplification at lower denaturation temperature PCR
CR	Complete remission
Ct	Cycle threshold
DIPNECH	Diffuse idiopathic pulmonary neuroendocrine cell hyperplasia
DISC	Death inducing signalling complex
DST	Downstream targets
EMA	European Medicines Agency
EMT	Epithelial to mesenchymal transition
ESMO	European Society of Medical Oncology
FDA	Food and Drug Administration
FFPE	Formalin fixed paraffin embedded
FRET	Förster resonance energy transfer
GABA	Gamma-aminobutyric acid
GF	Growth factor
GO	Gene ontology
HE	Haematoxylin and eosin staining
HG	High grade
HPF	High power field
HR	Hazard ratio
IASLC	International Association for the Study on Lung Cancer
IGV	Integrative Genome Viewer
IHC	Immunohistochemistry
IMDA	Isothermal multiple displacement amplification
LAR	Long-acting repeatable
LCNEC	Large-cell neuroendocrine cancer
LG	Low grade
LOF	Loss of function
LOH	Loss of heterozygousity
MIQE	Minimum Information for Publication of Quantitative Real-Time PCR Experiments
miRNA	Micro RNA
mRNA	Messenger RNA

Abbreviation	Full Name
NE	Neuroendocrine
NEB	Neuroepithelial body
NELC	Neuroendocrine lung cancer
NET	Neuroendocrine tumour
NGS	Next-generation sequencing
NSCLC	Non-small cell lung cancer
NTC	Non-template control
OS	Overall Survival
PCR	Polymerase chain reaction
PD	Progressive disease
PFS	Progression Free Survival
PNEC	Pulmonary neuroendocrine cells
PR	Partial remission
PSA	Polysialic acid
qPCR	Quantitative PCR
RISC	RNA-induced silencing complex
ROI	Region of interest
RTK	Receptor tyrosine kinase
RTK	Receptor tyrosine kinase
SCC	Small-cell cancer
SCLC	Small-cell lung cancer
SD	Stable disease
SNP	Single nucleotide polymorphism
SQCC	Squamous cell carcinoma
TC	Typical carcinoid
TSCP	TruSeq Amplicon Cancer Panel
TSG	Tumour suppressor gene
WGA	Whole-genome amplification
WGS	Whole-genome sequencing
WHO	World Health Organisation

9. List of Figures

Figure 5 Atypical carcinoid with two rosette structures (circles) and “salt and pepper chromatin” (arrow) stained with HE (400x magnification).

Figure 6 Large-cell lung cancer forming a so-called palisade structure (400x magnification).Figure 7 Small-cell lung cancer with HE staining (400x magnification). The neuroendocrine properties like granular chromatin and lack of prominent nucleoli serve as diagnostic criteria for diagnosis of SCLC.

Figure 7 Small-cell lung cancer with HE staining (400x magnification). The neuroendocrine properties like granular chromatin and lack of prominent nucleoli serve as diagnostic criteria for diagnosis of SCLC.

Figure 8 Suggested algorithm for the treatment of non-small cell pulmonary neuroendocrine tumours (Gridelli et al. 2013).

Figure 9 Boxplots depicting significant differences in miRNA expression in neuroendocrine pulmonary tumours. Expression of miR-18a and miR-15b* is increasing with increasing malignancy of the tumour. miR-335* and miR-1201 profiles show a decreased expression in carcinoids compared to the neuroendocrine carcinomas. For miR-22 and miR-367* increased malignancy is associated with decreased expression. In SCLC, miR-504 expression is dramatically decreased and for miR-513C, TC show the highest expression.

Figure 10 Boxplots showing the expression profiles of the miR-29 family displaying similar patterns between the different tumour entities. Decreasing expression of miR-29a-c correlates with increasing malignancy of the tumour.

Figure 11 Pie chart showing results of the pathway analysis in pulmonary neuroendocrine tumours: The pathways showing the most prominent alterations by

miRNAs were shown to be the MAPK pathway followed by PI3K- and TGF-β-pathway. Aberrations could also be found for Wnt-signalling, NFκB-pathway, JNK-pathway and mTOR-signalling.

Figure 12 Illustrated results of the GO analysis presenting most hits in gene expression and transcription. Similar hits for cell cycle and nervous system were found. Following, with decreasing impact, also proliferation, immune response, apoptosis, DNA-damage-response, growth factors and signalling, carriers, angiogenesis and expression of structural compounds is affected by differential miRNA expression.

Figure 13 mRNA expression patterns of different genes measured by the NanoString technology. All illustrated genes decrease in their gene expression with increasing malignancy of the NET. FOLR1, CDK6 and SYP show very low median expression levels in NE carcinomas, especially when compared to pulmonary carcinoids. MLH1 is significantly higher in carcinoids then in high-grade tumours, but also carcinomas still have a noteable expression level. CHGA was the strongest expressed gene of all targets. Its y-axis is logarithmically scaled.

Figure 14 mRNA expression patterns of different genes measured by the NanoString technology are shown. All illustrated genes increase in their expression level with higher aggressiveness of the tumour. TYMS, CDKN2A and SOX4 show nearly no expression in carcinoid tumours but a detectable (LCNEC) to strong (SCLC) expression in high-grade carcinomas. PAX6, RBP1 and SOX11 are absent in carcinoids and LCNEC but expressed in SCLC.

Figure 15 The boxplots present mRNA expression pattern of BCL2 investigated by NanoString nCounter technology and the BCL2/BAX-ratio as marker for evade of

apoptosis, respectively. The BCL2 expression increases with increasing malignancy of the tumour entity. Whereas the BCL2/BAX ratio is nearly even in TC, the potential to evade apoptosis increases from AC over LCNEC to the highest value in SCLC.

Figure 16 Kaplan-Meier curves for significant results regarding expression-dependent PFS in the group of high-grade pulmonary NET. A high expression level of NTS and HIF1A is associated with shortened time to progression, respectively. Low level expression of FOLR1 leads to an early recurrence of the tumour, whereas in contrast a loss of OCT4 expression is associated with prolonged PFS in this group of tumours.

Figure 17 Kaplan-Meier curves for significant results regarding expression-dependent OS. A low PAX6 or OCT4 expression is associated with prolonged, a low FPGS or MAN2B1 expression is associated with shortened overall survival in LCNEC and SCLC, respectively.

Figure 18 The chart pies summarises the algorithm used for variant filtering. Starting from 25,940 variants detected with the preliminary variant calling, going on with removing of synonymous variants that led to 18,899 variants. After a final filtering of variants below 10% of total reads or less than 25 mutated reads absolute 634 variants were determined.

Figure 19 The histogram demonstrates the distribution of the reads past filter (PF) from all targets and runs. The y-axis shows the number of clusters that passed the initial filter process, the x-axis shows the coverage of these loci merged from each sample. Most targets had a median coverage between 500 and 2,000bp.

Figure 20 Samples showing at least one TP53 variant regarding the tumour entity. The number of mutated samples increased from TC (below 30%) to SCLC (more

than 90%). A sharp edge can be seen between carcinoid tumours (30%-40%) and high-grade carcinomas (75-95%).

Figure 21 Kaplan-Meier curves of significant results regarding FBXW7. The occurrence of mutations within the coding sequence of FBXW7 is associated with shortened cumulative overall survival.

Figure 22 Kaplan-Meier curves of significant results regarding the mutation-dependent PFS analysis. Patients showing mutations in the CDS of either MET or KRAS have a highly significant shortened time to progression of the tumours. Also ATM and RB1 mutations significantly impact to progression of the tumours.

Figure 23 Box plots illustrating significantly upregulated mRNA expression in the different subtypes of pulmonary neuroendocrine tumours are shown. The gene expression measured by TaqMan qPCR is shown using log(2^-dCt) of each target. Horizontal bars indicate significant dependences. Note that any proteasomal subunit mRNA expression is significantly upregulated compared to controls obtained from non-tumorous lung tissue of patients with pneumothorax. Especially PSMB4 and PSMD1 show the strongest upregulation compared to benign lung. LCNEC show the broadest range of proteasomal expression pattern, maybe due to the heterogeneity of this entity. Remarkable is the relatively low PSMA5 expression level when compared to the control.

Figure 24 The figure illustrates the results of the immunohistochemical staining of the proteasomal subunit PSMB4 in both, low-grade (A+B) and high-grade (C+D) pulmonary NET. Immunohistochemically, PSMB4 reactivity is strong in any subtypes of pulmonary NET. All NET are silhouetted against the encircling stroma.

Immunohistochemical no differences between the four tumour entities could be detected.

Figure 25 Boxplot of PSMB4 expression levels between the different tumour types. In particular, the PSMB4 mRNA expression is upregulated in pulmonary NET compared to controls and differs significantly among the subtypes of pulmonary NET. PSMB4 shows the highest expression in LCNEC, the lowest expression in AC and SCLC. Nevertheless, immunohistochemically no differences between the four tumour entities could be detected, PSMB4 mRNA expression is higher in LCNEC/SCLC than in TC/AC. The gene expression measured by TaqMan qPCR is shown using log(2^-dCt) of each target. Horizontal bars indicate significant dependences.

Figure 26 Differential expression of PSMB4 between the two types of high-grade NELC. LCNEC shows a slightly higher expression level then SCLC. The gene expression measured by TaqMan qPCR is shown using log(2^-dCt) of each target. Horizontal bars indicate significant dependences.

Figure 27 Differential expression pattern of PSMA1 and PSMB5 in low-grade NELC. Among others, the gene expressions of PSMA1 ($p= 0.030$) and PSMB5 ($p= 0.035$) are significantly higher in TC compared to AC. The gene expression measured by TaqMan qPCR is shown using log(2^-dCt) of each target. Horizontal bars indicate significant dependences.

Figure 28 Boxplots illustrating results of the immunohistochemical staining of NELC against the neuroendocrine markers NCAM (CD56) and CHGA, CKMNF-116 and TTF1 as diagnostic standards, Ki67 for proliferation and CASP3 to determine the apoptotic activity fraction.

Figure 29 The visual analysis of the next generation sequencing data by integrative genomics viewer shows a high background of false-positive variants for APC exon 14. Pink bars show sequenced forward strand, blue bars show sequenced reverse strands. Colour dots within the strands display discrepancies between the base calls and the hg19 reference build.

Figure 30 Proposal for a model for classifying lung tumours. Despite the traditional morphologic view and classification into NSCLC and SCLC, which has been undisputed for generations of medical doctors, the family of pulmonary neuroendocrine tumours, although showing different morphological presentation, can be biologically distinguished from all other forms of lung cancers.

Figure 31 Overview of differences in signalling pathways and cellular processes between pulmonary neuroendocrine lung tumours. Red arrows indicate activation, green arrows downregulation of different key players for important cellular pathways. Also markers important for prognosis (OS/PFS) are highlighted. Of note are the different entries into the cell cycle between carcinoids and carcinomas and the strong activation of angiogenesis in pulmonary carcinoid tumours.

10. List of Tables

mRNAs are bolded; most significant mRNAs are highlighted grey. Highlighted genes are presented in boxplots in Figure 13.

Table 11 Significant p-values of mRNA expression correlating with tumour grade calculated with the Spearman Test. Highly significant mRNAs are bolded; most significant mRNAs are highlighted grey.

Table 12 P-values of mRNA expression regarding several clinical variables (TNM) using the Spearman Test are shown. Highly significant mRNAs are bolded; most significant mRNAs are highlighted in grey.

Table 13 Overview of the technical run parameters for all five MiSeq runs. In run 5, the 23 samples with the lowest median coverage or insufficient representation of some loci were resequenced.

Table 14 The table shows the results of the variant calling. The mutation frequency per gene as well as the percentage of samples of each entity showing at least one mutation at this locus is illustrated.

Table 15 Summary of significant results regarding the mutation-dependent survival analysis.

11. Acknowledgments

First I want to thank PD Dr. Jeremias Wohlschläger who was mentoring my work and especially this thesis. Despite his workload, he always took the time to discuss our results and offered me help in any way. His guidance into the world of lung cancer has been essential during this work.

I also want to express my sincere gratitude to Prof. Dr. Kurt Werner Schmid for the opportunity to develop this thesis at his institute. He allowed me great latitude to create this work and always offered me expert advice and support.

My very special thanks goes to Dr. Daniel Christoph, who had a lot of patience with me and always abets me during my work. I further want to thank him for helping me with all the clinical background I needed.

I deserve a special thanks to Saskia Ting and Dr. Thomas Hager for helping me with the histological and immunohistochemical evaluation as well as answering my pathological questions.

The skilful assistance of Gabriele Ladwig with the immunohistochemical staining is highly appreciated.

I am indebted to many of my colleagues, especially Robert Werner, who supported me in any aspect during this thesis.

I am very grateful to Robert F.H. Walter, who supported me under all circumstances, privately as well as professionally. This thesis would not have been possible without him and his help.

I owe my deepest gratitude to Claudia Vollbrecht. Without her continuous encouragement and support for me, privately and professionally, this thesis would hardly have been completed. She was my pillar of strength all the time.

Last but not least I want to express my deepest gratitude to my family. They kept me grounded in all highs and depths and stick to me, also when faced with difficult times. Without them I would have never been able to reach this point in my life.

12. Curriculum Vitae

Der Lebenslauf ist in der Onlineversion aus Gründen des Datenschutzes nicht enthalten.